REMOTE SENSING OF CYANOBACTERIA IN CASE II WATERS USING OPTICALLY ACTIVE PIGMENTS, CHLOROPHYLL *A* AND PHYCOCYANIN

Kaylan Lee Randolph

Submitted to the faculty of the University Graduate School
in partial fulfillment of the requirements
for the degree
Master of Science
in the Department of Geography,
Indiana University

March 2007

Accepted by the faculty of Indiana University, in partial fulfillment of the requirements for the degree of Master of Science.

Jeffery S. Wilson, Ph.D.

Master's Thesis
Committee

Lenore P. Tedesco, Ph.D.

Lin Li, Ph.D.

ACKNOWLEDGEMENTS

I wish to thank my advisors, Jeff Wilson, Lenore Tedesco, and Lin Li for their endless guidance, patience, and faith in me. Though it was evident that they were often concerned about the direction in which I was headed, they entertained my every hair-brained idea and whim. I am certain that my success as a graduate student has been primarily based in my relationship with them.

Specifically, I wish to thank my Chief Advisor, Jeff Wilson, for providing me with the opportunity to experience and guidance in this graduate program, which has far exceeded all of my expectations. I want to thank Lenore Tedesco, whose amazing enthusiasm for the work that she does ultimately transfers to those working for and around her. She is closely tied to the community and performs research that is both scientifically relevant and applicable and has instilled the passion to development practices and strategies to improve environmental health in me. I would like to thank Lin Li for proposing this ambitious project, the first of its kind at IUPUI, and encouraging me to join his team.

I also want to thank Lani Pascual, who took on many roles in this project. Her unconditional support and encouragement and persistent enthusiasm propelled the project, and more specifically, me forward. Thank you to Lani for being my support system, my mentor and confidant.

I wish to thank my family for actively listening to my endless rants about remote sensing of cyanobacteria, a topic in which the have no experience and likely little interest. Thank you to my parents who have faith in my every decision and who recognize and willingly acknowledge that the outcome won't always be brilliant.

I wish to thank the graduate students and faculty in the Department of Earth Sciences at IUPUI for participating in the field sampling campaign, which proved to be a logistical nightmare. Specifically, I wish to thank Becky Sengpiel who has become a great friend both in and out of the laboratory. I wish also to thank my officemates Bob Hall, Vince Hernly, and Bob Barr for their good spirit, understanding, and tolerance on those days when things were looking less than favorable.

Finally, I also wish to thank the Veolia Water Indianapolis, LLC White River Laboratories for all of their assistance with sample analyses; IndyParks and Eagle Creek Park for dock space and launch access; and Kent Duckwell for access to Geist and Morse Reservoirs.

Without the patience and support of these people, this research would not have been possible.

ABSTRACT

Kaylan Lee Randolph

REMOTE SENSING OF CYANOBACTERIA IN CASE II WATERS USING OPTICALLY ACTIVE PIGMENTS, CHLOROPHYLL *A* AND PHYCOCYANIN

Nuisance blue-green algal blooms contribute to aesthetic degradation of water resources and produce toxins that can have serious adverse human health effects. Current field-based methods for detecting blooms are costly and time consuming, delaying management decisions. Remote sensing techniques which utilize the optical properties of blue-green algal pigments (chlorophyll *a* and phycocyanin) can provide rapid detection of blue-green algal distribution. Coupled with physical and chemical data from lakes, remote sensing can provide an efficient method for tracking cyanobacteria bloom occurrence and toxin production potential to inform long-term management strategies. *In-situ* field reflectance spectra were collected at 54 sampling sites on two turbid, productive Indianapolis reservoirs using ASD Fieldspec (UV/VNIR) spectroradiometers. Groundtruth samples were analyzed for *in-vitro* pigment concentrations and other physical and chemical water quality parameters. Empirical algorithms by Gitelson *et al.* (1986, 1994), Mittenzwey *et al.* (1991), Dekker (1993), and Schalles *et al.* (1998), were applied using a combined dataset divided into a calibration and validation set. Modified semi-empirical algorithms by Simis *et al.* (2005) were applied to all field spectra to predict phycocyanin concentrations. Algorithm accuracy was tested through a least-squares regression and residual analysis. Results show that for prediction of chlorophyll *a* concentrations within the range of 18 to 170 ppb, empirical algorithms yielded coefficients of determination as high as 0.71, RMSE 17.59 ppb, for an aggregated

dataset (n=54, p<0.0001). The Schalles *et al.* (2000) empirical algorithm for estimation of phycocyanin concentrations within the range of 2 to 160 ppb resulted in an r^2 value of 0.70, RMSE 23.97 ppb (n=48, p<0.0001). The Simis *et al.* (2005) semi-empirical algorithm for estimation of chlorophyll *a* and phycocyanin concentrations yielded coefficients of determination of 0.69, RMSE 20.51 ppb (n=54, p<0.0001) and 0.85, RMSE 24.61 pbb (n=49, p<0.0001), respectively. Results suggest the Simis *et al.* (2005) algorithm is robust, where error is highest in water with phycocyanin concentrations of less than 10 ppb and in water where chlorophyll *a* dominates (Chl:PC>2). A strong correlation between measured phycocyanin concentrations and blue-green algal biovolume measurements was also observed (r^2=0.95, p<0.0001).

Jeffrey S. Wilson, Ph.D.
(Committee Chair)

TABLE OF CONTENTS

LIST OF TABLES

LIST OF FIGURES

INTRODUCTION

Nuisance algal blooms cause aesthetic degradation to lakes and reservoirs resulting in surface scum, unpleasant taste and odor in drinking water (from the production of metabolites such as Methyl Isoborneol and Geosmin), and possible adverse effects to human heath from blue-green algal toxins. Harmful algal blooms of cyanobacteria (CyanoHABs) have been known to produce the following toxins: Anatoxin-a, Microcystin, and Cylindrospermopsin. Anatoxin-a, produced by cyanobacterial genera such as *Anabaena*, *Oscillatoria*, and *Cylidrospermopsis*, among others, has an acute neurotoxic effect. As an acetylcholine mimic, Antatoxin-a acts as a powerful acetylcholine receptor agonist, attaching to a cell receptor to produce a negative physiological reaction. Symptoms of exposure include salivation, muscle tremors, convulsions, and sometimes death. Microcystins, produced by cyanobacterial genera such as *Anabaena* and *Microcystis*, has an acute hepatotoxic effect. Microcystin, a microfilament disruptor, damages liver cell integrity. Symptoms of exposure include vomiting, diarrhea, hemorrhaging of the liver, seizures, shock, and sometimes death from respiratory arrest. Cylindrospermopsin is also a hepatotoxin which acts by inhibiting protein phosphatase. Symptoms of exposure include anorexia, diarrhea, gasping respiration, enlarged liver, vomiting, headache, and malaise. Though these strains have been documented as toxin producers, the conditions in which they produce toxins are highly variable (Backer, 2002).

Several cases of human poisoning as a result of microcystin hepatotoxicity have been documented. These cases mostly include onset of severe illness and liver damage, however, some have resulted in death. In 1988, a CyanoHAB containing *Anabaena* and *Microcystis* was found in a drinking water reservoir in Brazil. Two thousand recipients of

the reservoir's water contracted gastroenteritis, 88 of these cases resulted in death (Teixeira *et al.*, 1993). The U.S. saw its first death potentially attributed to a CyanoHAB in July of 2002. In Dane County, Wisconsin a teenage boy swimming in a golf course pond described as scummy, suffered a seizure and died of heart failure. Blood and stool tests revealed the presence of *Anabaena* and anatoxin-a (Behm, 2003). Because the acute effects of intoxication are severe, stringent monitoring programs of Cyanobacteria blooms in drinking water and recreational reservoirs are necessary.

Predicting the locations and timing of blue-green blooms using traditional sampling techniques is difficult, if not impossible, due to high variability of conditions in which blooms form and produce toxins (Pitois *et al*., 2000). Current methods consist of field sample collection, laboratory analysis, and identification and enumeration of phytoplankton, which can take days to weeks. These methods are neither timely nor cost efficient for drinking water mangers since blooms can be as ephemeral as a few days. Because some phytoplankton pigments are optically active and their properties can be measured using spectroscopy, researchers have evaluated the utility of field-collected spectral response patterns for determining concentrations of both chlorophyll *a* and phycocyanin pigments in lake water (*e.g*., Gitelson *et al.*, 1986; Schalles and Yacobi, 2000; Mitzenzway *et al.*, 1992; Simis *et al.,* 2005). These researchers have developed models based on variability of spectral response gathered by medium to high resolution spectroradiometers (spectral range approximately 300 to 1100 nm) for sites with differing algal density. Since the optical properties of nuisance algal blooms have been discerned in field reflectance spectra, these remote sensing techniques can be extended to airborne and spaceborne satellite imaging systems to map chlorophyll *a* and phycocyanin concentrations and, therefore, blue-green algal distribution in inland reservoirs.

The purpose of this research is to extend remote sensing methods for mapping the spatial distribution and concentration of phytoplankton in inland reservoirs. Previously developed algorithms (Table 1) were chosen for evaluation. Developed in case II waters, inland water where chemistry is complex including high concentrations of suspended material, dissolved organic matter, and yellow substances, these algorithms have potential to extend well to the turbid, eutrophic reservoirs in Indiana. The algorithms were evaluated for accuracy in estimating analytically measured chlorophyll *a* and phycocyanin concentrations from field spectral response measurements collected in two Indianapolis water supply reservoirs. Algorithm accuracy was evaluated using least-squares regression. Algorithm robustness was then tested through a residual analysis in which confounding water quality parameters were identified. The utility of field spectroscopy was evaluated, as it is reported in the literature, as a real-time cyanobacteria bloom assessment method and remote sensing algorithms were be established for these systems that can be extended to air and spaceborne imaging systems and to other water bodies.

Table 1: Algorithms relating field spectral response to measured chlorophyll *a* and phycocyanin concentrations.

Chlorophyll *a*	**Phycocyanin**
$[R(705)][R(670)]^{-1}$ $[R(705)-R(670)][R(550)]^{-1}$ $[R(705)-R(670)][R(550)^{-1}-R(670)^{-1}]$ $[R(705)-R(670)][R(550)^{-1}-R(760)^{-1}]$ $[R_{max}\lambda_{(695-715)}][R_{min}\lambda_{(665-685)}]^{-1}$ Gitelson *et al.* (1986); Mittenzwey and Gitelson (1988); Gitelson (1992); Mittenzwey *et al.* (1991); Dekker (1993)	$PC = R_{648}/R_{624}$ Schalles and Yacobi (2000)
$RH_{670-730}$ $SUM_{670-730}$ $R_{(maxred)}/R(560)$ $R_{(maxred)}/R(675)$ Dekker (1993)	$PC = 0.5(R_{600} + R_{648}) - R_{624}$ Dekker (1993)
$a_{chl}(665) = (\{[R(709)/R(665)] \times [a_w(709) + b_b]\} - b_b - a_w(665)) \times \gamma^{1}$ $a_w(\lambda)$ are pure water absorption coefficients at λ b_b is the backscattering coefficient obtained from: $b_b = [a_w(778) \times R(778)] \times [(f - R(778)]^{-1}$ f is an estimate based on average cosine of downward irradiance γ is derived from the linear least-squares fit of measured versus estimated chlorophyll *a* absorption Simis *et al.* (2005)	$a_{pc}(620) = (\{[R(709)/R(620)] \times [a_w(709) + b_b]\} - b_b - a_w(620)) \times \delta^{-1} - [\varepsilon \times a_{chl}(665)]$ $a_w(\lambda)$ are pure water absorption coefficients at λ b_b is the backscattering coefficient at 778 nm δ is derived from the linear least-squares fit of measured versus estimated phycocyanin absorption $a_{chl}(665)$ absorption of chlorophyll *a* at 665 nm ε is a conversion factor to define absorption of chlorophyll *a* at 620 nm relative to 665 nm Simis *et al.* (2005)

Background on Remote Sensing of Water Quality

Remote sensing allows the collection of information about water quality without obtaining direct contact. Downwelling irradiant energy provided by a source such as the sun, is transmitted along a pathway through the atmosphere, reflected off of a target, back into the atmosphere, and then recorded by a sensor. In aquatic systems, the total recorded radiance of water is a function of path, surface, volumetric, and bottom radiance (Jensen, 2005). Path radiance is the result of atmospheric scattering and is classified as noise because it does not contain information about the target water feature. Surface radiance describes the top few millimeters of water, the boundary layer between the atmosphere and the water. Volumetric radiance penetrates the boundary layer and provides information about the material suspended in the water column. Bottom radiance passes through the water column and reflects off of bottom sediments. Display of spectral reflectance as a function of wavelength can be used to identify the properties and condition of the target water feature because any optically active water constituents will attenuate or augment the original radiance signal along the spectrum.

Since any optically active particle suspended in the water column will affect the irradiance signal, reflectance spectra can be used to estimate productivity, as measured using chlorophyll *a* concentrations. Green algae contain the pigment chlorophyll *a* and have two absorption maxima at approximately 425 and 675 nm. Ocean mapping of chlorophyll *a* using spaceborne systems has produced promising results for monitoring productivity. Oceans are classified as case I water, where optically active constituents mostly include water, phytoplankton, and its products. Ocean color sensors with the necessary spectral bands for detecting phytoplankton pigments, including MODIS, SeaWIFS and MERIS, however, have spatial resolutions that are too coarse for mapping

small, inland water bodies, classified as case II. Case II water chemistry is more complex, including high concentrations of suspended material, dissolved organic matter, and yellow substances borne from terrestrial influence. The presence of elevated levels of chlorophyll *a* in inland water is typically an indicator of high productivity and potentially harmful blue-green algal blooms. Freshwater blue-green algae have an accessory pigment to chlorophyll *a*, the biloprotein phycocyanin. This accessory pigment allows cyanobacteria to have an additional absorption maximum in the red portion of the spectrum at approximately 620 nm (Jupp *et al.*, 1994; Gons *et al.*, 1992; Dekker, 1993). Greater variability in the optically active constituents of inland waters also requires increased spectral resolution.

Summary of Spectral Reflectance Features of Case II Water

Three optically active components affect the features found in the spectral reflectance curve of freshwater: phytoplankton pigments, particulate matter, and yellow substances. Previous research has identified some of the sources of the features found in this curve (Figure 1). The first is an absorption feature found at approximately 440 nm (a), attributed to absorption by chlorophyll *a* (Gordon and Morel, 1983; Gitelson *et al.*, 1999). This feature is used in ocean color models but not in case II waters because the presence of dissolved organic matter and suspended sediment significantly affect the signal. An additional absorption feature within the range of 450 and 525 nm (b) is caused by presence of carotenoids (Rowan, 1989; Gitelson *et al.*, 1999; Jensen 2005). Carotenoids are a class of yellow to red pigments that include carotenes and xanthophylls. The spectral range of 550 to 600 nm (c) contains the green peak, mostly due to minimal absorption by phytoplankton pigments and, thus, maximum scattering by algal cells (Dekker *et al.*, 1991; Gitelson, 1992; Jensen, 2005). It has been suggested that a shift in this peak toward longer wavelengths is a result of absorption of the shorter

wavelengths by carotenoids, indicating an increased carotenoid concentration. A shift in the green peak toward shorter wavelengths (540 nm) is caused by absorption of the longer wavelengths by phycocyanin, a pigment found in cyanobacteria, indicating an increase in phycocyanin concentration (Schalles *et al.*, 1998; Gitelson *et al.*, 1999). The subsequent trough, within the range of 620 and 630 nm (d), is the result of absorption by phycocyanin (Gitelson *et al*., 1986). The minor reflectance peak at approximately 650 nm (e) is attributed to backscattering from dissolved organic matter (Gitelson, 1992). This feature is also known to be affected by phycocyanin concentration because it is the location of the phycocyanin fluorescence emission maximum (Ahn *et al.*, 1992). The trough feature at approximately 675 nm is the chlorophyll *a* absorption maximum (f) (Rundquist *et al.*, 1996; Han and Rundquist, 1997). Reflectance here depends mainly on the presence of non-organic suspended matter (Gitelson *et al.*, 1993; Dekker, 1993; Yacobi *et al.*, 1995). The reflectance peak in the NIR portion of the spectrum, within the range of 698 and 712 nm (g), is the result of scattering from algal cells, the pigment and water combination, and particulate matter. The location and height of this peak is a function of chlorophyll *a* concentration. Peak shifts toward longer wavelengths and increase in height are indications of increased chlorophyll *a* concentration (Dekker *et al.*, 1991; Han and Rundquist, 1997; Gitelson, 1992; Mittenzwey *et al.*, 1992; Rundquist *et al.*, 1996; Schalles *et al.*, 1998). Reflectance features at wavelengths longer than 750 nm are attributed to organic and non-organic suspended matter concentrations (Han *et al.,* 1994).

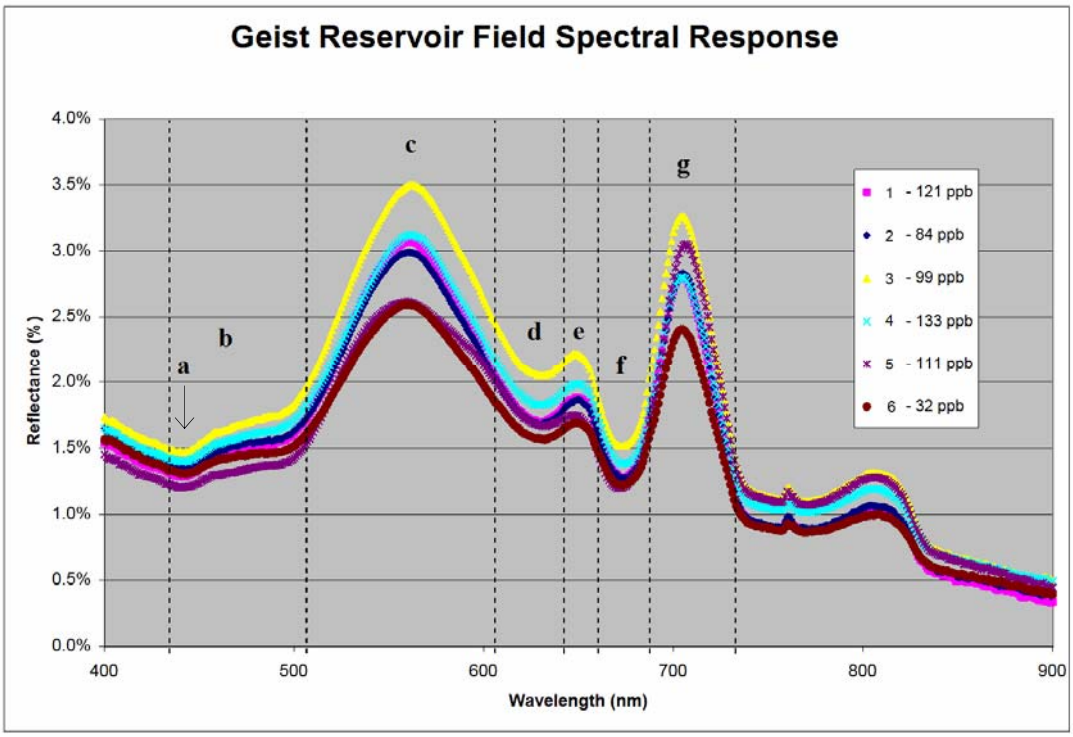

Figure 1: Spectral Reflectance for six sites on Geist Reservoir collected September 6, 2005 and corresponding measurements of chlorophyll *a*.

Background on Model Types

Although very few models exist for predicting phycocyanin concentration in productive, inland, case II water, many algorithms have been proposed for estimating chlorophyll *a* concentration as a proxy for measuring productivity in both case I and II systems. Morel and Gordon (1980) described three methods for algorithm derivation:

i. Empirical method – Relationships between spectral reflectance values, $R_{rs}(\lambda)$, and laboratory measured constituent concentrations collected simultaneously are developed using statistical methods.

ii. Semi-empirical method – Models are based on known spectral features and previously discovered empirical relationships are employed. Measured inherent optical properties of the water column are included to derive absorption coefficients for optically active constituents.

iii. Analytical method – The inherent and apparent optical properties are measured and included in the model as specific absorption and backscatter coefficients. Constituent concentrations are determined using the reflectance, absorption, and backscatter coefficients. Bio-optical models are constructed based on the biophysical characteristics of a system using radiative transfer equations with the purpose of separating the total radiance into its basic components.

Remote sensing reflectance (R_{rs}) at a specific wavelength (λ) is obtained using the ratio of upwelling radiance (L_u) above the waters surface (0^+) at a nadir viewing angle to the downwelling irradiance (E_d) provided by the sun:

$$R_{rs} = \frac{L_u(0^+, \lambda)}{E_d(0^+, \lambda)} \qquad \text{Equation 1}$$

Statistically significant relationships between above-water remote sensing reflectance ($R_{rs}(0^+, \lambda)$) and constituent concentrations, such as correlation between change in reflectance with change in constituent concentration as a function of wavelength, are sought and used in algorithm derivation. Recent research suggests a movement from the empirical to an analytical or bio-optical modeling technique, where theoretical radiative transfer equations (RTE) based on the inherent optics (the reflection, absorption, and transmission of light interacting with an individual particle) are employed. Because bio-optical modeling is based on physical properties, it eliminates the need for gathering water samples to provide statistical analysis linking phytoplankton concentration to reflectance, thus improving the accuracy of algorithms across water bodies. Likewise, bio-optical modeling techniques are more easily extended to air and space-borne systems. The following Gordon *et al*. (1975) described the relationship between the inherent optical properties (IOPs), properties of a specific medium independent of a light source, and apparent optical properties (AOPs), properties that are a combination of the IOPs and the light field in which they are measured, is used in development of bio-optical models for homogeneous water bodies with the equation:

$$R(0^-,\lambda) = f\,\frac{b_b(\lambda)}{a(\lambda)+b_b(\lambda)}$$ Equation 2

Where:

$R(0^-, \lambda)$	=	subsurface reflectance at a specified depth and wavelength
f	=	experimental factor dependent on the light field (sun angle) and volume scattering function (VSF) (Morel and Gentili, 1991)
$b_b(\lambda)$	=	backscatter coefficient (attenuation caused deflection of energy at 90º to 180º angle)
$a(\lambda)$	=	absorption coefficient (efficiency of a material at absorbing energy)

Subsurface irradiance $R(0^-, \lambda)$ is related to surface reflectance $R_{rs}(0^+, \lambda)$ by the inclusion of an empirical factor Q, which is the ratio of subsurface downwelling irradiance to $E_u(0^-, \lambda)$ subsurface upwelling radiance $L_u(0^-, \lambda)$. Specifically $f:Q$ accounts for the geometry of light exiting the water body on the remote sensing reflectance measured above the water surface. With inclusion of the ratio $f:Q$, $R_{rs}(0^+,\lambda)$ is written as (Dall'Olmo and Gitelson, 2005):

$$R_{rs}(0^+,\lambda) \propto \frac{f}{Q}\,\frac{b_b(\lambda)}{a(\lambda)+b_b(\lambda)}$$ Equation 3

The bio-optical modeling technique requires the inclusion of total absorption, scattering, and backscatter coefficients. In the radiative transfer model for case II waters, total absorption and backscattering coefficients for three optically active constituents of natural water bodies and pure water are included:

$$a(\lambda) = a_w(\lambda) + a_{ph}(\lambda) + a_{ISM} + a_{CDOM}(\lambda)$$ Equation 4

$$b_b(\lambda) = b_{b,w}(\lambda) + b_{b,ph}(\lambda) + b_{b,ISM}(\lambda) + b_{b,CDOM}(\lambda)$$ Equation 5

Where:

$a_w(\lambda)$, $b_{b,w}(\lambda)$	=	absorption and backscatter coefficients for pure water at wavelength (λ) (Buitevled *et al.*, 1994)
$a_{ph}(\lambda)$, $b_{b,ph}(\lambda)$	=	absorption and backscatter coefficients for phytoplankton at wavelength (λ)
$a_{ISM}(\lambda)$, $b_{b,ISM}(\lambda)$	=	absorption and backscatter coefficients for inorganic suspended matter at wavelength (λ)
$a_{CDOM}(\lambda)$, $b_{b,CDOM}(\lambda)$	=	absorption and backscattering coefficient for colored dissolved organic matter at wavelength (λ)

According to Beer's Law, it is assumed that absorption and scattering properties of a water body are a linear function of the concentration of its constituents (Jensen, 2005). The absorption coefficient for the optically active constituent of interest divided by the specific absorption coefficient, $a_i^*(\lambda)$, absorption per unit path length and mass concentration, can yield pigment concentration (Gons, 1999):

$$[\text{Pigment}_i] = a_i(\lambda) / a_i^*(\lambda) \qquad \text{Equation 6}$$

Where:

$a_i(\lambda)$ = absorption coefficient for the constituent of interest (i) at wavelength (λ) (Buitevled *et al.*, 1994)

$a_i^*(\lambda)$ = specific absorption coefficient for the constituent of interest (i) at wavelength (λ)

Bio-optical modeling for case II waters has proven difficult because the optical properties of the water body are not solely dependent on phytoplankton and its byproducts, but also on chromophoric dissolved organic matter (CDOM), the portion of dissolved organic matter (humic and fluvic acids) that are colored, and inorganic suspended matter (ISM), mostly comprised of sands, silts and clays. The spectral characteristics of CDOM and ISM are highly variable due to differences in particle shape, size, and composition (Morel, 2001). Likewise, researchers exploring the optical characteristics of cyanobacteria have discovered that the specific absorption coefficient is highly variable both inter- and intra-species, dependent on the cell physiology and morphology and the photoadaptive response of cells to change in the environmental conditions (Morel, 2001). Semi-empirical models, which include both the properties of phytoplankton and also organic and inorganic suspended matter, sometimes referred to as bio-geo-optical models, have proven successful (Morel, 2001).

Color Ratio and Band Combination Algorithms

Simple color ratio algorithms, also called reflectance quotients, first developed on oligotrophic systems (Morel and Prieur, 1977; Gordon and Morel, 1983) were modified to predict chlorophyll *a* concentration in case II, productive systems. Color ratios utilize the relationship between remote sensing reflectance (*R*) and the ratio of backscattering from the surface of an algal cell to its pigment absorption efficiency (Morel and Prieur, 1977; Gitelson *et al.*, 1999):

$$R = r\frac{b_b(\lambda)}{a(\lambda)} \qquad \text{Equation 7}$$

Where:

r	=	a constant usually between 0.12 and 0.55 in inland turbid waters (Dekker, 1993)
$b_b(\lambda)$	=	backscattering coefficient
$a(\lambda)$	=	absorption coefficient

Increased algal density will cause an increase in both the absorption and scattering coefficients seen in the spectra. Reflectance features for algorithm development are therefore chosen based on the properties of the photosynthetic pigment of interest. Chlorophyll *a* absorbs most energy in the blue and red portion of the spectrum and is less efficient at absorbing energy in the green portion of the spectrum. Proposed chlorophyll *a* ratios therefore utilize the chlorophyll *a* absorption band in the red region (at approximately 670 nm) and the chlorophyll *a* fluorescence band in the NIR region (at approximately 700 nm), resulting in what is known as the NIR:red ratio. The sensitivity of the features found at 700 and 670 nm to change in chlorophyll *a* concentration demonstrates that variability along a continuum of pigment density could be used to derive an algorithm for predicting chlorophyll *a* pigment concentration from spectra (Gitelson *et al.*, 1986; Mittenzwey and Gitelson, 1988; Mittenzwey *et al.*, 1992; Gitelson *et al*., 1993; Dekker, 1993). Slight variations on the NIR:red algorithm have been

proposed, including R(705)/R(670) (Mittenzwey *et al.*, 1991) and R(706)/R(676) (Dekker, 1993), due to the change in peak position depending on water composition, specifically pigment, seston, and organic matter concentrations. Strong relationships (r^2=0.87-0.92) between the NIR:red reflectance ratio and chlorophyll *a* concentration were reported by Gitelson *et al.* (1986), Mittenzwey and Gitelson (1988), and Gitelson *et al.* (1993) with a low standard error of chlorophyll estimation, 13.5-19.5 ppb. The reflectance peak found in the green portion of the visible spectrum, within the range 550 to 570 nm, is attributed to scattering by algal cells (Dekker *et al.*, 1991; Gitelson, 1992; Jensen, 2005). Other variations on the simple NIR:red reflectance ratio include the addition of the green peak, the reflectance feature at 550 nm and the global maximum for the spectral range sensitive to phytoplankton pigment concentration (Table 2). Also included in one of the four-band algorithms is the reflectance peak at approximately 750 nm; features beyond 750 nm are dependent on the presence of organic and inorganic matter but insensitive to phytoplankton pigments (Gitelson *et al.*, 2000; Table 2). Mittenzwey *et al.* (1991) reported higher r^2 values for the three and four-band algorithms compared to the two-band NIR:red ratio, suggesting algorithm accuracy increases with the inclusion of the green peak.

Table 2: Color-ratio and band-combination algorithms presented by Gitelson *et al.* (1986), Mittenzwey *et al*. (1991), Dekker (1993), and Schalles and Yacobi (2000).

Chlorophyll *a* Band Combinations	**Phycocyanin Band Combinations**
$[R(700)]\times[R(670)^{-1}]$*	$0.5[R(600)+R(648)]-R(624)$ ‡
$[R(705)-R(670)]\times[R(550)^{-1}]$ †	$[R(650)][R(625)^{-1}]$ •
$[R(705)-R(670)]\times[R(550)^{-1}-R(670)^{-1}]$ †	
$[R(705)-R(670)]\times[R(550)^{-1}-R(760)^{-1}]$ †	

*Gitelson *et al.* (1986)
†Mittenzwey *et al*. (1991)
‡Dekker (1993)
•Schalles and Yacobi (2000)

Chlorophyll *a* is found in all algal species, thus it is the chosen pigment for measuring the productivity of a water body using remote sensing. The spectral response of algae is dependent on several factors including cell morphology and physiology (Gitelson *et al.*, 1999). The same technique used to determine chlorophyll *a* concentration can therefore be applied to identify accessory algal pigments and, ultimately, the concentration of specific algal groups such as cyanobacteria. Dekker *et al.* (1991), Gons (1999), and Jupp *et al.* (1994) identified the absorption trough found at 620 nm as the most prominent spectral feature specific to cyanophyte density. Dekker (1993) devised an algorithm which exploits the 620 nm phycocyanin absorption feature for determination of phycocyanin concentration in shallow, eutrophic lakes using the following empirical relationship:

$$[PC] = 0.5(R(0^-)_{600} + R(0^-)_{648})\text{-}R(0^-)_{624} \qquad \text{Equation 8}$$

Where:

[PC] = concentration of phycocyanin
$R(0^-)_\lambda$ = subsurface reflectance at a specified wavelength

The algorithm was based on four identified responses within the reflectance spectra with increasing phycocyanin concentration:

(i) a decrease in the reflectance at 620 nm, resulting from absorption by phycobilins, photosynthetic pigments efficient at absorbing yellow/red light (Dekker, 1993; Gitelson *et al.*, 1995),

(ii) a shift in the green peak toward shorter wavelengths (540 nm), caused by absorption of the longer wavelengths by phycobilins (Schalles *et al.*, 1998; Gitelson *et al.*, unpublished),

(iii) an increase in the minor reflectance peak at approximately 648 nm, the fluorescence emission maximum of phycocyanin (Dekker, 1993; Gitelson, 1992) , and

(iv) a decrease in reflectance at approximately 440 nm attributed to the lack of accessory chlorophyll pigments in cyanophytes (Gitelson *et al.*, 1999).

Application of the Dekker (1993) phycocyanin algorithm, however, has been reported as having low predictive power, with an r^2 of 0.384 (Schalles and Yacobi, 2000). Schalles and Yacobi (2000) further investigated the absorption feature at 620 nm, caused by the presence of phycocyanin, since it frequently occurred in spectral response obtained from Carter Lake, a turbid, eutrophic lake located on the Iowa-Nebraska border. Schalles and Yacobi (2000) applied the ratio $R(650)/R(625)$ to determine phycocyanin concentration (Table 2). Regression of groundtruth phycocyanin concentration against estimates resulting from application of the Schalles and Yacobi (2000) ratio index to reflectance values resulted in an r^2 value of 0.61. Schalles *et al.* (1998) noted the dynamic nature of the green peak as a function of phycocyanin concentration change: peak height decreased and shifted towards shorter wavelength (540 and 550 nm) at times of high phycocyanin concentration and shifted toward longer wavelengths (560 to 570 nm), likely due to the presence of diatoms, at times of low phycocyanin concentration.

Near-Infrared Peak Algorithms

Gitelson *et al.* (1993, 1994) and Yacobi *et al.* (1995) used factor analysis and statistical modeling to devise an additional index for determination of chlorophyll *a* concentration in highly productive, case II waters with differing dominant phytoplankton species. Further study of the nature of the NIR peak (Gitelson *et al.*, 1993) encouraged the creation of two new chlorophyll *a* algorithms, the Reflectance Height (RH) and SUM algorithms (Gitelson *et al.*, 1993):

$RH_{670\text{-}750}$ Equation 9

$SUM_{670\text{-}750}$ Equation 10

These algorithms were based on four identified responses of the NIR peak with increasing chlorophyll *a* concentration (Gitelson *et al*., 1993):

(i) Increase in peak magnitude,
(ii) Increase in peak height measured from a baseline (670 to 750 nm),
(iii) Increase in peak area measured above a baseline (670 to 750 nm), and
(iv) Shift in peak position toward longer wavelengths.

To quantify peak height and sum, the NIR peak was normalized to a baseline from approximately 670 to 750 nm (drawn from the left to right edge of the NIR peak). Several baseline lengths have been suggested, all beginning at 670 nm, however ending at varying locations including 850 nm (Schalles *et al.*, 1998), 750 nm (Gitelson *et al.*, 2000), and 730 nm (Gitelson, 1992). The reason for normalization of the NIR peak to a baseline is simply that the slope is said to be unaffected by phytoplankton concentration and instead by scattering caused by other water constituents.

The regression of the reflectance height index values and chlorophyll *a* concentration from data collected at Lake Kinneret, Haifa Bay, and the hypereutrophic fish ponds produced coefficients of determination ranging from 0.83 to 0.96 (Gitelson *et al.*, 2000). Schalles *et al.* (1998) tested the extendibility of the RH and SUM algorithms with a baseline from 670 to 850 nm to estimate chlorophyll *a* concentration over a year period at Carter Lake, a turbid, eutrophic lake located on the Iowa-Nebraska border, and retrieved r^2 values of 0.83 and 0.91, respectively between analytically measured chlorophyll *a* concentration and the regression equation obtained from the model development dataset. Schalles *et al.* (1998) used 13 sample sites as a validation set and retrieved a standard error of less than 28 ppb. Schalles *et al.* (1998) reported high positive correlations between chlorophyll *a* concentration, turbidity, and the presence of organic seston.

For systems with differing trophic states, the following variations on the reflectance height algorithm are proposed (Gitelson, 1992):

$R_{(maxred)}/R(560)$ Equation 11

$R_{(maxred)}/R(675)$ Equation 12

Where:

$R_{(maxred)}$ = is reflectance height (different notation for RH),
R(560) = is the global maximum in the spectra, and
R(675) = is the chlorophyll *a* absorption maximum

Reflectance at 560 nm, the global maximum, is said to be efficient for removing errors in chlorophyll *a* prediction caused by waters with differing levels of productivity. Because the presence of suspended matter affects the reflectance signal at 675 nm and at the R_{maxred} equally, normalization of reflectance height by R(675) can reduce error introduced by increased suspended matter concentrations (Gitelson, 1992).

Recent research performed by Dall'Olmo and Gitelson (2005) suggests movement away from the use of the reflectance height and sum algorithms because of an inability to account for backscattering between samples. Application of the reflectance height algorithm to two turbid, Nebraska water bodies resulted in a low r^2 of 0.57 and root mean square error of 28.5 ppb.

Optimized Color Ratio Algorithms

Simis *et al.* (2005) encouraged movement from the empirical to semi-empirical technique for estimating phycocyanin pigment concentration. Simis *et al.* (2005) increased the predictive power of the simple ratio R(709)/R(620) for phycocyanin by incorporating measured specific absorption coefficients of phycocyanin, $a_{PC}^*(620)$, pure water coefficients at specified wavelengths $a_w(\lambda)$ (Buiteveld *et al.*, 1994), and backscatter

coefficients (b_b) retrieved from 778 nm to obtain the absorption coefficients of phytoplankton pigments. Spectral response was collected using a medium resolution imaging spectroradiometer, conforming to the spectral resolution of Medium Resolution Imaging Spectrometer (MERIS) to create an optical model for determining both chlorophyll *a* (Chla) and phycocyanin (PC) pigment presence in turbid inland water. Reflectance spectra from two hypereutrophic lakes in the Netherlands were taken using an instrument with a spectral range of 380 to 780 nm (4 nm spectral resolution). The following simple band reflectance ratios were reintroduced:

Chlorophyll *a*: R(709)/R(665) Equation 13

Phycocyanin: R(709)/R(620) Equation 14

Reflectance ratios were then optimized by the introduction of absorption properties, the backscattering coefficient, and a correction factor for the difference between observed and measured concentrations. Backscattering (b_b) was determined following Gons (1999) by the use of a 15 nm wide band at 778 nm.

The following algorithms for chlorophyll *a* and phycocyanin estimation were introduced:

Chlorophyll *a*: $a_{chl}(665) = (\{[R(709)/R(665)] \times [a_w(709) + b_b]\} - b_b - a_w(665)) \times \gamma'$ Equation 15

Phycocyanin: $a_{pc}(620) = (\{[R(709)/R(620)] \times [a_w(709) + b_b]\} - b_b - a_w(620)) \times \delta^{-1} - [\varepsilon \times a_{chl}(665)]$ Equation 16

Where: Simis *et al.* (2005)

$a_{chl}(665)$ = absorption of chlorophyll *a* at 665 nm

$R(\lambda)$ = reflectance value at a specified wavelength

$a_w(\lambda)$ = pure water absorption coefficients at specified locations
$a_w(709) = 0.70\ m^{-1}$ (Buitevled *et al*., 1994)
$a_w(665) = 0.40\ m^{-1}$ (Pope and Fry, 1997)
$a_w(620) = 0.30\ m^{-1}$ (Buitevled *et al*., 1994)

b_b backscattering coefficient obtained from
$b_b = [a_w(778)R(778)] \times [(f - R(778)^{-1}]$ (Gons, 1999)
$a_w(778) = 2.71\ m^{-1}$ (Buitevled *et al.*, 1994)
f = 0.275, estimate based on average cosine of downward irradiance (Gons, 1999; Krijgsman, 1994)

γ' = 0.082, a constant derived from the linear least-squares fit of measured to estimated chlorophyll *a* absorption

$a_{PC}(620)$ = absorption of phycocyanin at 620 nm

δ^{-1} = correction factor derived from the linear least-squares fit of measured versus estimated phycocyanin absorption

ε = 0.24; correction factor to define absorption of chlorophyll *a* at 620 nm relative to 665 nm, derived from Lake Loosdrecht data (Simis *et al.*, 2005)

Concentration of chlorophyll *a* and phycocyanin can then be determined from:

$[Chla] = a_{chl}(665)/a^*_{chl}(665)$ Equation 17

$[PC] = a_{PC}(620)/a^*_{PC}(620)$ Equation 18

Where:

$a_{chl}(665)$ = absorption by chlorophyll *a* pigments at 665 nm

$a^*_{chl}(665)$ = 0.0153 mg Chl/m^2, average pigment specific absorption value for chlorophyll *a* at 665 nm obtained for Lake Loosdrecht (Simis *et al.*, 2005)

$a_{PC}(620)$ = absorption by phycocyanin pigments at 620 nm

$a^*_{PC}(620)$ = 0.0095 mg Chl/m^2, average pigment specific absorption value for phycocyanin at 620 nm obtained for Lake Loosdrecht (Simis *et al.*, 2005)

Application of the Simis *et al.* (2005) PC algorithm including sampling site specific values for ε and specific absorption coefficients (calculated from absorption measurements)

resulted in a 20% error in estimated PC concentrations, with an r^2 value of 0.94 (n=34). Simis *et al.* (2005) measured the predictive power of applying a fixed phycocyanin specific absorption coefficient, taken as the average of all $a_{PC}^*(620)$ measured from Lake Loosdrecht from March through November, for retrieval of phycocyanin concentration from the Lake IJsselmeer September cruise. The "fixed" PC algorithm resulted in an r^2 value of 0.77 (n=12). Simis *et al.* (2005) reported low predictive power of the fixed algorithm on Lake IJsselmeer for phycocyanin for cruises when the phycocyanin-to-chlorophyll *a* ratio was low. The algorithm was effective, however, for inland lakes dominated by cyanobacteria. Since other pigments can contribute to the signal at 620 nm, it is suggested that the Simis *et al.* (2005) algorithm has reduced predictive power in non-cyanobacterial dominated water. For systems dominated by green algae, overestimation of phycocyanin concentration is suggested as a source of error without use of the correction factor for chlorophyll *a* absorption at 620. Simis *et al.* (2005) also reported high variability among phycocyanin specific absorption coefficients $a^*_{PC}(620)$, mostly due to varying cell morphology and differing phytoplankton composition.

Summary of the Systems on which the Previously Developed Algorithms have been Tested and Validated

The previously developed algorithms (Table 1) were chosen for evaluation in the current study because they were developed on case II waters (inland water where chemistry is complex due to high concentrations of suspended material, dissolved organic matter, and yellow substances; Table 3) with characteristics similar to the Indianapolis reservoirs.

The robustness of the Gitelson *et al.* (1993) Reflectance Height and Sum algorithms have been evaluated internationally on lakes and reservoirs spanning a wide range of

trophic states. The results of the Reflectance Height algorithm regressed against measured chlorophyll *a* concentration in international tests produced a range of determination coefficients from 0.83 to 0.96. Though these algorithms seem robust, the heterogeneous nature of the Indianapolis reservoirs and tendency to stratify will likely require optimization of the Gitelson *et al.* (1993) algorithms.

The extendibility of the Schalles and Yacobi (2000) algorithm, tested on Lake Carter in Nebraska, and the Simis *et al*. (2005) algorithm, tested on two lakes in the Netherlands, has not been evaluated elsewhere (Table 3). Although these performed well for the reservoirs on which they were created, they have not been validated on systems in different locations with dissimilar water quality characteristics. Because concentrations of optically active water constituents in the Indianapolis reservoirs do not necessarily vary together, inclusion of the spectral response patterns of other constituents will be required to accurately predict pigment concentration.

Table 3: Summary of the systems on which the previously developed algorithms (Table 1) were created and validated (Gitelson *et al.,* 2000 [1]; Simis *et al*., 2005 [2]; Mittenzwey *et al*., 1991 [3], Schalles and Yacobi, 2000 [4].

Site	Period	Chla (mg/m^3)	Dominant Phytoplankton	Trophic Status	Algorithm Tested/Validated
Lake Kinneret, Israel* [1]	winter-spring	2.4 – 330	*Peridinium gatunense*	Eutrophic	NIR:red
Lake Kinneret, Israel* [1]	summer-fall	3.8 – 26	Chlorophytes	Eutrophic	RH, SUM
Iowa Lakes, US† [1]	summer-fall	2.0 – 55	Diatoms	Mesotrophic	RH, SUM
Carter Lake, US† [1], [4]	year round	20 – 280	*Anabaena sp.*	Eutrophic	NIR:red, RH, SUM R_{650}/R_{625},
Fish Ponds, Israel† [1]	winter-spring	2.1 – 674	*Microcystis aeruginosa*	Eutrophic	RH, SUM, NIR:red
Wastewater ponds, Israel† [1]	spring-summer	69 – 2700	Chlorophytes	Hypereutrophic	NIR:red, RH, SUM,
Haifa Bay, Israel† [1]	spring-summer	1 – 70	Dinoflagellates, diatoms	Oligotrophic	NIR:red, RH, SUM
Lake Loosdrecht, Netherlands* [2]	spring-fall	66 (average)	*Limnothrix/Pseudanabaena*	Eutrophic	Simis *et al.* (2005) Semi-empirical
Lake Ijsselmeer, Netherlands* [2]	spring-fall	200 (maximum)	*Microcystis sp./ Aphanizomenon*	Eutrophic	Simis *et al.* (2005) Semi-empirical
Spree, Dahme, and Seddin-See, Dämeritzsee, Müggelsee waterways and shallow lakes, Berlin* [3]	2 year	5 – 350	Unknown	Mesotrophic-Eutrophic	NIR:red

* Reservoir on which previously developed algorithms were created

† System on which the previously developed algorithms have been validated

STUDY SITE DESCRIPTION

Geist and Morse Reservoirs are part of the main flood, drinking, and recreational water system for the City of Indianapolis. Using the Indiana Trophic State Index, an estimate of lake condition based on the concept that change in nutrient influx causes change in phytoplankton biomass, and ultimately lake clarity, these reservoirs are categorized as mesotrophic to eutrophic (Table 4; Tedesco *et al*., 2003). High concentrations of phosphorus and chlorophyll *a* and low transparency in the reservoirs suggest a eutrophic state. These waters are referred to as case II. Trophic status of the reservoirs is directly related to surrounding land use which is comprised primary of agricultural and residential development (Tedesco *et al*., 2003).

Table 4: Description of Geist and Morse Reservoirs and their corresponding watersheds, Fall Creek and Cicero Creek.

Reservoir	Geist	Morse	Units
Original Purpose	Water Supply	Water Supply	
Date of Service	1943	1956	
Surface Area	2.9	2.3	mi^2
	7.5	6.0	km^2
Reservoir Volume	6,300	7,400	million gallons
	23.8	28.0	million m^3
Maximum Depth	48	42	Ft
	14.7	12.9	m
Mean Depth	3.2 m	4.7	m
	3.2	4.7	m
Residence Time	55	70	Days
Watershed Area	215	227	mi^2
above Dam	560	590	km^2
Trophic Status	Mesotrophic*	Eutrophic*	
Mean Total P	100†	94†	µg P/L
Mean Total N	2.0†	4.1†	mg N/L
% Agriculture in Watershed	58.3%‡	76.9%‡	
Trunk Stream (median flow)	Fall Creek (2.6) (91.8)	Cicero Creek (1.0) (35.3)	m^3/s cfs
Other Inflow Streams	Thorpe Creek, Bee Camp, and Dry Branch	Little Cicero Creek, Bear Slide Creek, and Hinkle Creek	
Dominant Phytoplankton	*Aulacoseira, Scenedesmus/ Ankistrodesmus, Aphanizomenon/Anabaena*	*Aulacoseira, Scenedesmus/ Ankistrodesmus, Aphanizomenon/Anabaena*	

* (IDEM 2002, 2004, and 2006)
† Various CIWRP studies, including this study, from 2003 – 2005
‡ Eagle Creek Land cover assessments (Tedesco *et al*., 2005) and 2000 land use/land cover assessments for Fall Creek and Cicero Creek Watersheds (Tedesco *et al.*, 2003)

Geist Reservoir was constructed in 1943 to regulate the flow of Fall Creek, a water source for the Indianapolis drinking water supply. Geist Reservoir, located on the border between Marion and Hamilton counties (-85º56'29.5749"W, 39º55'32.1001"N), is a small, shallow (mean depth 3.2 m) reservoir, covering 7.5 km^2 (USGS, 2003). Estimated reservoir volume is 23,810,000 m^3 (Wilson *et al.*, 1996). Four streams contribute the

majority of flow into the reservoir, with Fall Creek contributing the largest flow volume (Tedesco *et al.*, 2003). Fall Creek drains the Fall Creek Watershed, a 560 km^2 area. USGS Stream Gage data from Fall Creek (1941-2003) show a median daily instantaneous flow into Geist Reservoir of 2.6 m^3/s. Residence time based on the USGS stream gage data from Fall Creek (1941-2003) is estimated at 55 days. The Fall Creek Watershed is comprised mainly of agricultural land, 58.3% in 2000 (Tedesco et al., 2003). Based on research conducted by the Central Indiana Water Resources Partnership (CIWRP), bi-weekly monitoring of Geist Reservoir during the growing season from 2003-2005 showed a mean total phosphorus concentration of 100 µg/L (Table 4).

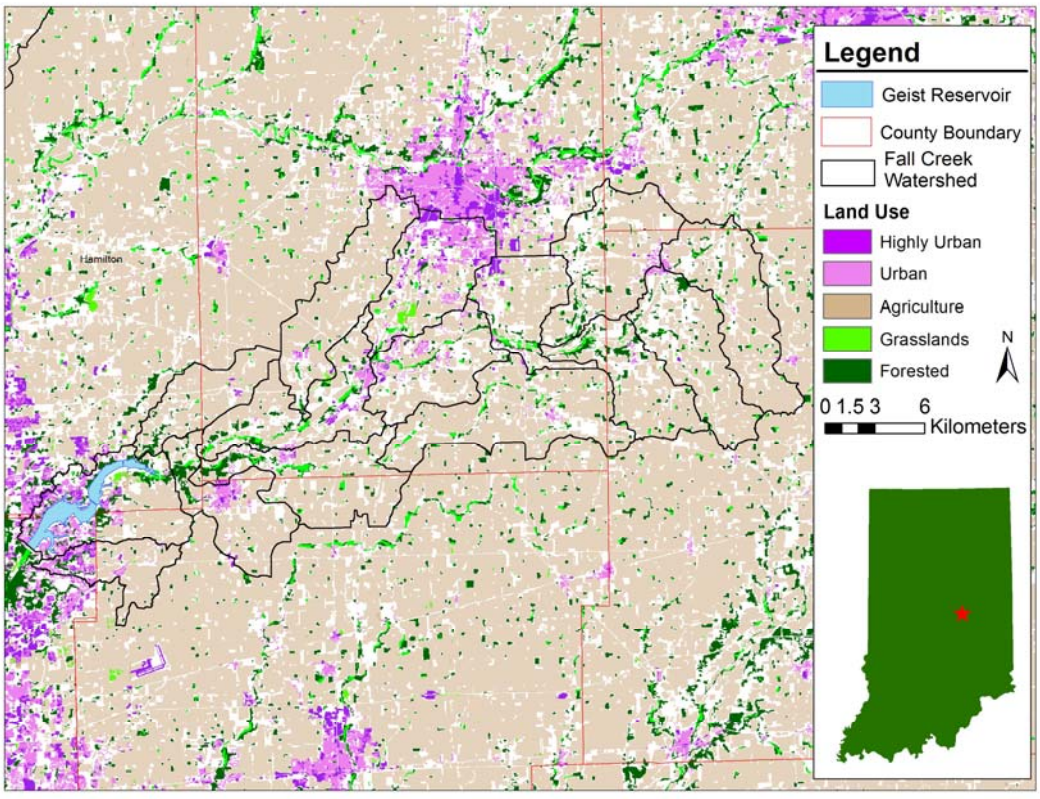

Figure 2: Geist Reservoir and Fall Creek watershed land use/land cover (Tedesco *et al.,* 2003).

Morse Reservoir was constructed in 1956 in the center of Hamilton County (-86º2'17.2291"W, 40º6'16.84512"N) to regulate flow to Cicero Creek and the White River, a drinking water resource for the City of Indianapolis. Morse is classified as a small, shallow (mean depth of 4.7 m) reservoir, covering 6 km^2 (USGS, 2003). Estimated reservoir volume is 28,012,000 m^3 (USGS, 2003). Cicero Creek drains the Cicero Creek Watershed, a 590 km^2 area (Figure 3). Four streams contribute the majority of flow into Morse with Cicero Creek contributing the highest flow volume to the reservoir (Tedesco *et al.*, 2003). According to USGS Stream Gage data from Cicero Creek (2004-2006), estimated median daily instantaneous flow into Morse Reservoir is 1.0 m^3/s. Residence time based on the USGS stream gage data from Cicero Creek (2004-2006) is estimated at 70 days. Long water residence time in Morse and a high percentage of agricultural land use in Cicero Creek Watershed, 76.9% in 2000, contribute high phosphorus loading into Morse Reservoir (Tedesco *et al.*, 2003; Figure 3). The mean total phosphorus concentration for Morse Reservoir during the growing season, sampled bi-weekly during various CIWRP studies from 2003-2005, was 94 µg P/L (Table 4).

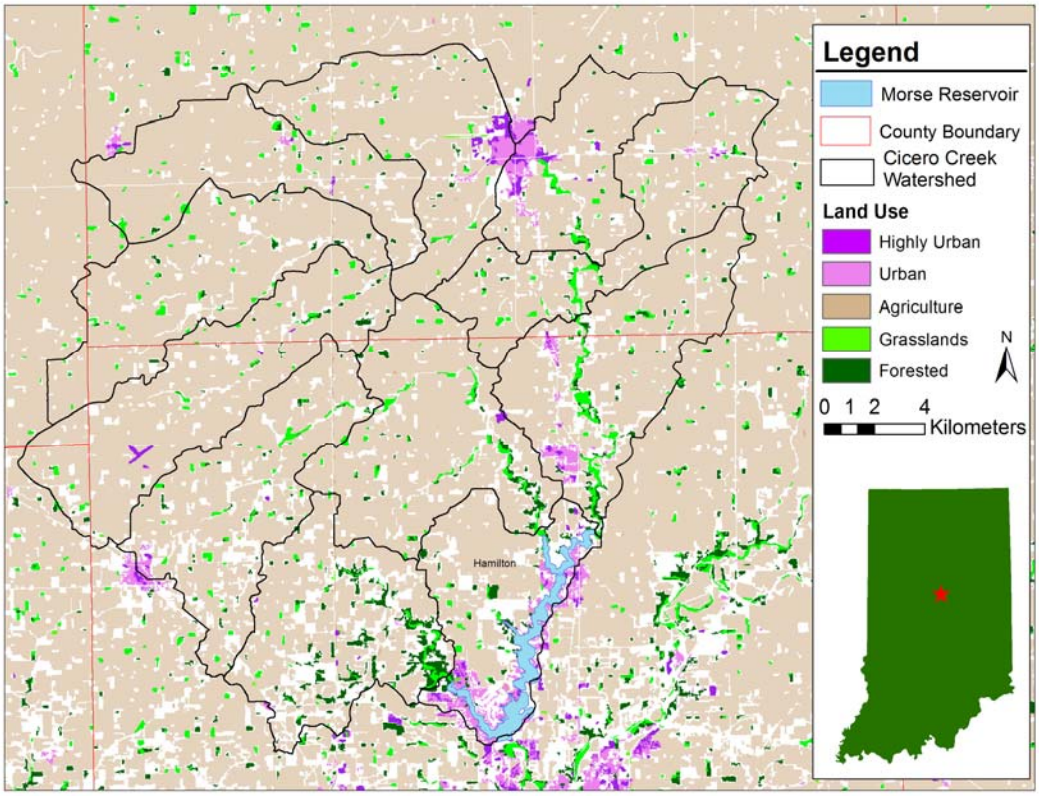

Figure 3: Morse Reservoir and Cicero Creek watershed land use/land cover (Tedesco *et al.*, 2003).

METHODOLOGY

General Study Design

On September 6 and 7, 2005, field spectral measurements and ground truth data were collected at 55 sampling sites on two Indianapolis reservoirs: Morse (28 sites) and Geist (27 sites) (Figure 4). Duplicate samples were collected at three of the sites for each reservoir. Reflectance measurements were collected using ASD FieldSpec UV-VNIR high resolution spectroradiometers. Hyperspectral imagery was acquired using the AISA sensor, Airborne Imaging Spectrometer for Applications, concurrent with field spectra and groundtruth sample collection. CALMIT, the Center for Advanced Land Management Information Technologies, stationed at University of Nebraska-Lincoln, collected the airborne imagery for the reservoirs[1]. Sampling was coordinated according to optimal airborne imagery acquisition time and required the use of two boats, two field spectroradiometers, and 15 participants. This study was designed to determine the relationship between ground spectral response and *in-vitro* phytoplankton pigment concentrations and blue-green algal biomass and biovolume.

[1]Assessment of airborne hyperspectral imagery for mapping phytoplankton pigments is a companion study that will use field spectral measurements to calibrate the airborne sensor.

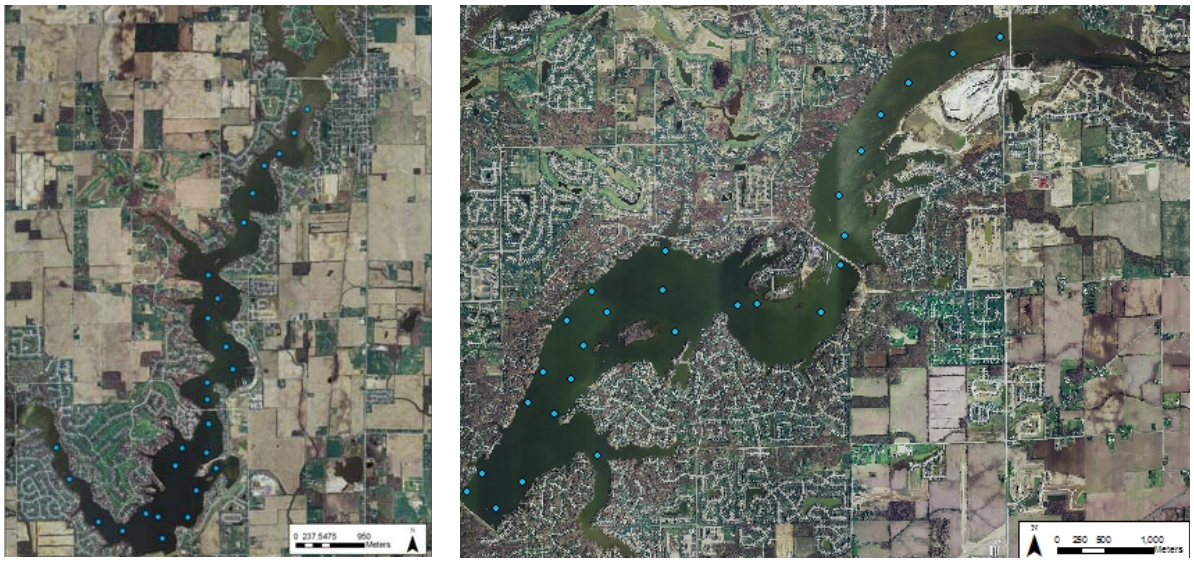

Figure 4a and b: Geo-referenced sampling sites on Morse (a) and Geist (b) Reservoirs (March 2005, IGIC).

Field Methodology

The following physical parameters were measured at the 55 sampling sites on Geist and Morse reservoirs using YSI multi-parameter probes (model 600XLM-SV) positioned 25 cm below the water surface: temperature (ºC), specific conductance (mS), total dissolved solids (g/L), salinity (ppt), DO (% and mg/L), and pH. Secchi Depth (cm) was collected at each site using a Secchi disk to estimate water transparency. A Trimble Pro-XRS (Trimble Navigation, Inc.) global positioning system receiver was used to determine the coordinates for each sample site. The accuracy of each position is ≤10 m.

Radiance measurements, recorded in a continuous spectrum in 708 bands within a spectral range from 348 to 1074 nm, were collected at each of the sampling sites using two ASD FieldSpec UV-VNIR (Analytical Devices, Inc., Boulder, CO) spectroradiometers. Radiance recorded within the spectral range of 400-900 nm were used in this analysis. The fiber optic cable was attached to an extendable pole pointed

in a nadir viewing angle and was set at a height of approximately 0.5 m above the water surface. The instantaneous-field-of-view (IFOV) of the bare fiber optic cable was 0.17 rad, producing a diameter of 0.04 m on the water surface. Downwelling irradiance measurements were also collected at each sample site using a white reference panel as an optical standard for calibrating upwelling irradiance. To reduce the amount of noise in the spectra, the radiance reflectance spectrum at each site was averaged over 15 readings.

Water Sample Analysis

Surface water grab samples (obtained approximately 0.3 m below the surface) were collected at each station and analyzed for chlorophyll *a*, phycocyanin, and other water quality constituents including total suspended solids (TSS), turbidity, total Kjehldahl nitrogen (TKN), total phosphorus, ortho-phosphorus, and loss-on-ignition carbon (LOI) at IUPUI laboratories. Other secondary physical and chemical analyses were performed by Veolia Water Indianapolis, LLC using Environmental Protection Agency and American Public Health Association standards (Appendix A).

Pigment Analysis

Samples to be analyzed for chlorophyll *a* and phycocyanin were collected in 1 L amber HDPE bottles and filtered and frozen within four hours to preserve pigments. For each sample, a replicate was also filtered. All steps in the chlorophyll *a* extraction process were performed under subdued light conditions.

Chlorophyll a

Samples to be analyzed for chlorophyll *a* were filtered in 150 to 200 mL aliquots through 47 mm, 0.45 micron pore size acetate filters using a filtration manifold. Filters were then placed into a 15 mL falcon tube then frozen for 20-30 days, until analysis. Prior to analysis, filters were dissolved in 10 mL of 90% buffered acetone and allowed to extract in the freezer (-3ºC) for at least 24 hours and no longer than 48 hours. Extracted chlorophyll *a* was analyzed using the Environmental Protection Agency Method 445.0 (1983). After a 1:5 or 1:10 dilution, pheophytin corrected chlorophyll *a* was measured fluormetrically using a TD-700 Flourometer (Turner Designs, Inc.) equipped with a Daylight White Lamp and Chlorophyll Optical Kit (340-500 nm excitation filter and emission filter > 665 nm) and calibrated with chlorophyll *a* from spinach standard (Sigma-Aldrich 10865).

Phycocyanin

Samples to be analyzed for phycocyanin were filtered in 200 mL aliquots through 47 mm, 0.7 micron pore size glass fiber filters using a filtration manifold and frozen within four hours to preserve pigments. For each sample, a replicate was also filtered. Filters were placed into a 10 mL falcon tube then frozen until analysis. Prior to analysis, filters were transferred to a 50 mL polycarbonate centrifuge tube and suspended in 15 mL of 50 mM phosphate buffer. Phycocyanin was determined by homogenization of cells using a tissue grinder as described in Sarada *et al.* (1999). Filters were broken up using a stainless steel spatula. The spatula was rinsed with 5 mL of 50 mM phosphate buffer with the rinse collected in the centrifuge tube. The filter and 20 mL of buffer were homogenized for 2 minutes using a Teflon coated pestle. Pestles were rinsed into the sample with an additional 5 mL of buffer with the rinse collected in the centrifuge tube. Samples (now with 25 mL of buffer) were centrifuged at 5ºC, 27,200 x g for 25 minutes

using a Beckman J2-21M centrifuge. Filters were homogenized again and the pestle was rinsed using 5 mL buffer. As before, rinse buffer was collected in the centrifuge tube. The sample was centrifuged again using the same settings. Supernatant was collected, diluted using a 1:5 or 1:10 dilution (Sarada *et al.*, 1999). Extracted samples were analyzed for Phycocyanin concentrations flourometrically using a TD-700 Flourometer (Turner Designs, Inc.) equipped with a Cool White Mercury Vapor Lamp and a Phycocyanin Optical Kit (630 nm excitation and 660 nm emission filters) and calibrated using C-phycocyanin from *Spirulina sp*. (Sigma-Aldrich P6161). All steps in the phycocyanin extraction process were performed under subdued light conditions. Sarada *et al.* (1999) reported 99% recovery of phycocyanin using this homogenization technique.

Pigment Extraction Error Analysis

Percent error was calculated between each sample and its replicate ($\frac{\bar{x}}{\sigma}$). Samples with error > 20% were not used in further data analysis.

Phytoplankton Identification and Enumeration

The identification and enumeration of phytoplankton for the samples was completed by research staff at the Center for Earth and Environmental Science (CEES) at IUPUI. A subset of 25 samples were randomly selected and poured into 50 mL centrifuge tubes and preserved with 0.5 mL of Lugol's solution. Samples were stored at 5ºC until concentrating and analyzing. Phytoplankton were identified to species and measured for biovolume. A minimum of 400 natural units were counted in each sample and each

measured for biovolume. Cell volumes were estimated by approximation to the nearest simple geometric solid (*i.e.,* sphere, ovoid, or rod) (Lund *et al.*, 1958).

Total Suspended Solids and Inorganic Suspended Solids

Samples to be analyzed for TSS were stored in a refrigerator maintained at 5ºC until filtration. Samples were filtered within 48 hours of sample collection. Samples were filtered in amounts of 150 – 200 mL through pre-ashed, pre-weighed 47 mm, 0.7 micron pore size glass fiber filters. Samples were dried at 60ºF then placed in a dessicator. Dried and cooled samples were weighed using a Top Loading Pinnacle Series Balance (Denver Instrument Co.). TSS in mg/L was calculated by subtracting the post-ashed from the pre-ashed (SM2540D).

Loss on Ignition (LOI) Organic Carbon

Samples used to determine TSS were weighed on a Micro-balance MX5 (Mettler-Toledo) then ashed for 75 minutes at 550ºC in porcelain crucibles. Inorganic suspended solids (mg/L) was calculated by subtracting the weight before ashing from the weight after ashing.

Other Physical and Chemical Analyses

Collected water samples were analyzed for nutrients and other water quality constituents. IUPUI laboratories analyzed for ortho-phosphate colormetrically using the ascorbic acid-Molybdate blue method (SM 4500) on a Konelab 20 Photometric Analyser. Total Kjehldahl Nitrogen (TKN) was analyzed by ESG Laboratories (Indianapolis, IN).

The following analytes were processed by Veolia Water Indianapolis, LLC Laboratories using the Environmental Protection Agency and American Public Health Association Standard Methods (APHA, 1998):

- alkalinity (mg/L as $CaCO_3$)
- total hardness (mg $CaCO_3$/L)
- dissolved organic carbon (mg C/L)
- total organic carbon (mg C/L)
- chloride (mg/L)
- sulfate (mg/L)
- total phosphorus (mg/L)
- NH_4-N (mg/L)
- nitrate (mg/L)
- nitrite (mg/L)
- total and dissolved silica (mg/L)
- calcium (mg/L)
- magnesium (mg/L)
- potassium (mg/L)
- sodium (mg/L)
- MIB/Geosmin
- Turbidity

Data Analysis

Spectral Analysis

The relationship between field spectral responses and analytically measured phytoplankton pigment concentrations, chlorophyll *a* and phycocyanin, was determined by the application and optimization of the previously developed algorithms (Table 1). The strength of the relationship between the empirical algorithm and analytically measured pigment concentrations were evaluated using least-squares regression analysis. Statistically obtained coefficients for empirical models are reservoir specific. Coefficients derived using regression analysis were applied to data stratified by reservoir, as is suggested by previous research (Bukata *et al.*, 1991; Gitelson, 1992; Gitelson *et al.*, 1993; Schalles *et al.*, 1998; Schalles and Yacobi, 2000). If a strong relationship proved to exist between index values obtained from the algorithm application and analytically measured phytoplankton pigment concentrations, then empirical models were also applied to a combined Morse and Geist Reservoir dataset. The semi-empirical model employed used the Simis *et al.* (2005) previously published specific absorption coefficients for derivation of pigment concentration. Algorithm

accuracy was reported using root-mean-square error (RMSE) of the estimated concentration.

Reflectance Band Combination and Color Ratio Algorithms

The Mittenzwey *et al*. (1991) ratio R(705)/R(670) as a predictive index to estimate chlorophyll *a* concentration was extended to the Indianapolis reservoirs by extracting the reflectance values at exactly 705 nm and 670 nm (Figure 5). Also, as an attempt to capture the fluorescence peak and absorbance trough reflectance values, the maximum reflectance value between 695 and 715 nm (Figure 5, Feature b) and the minimum reflectance value between and 665 and 685 nm (Figure 5, Feature a) were extracted and input into the NIR:red ratio as:

$[R_{max}\lambda_{(695\text{-}715)}][R_{min}\lambda_{(665\text{-}685)}]^{-1}$

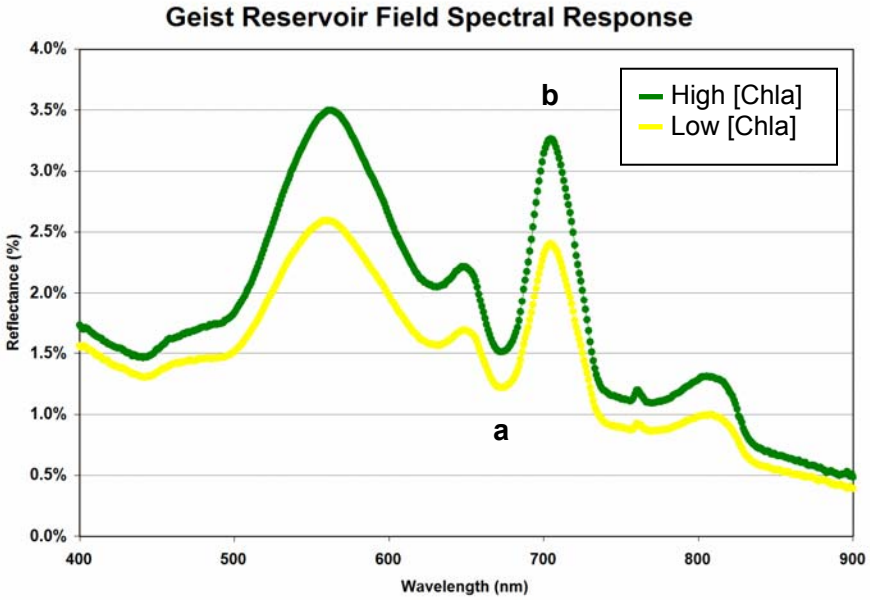

Figure 5: Sites with high (99 ppb) and low (32 ppb) concentrations of chlorophyll *a* at Geist Reservoir. The chlorophyll *a* absorption maximum (a) is located at approximately 670 nm and algal cell scattering maximum (b) at 705 nm.

The NIR:red reflectance ratio including the addition of the green peak, the reflectance feature at approximately 550 nm, was also applied to Indianapolis reservoir data to remove errors caused by varying levels in productivity. Similarly, to improve the effectiveness of the Reflectance Height algorithm in conditions of high suspended matter concentrations, the reflectance signal at 675 nm, a feature affected equally by suspended matter as the fluorescence peak at 700 nm, was applied (Table 5). Both techniques, including extraction of reflectance value at the location specified by the algorithm and the procedure of peak and trough reflectance value extraction were employed (Table 5).

Table 5: Color-ratio and band-combination algorithms presented by Gitelson *et al.* (1986) and Mittenzwey *et al*. (1991) for use in predicting chlorophyll *a* concentration and variations on the proposed algorithms for extracting absorption and scattering maximum values.

Band Combinations	**Variation on Simple color ratios**
$[R(700)]\times[R(670)^{-1}]$*	$[R_{max}\lambda_{(695\text{-}715)}][R_{min}\lambda_{(665\text{-}685)}{}^{-1}]$
$[R(705)-R(670)]\times[R(550)^{-1}]$†	$[R_{max}\lambda_{(695\text{-}715)}]\text{-}[R_{min}\lambda_{(665\text{-}685)}][\ R_{max}\lambda_{(540\text{-}570)}{}^{-1}]$
$[R(705)-R(670)]\times[R(550)^{-1}-R(670)^{-1}]$†	$\{[R_{max}\lambda_{(695\text{-}715)}]\text{-}[R_{min}\lambda_{(665\text{-}685)}]\}\{[\ R_{max}\lambda_{(540\text{-}570)}{}^{-1}]\text{-}[R_{min}\lambda_{(665\text{-}685)}{}^{-1}]\}$
$[R(705)-R(670)]\times[R(550)^{-1}-R(760)^{-1}]$†	$\{[R_{max}\lambda_{(695\text{-}715)}]\text{-}[R_{min}\lambda_{(665\text{-}685)}]\}\{[\ R_{max}\lambda_{(540\text{-}570)}{}^{-1}]\text{-}[R_{min}\lambda_{(665\text{-}685)}{}^{-1}]\}$

*Gitelson *et al.* (1986)
†Mittenzwey *et al*. (1991)

A similar empirical technique was used to determine the concentration of phycocyanin. Following Dekker (1993), an algorithm exploiting the absorption features (Figure 6, Feature a) and fluorescence (Figure 6, Feature b) of phycocyanin was employed:

PC = $0.5[R(600)+R(648)]-R(624)$ Equation 19

Reflectance values at 600 nm, 648 nm, and 624 nm were extracted from reflectance spectra collected at each sampling site. Likewise, application of the Schalles and

Yacobi (2000) ratio *R*(648)/*R*(620) to retrieve phycocyanin concentration required the extraction of reflectance 648 and 620 nm. Because of the dynamic nature of the reflectance and absorption peaks as a function of phycocyanin, chlorophyll *a*, seston and suspended sediment concentration, both of these algorithms were adjusted to be flexible to peak and trough shift. The variations on the simple color reflectance ratios were also applied to reflectance data (Table 6).

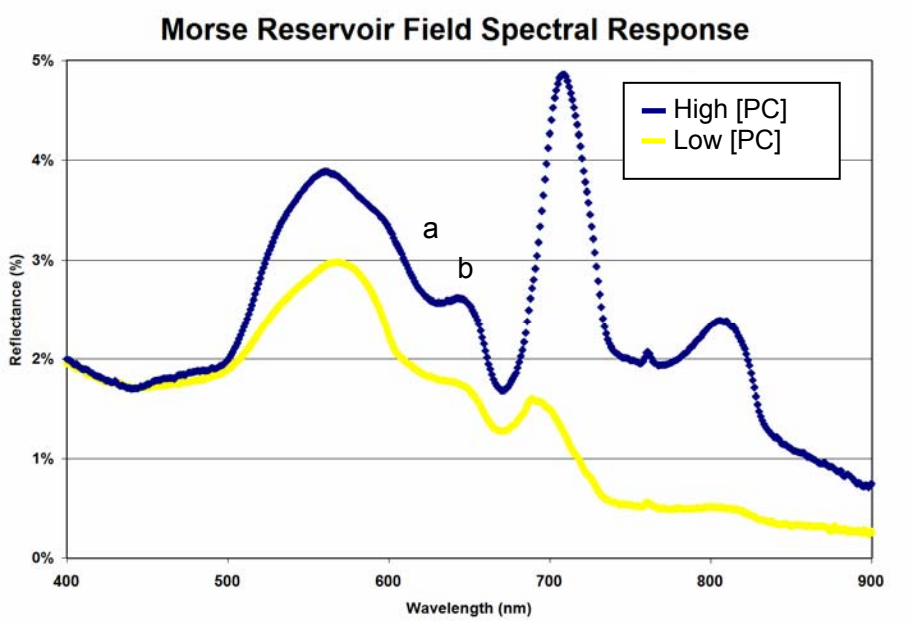

Figure 6: Sites with high (132 ppb) and low (2 ppb) concentrations of phycocyanin at Morse Reservoir. The phycocyanin absorption maximum (a) is located at approximately 620 nm and the phycocyanin fluorescence maximum (b) at 648 nm.

Table 6: Color-ratio and band-combination algorithms presented by Dekker (1993) and Schalles and Yacobi (2000) for use in predicting phycocyanin concentration and variations on the proposed algorithms (this study) for extracting absorption and scattering maximum values.

Phycocyanin Band Combinations	**Variation on Simple Color Ratios**
$0.5[R(600)+R(648)]-R(624)$ ‡	$0.5[R(600) + R(_{max}\lambda_{645\text{-}655}) - [R_{min}\lambda_{(665\text{-}685)}^{-1}]$
$[R(650)][R(625)^{-1}]$ •	$[R_{max}\lambda_{(640\text{-}660)}][R_{min}\lambda_{(615\text{-}635)}^{-1}]$

‡Dekker (1993)
•Schalles and Yacobi (2000)

Near-Infrared Peak Algorithms

Implementation of the reflectance height algorithm, $RH_{670\text{-}850}$, required normalization of the NIR peak to a baseline from 670 to 850 nm (Gitelson, 1992; Gitelson *et al.*, 1994; Yacobi *et al.*, 1995; Schalles *et al.*, 1998). The algorithm, originally developed on Lake Kinneret, was later modified to better fit Midwestern, inland lakes by adjusting the baseline from 670 to 750 nm (Gitelson *et al.*, 1994) to 670 to 730 nm (Gitelson *et al.*, 2000), due to a narrower NIR peak. The NIR peak in Indianapolis reservoir data was found within 670 and 730 nm. The algorithm was modified to reflect this difference and, therefore, maximum height of the NIR peak was determined from a baseline of 670 to 730 nm, thus $RH_{670\text{-}730}$ (Figure 7). Implementation of the second algorithm, $SUM_{670\text{-}730,}$ required the extraction and summation of all reflectance values under the NIR peak and above a baseline drawn from 670 and 730 nm (Figure 8).

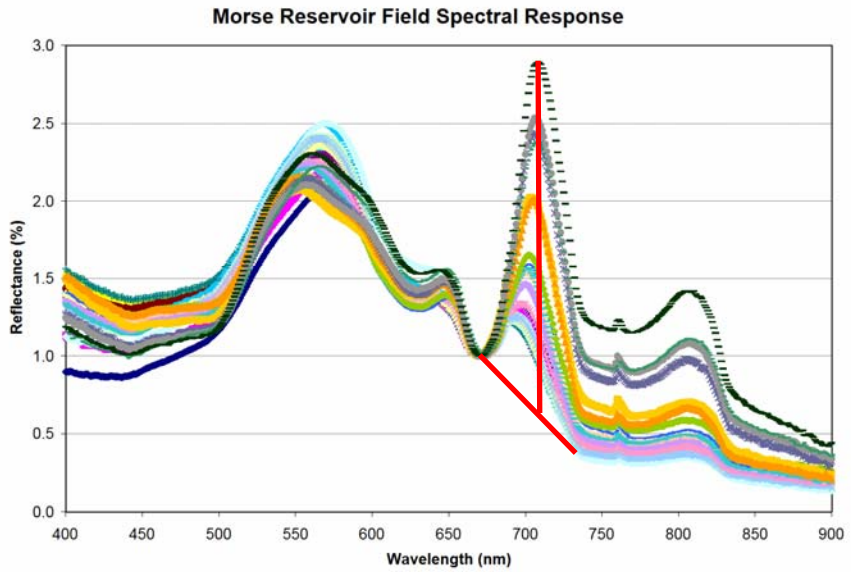

Figure 7: Reflectance Height (RH) of the NIR peak is determined from a baseline drawn from 670 to 730 nm.

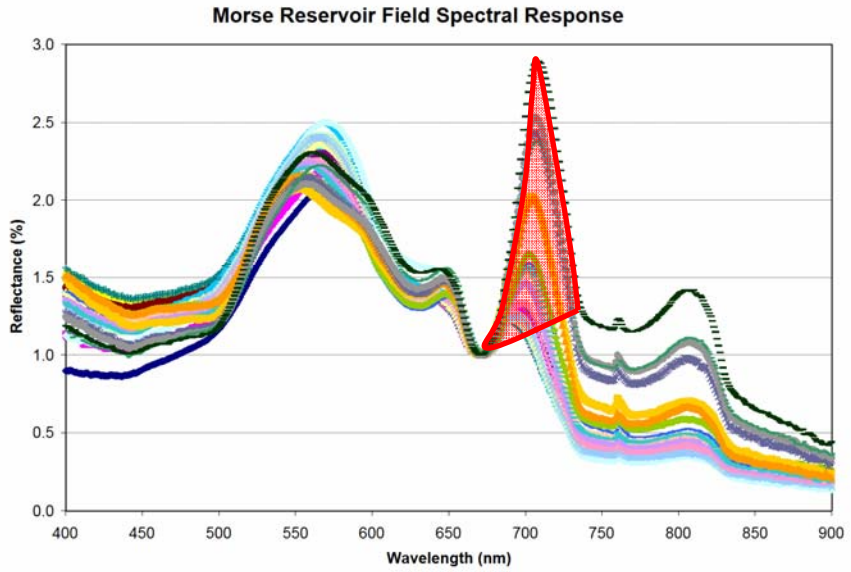

Figure 8: Reflectance Sum (SUM) of the NIR peak is the addition of all reflectance values (highlighted in red) above a baseline drawn from 670 to 730 nm.

Because the inclusion of reflectance at 560 nm, often the global maximum, is said to be efficient for removing errors in chlorophyll *a* prediction caused by waters with differing levels of productivity, the following variation on the Reflectance Height algorithm (denoted here as $R_{(maxred)}$) was employed (Gitelson, 1992):

$R_{(maxred)}/R(560)$ Equation 20

The reflectance signals at 675 nm and at R_{maxred} are affected equally by suspended matter concentrations, thus to improve the effectiveness of the reflectance height algorithm when suspended matter concentrations are high, the chlorophyll *a* absorption maximum is included, resulting in the following (Gitelson, 1992):

$R_{(maxred)}/R(675)$ Equation 21

To account for the dynamic nature of the reflectance features used in the Reflectance Height algorithms, change in position and magnitude as a function of water constituent composition, the following variations on the band combination algorithms were introduced to predict chlorophyll *a* concentrations:

$R_{(maxred)}/R_{max}\lambda_{(540\text{-}570)}$ Equation 22
$R_{(maxred)}/R_{min}\lambda_{(665\text{-}685)}$ Equation 23

Where:

$R_{(maxred)}$	=	The maximum reflectance value of the NIR peak above a baseline drawn from 670 and 730 nm
$R_{max}\lambda_{(540\text{-}570)}$	=	The maximum reflectance value within a wavelength range 540 to 570 nm
$R_{min}\lambda_{(665\text{-}685)}$	=	The minimum reflectance value within a wavelength range 665 to 685 nm

Regression equations relating the index values (*x*) to measured chlorophyll *a* and phycocyanin concentrations resulted in site specific coefficients *a* and *b* from the linear least squares regression analysis of the following form:

[*pigment*] = $a + bx$ Equation 24

Regression equations developed using the calibration datasets were then applied to validation datasets to obtain measured chlorophyll *a* concentration.

Semi-empirical Algorithms

The following Simis *et al.* (2005) algorithm, a further modification of the Mittenzwey *et al.* (1992) ratio R(709)/R(670), was implemented for determining the chlorophyll *a* absorption coefficient at 665 nm, $a_{chl}(665)$:

$a_{chl}(665) = (\{[R(709)/R(665)] \times [a_w(709) + b_b]\} - b_b - a_w(665)) \times \gamma'$ Equation 25

Where:

- $a_{chl}(665)$ = absorption of chlorophyll *a* at 665 nm
- R(λ) = reflectance value at a specified wavelength
- $a_w(\lambda)$ = pure water absorption coefficients at specified locations
  - $a_w(709) = 0.70\ m^{-1}$ (Buitevled *et al*., 1994)
  - $a_w(665) = 0.40\ m^{-1}$ (Pope and Fry, 1997)
- b_b = backscattering coefficient obtained from $b_b=[a_w(778)\ \alpha\ R(778)] \times [(\delta - R(778))^{-1}]$ (Gons, 1999; Astoreca *et al.,* 2006)
  - $a_w(778)$ = $2.71\ m^{-1}$ (Buitevled *et al*., 1994)
  - α = 0.60, constant accounting for refraction and reflection at the water's surface (Gordon *et al.*, 1988; Astoreca *et al*., 2006)
  - δ = 0.082, accounts for the reflectance-IOP model, taken from Astoreca, 2006 (based on Gordon *et al*., 1988)
- γ' = correction factor derived from the linear least-squares fit of measured versus estimated chlorophyll *a* absorption

Algorithm adapted from Simis *et al*., 2005

Concentration of chlorophyll *a* can then be determined from:

[Chla] = $a_{chl}(665)/a^*_{chl}(665)$ Equation 26

The following Simis *et al.* (2005) algorithm was implemented for the determination of the phycocyanin absorption coefficient at 620 nm, $a_{PC}(620)$:

$$a_{PC}(620) = (\{[R(709)/R(620)] \times [a_w(709) + b_b]\} - b_b - a_w(620)) \times \varsigma - \varepsilon \times a_{chl}(665)] \quad \text{Equation 27}$$

Where:

$a_{PC}(620)$	= absorption of phycocyanin at 620 nm
$R(\lambda)$	= reflectance value at a specified wavelength
$a_w(\lambda)$	= pure water absorption coefficients at specified locations $a_w(709) = 0.70\ m^{-1}$ (Buitevled *et al*., 1994) $a_w(620) = 0.30\ m^{-1}$ (Pope and Fry, 1997)
b_b	= backscattering coefficient obtained from $b_b=[a_w(778)\ \alpha\ R(778)] \times [(\gamma' - R(778))^{-1}]$ (Gons, 1999; Astoreca *et al.,* 2006) $a_w(778)$ = $2.71\ m^{-1}$ (Buitevled *et al.*, 1994) A = 0.60, constant accounting for refraction and reflection at the water's surface (Gordon *et al.*, 1988; Astoreca *et al.*, 2006) γ' = 0.082, accounts for the reflectance-IOP model, taken from Astoreca *et al.*, 2006 (based on Gordon *et al.*, 1988)
ς	= correction factor derived from the linear least-squares fit of measured versus estimated phycocyanin absorption, derived from Lake Loosdrecht data (Simis *et al.*, 2005)
$a_{chl}(665)$	= absorption of chlorophyll *a* at 665 nm, determined using the equation $(\{[R_{709} / R_{665}] \times [a_w(709) + b_b]\} - b_b - a_w(665)) \times \gamma'$
ε	= 0.24; conversion factor to define absorption of chlorophyll *a* at 620 nm relative to 665 nm, derived from Lake Loosdrecht data (Simis *et al.*, 2005)

Algorithm adapted from Simis *et al.* 2005

Concentration of phycocyanin can then be determined from:

$$[PC] = a_{PC}(620)/a^*_{PC}(620) \quad \text{Equation 28}$$

Measuring Algorithm Accuracy and Robustness

The algorithms' accuracy in predicting chlorophyll *a* and phycocyanin concentrations in Indianapolis reservoirs was tested through a least-squares regression. The coefficients, and their corresponding standard error (STE), obtained from the linear least-squares regression analysis of measured versus estimated concentrations of phytoplankton

pigments describe the algorithms' fit. Overall model performance was reported using the root-mean-square error (RMSE) of the estimated chlorophyll *a* and phycocyanin concentration:

$$\text{RMSE} = \sqrt{\frac{\sum_{i=1}^{n}(Y_i - \hat{Y}_i)^2}{(n-2)}} \qquad \text{Equation 29}$$

Where:

$\hat{Y}_i$ = estimated concentration of pigment *i*

Y_i = measured concentration of pigment *i*

n = number of observations

Confounding parameters were investigated through a residual analysis where residuals (e_i) were calculated as:

$$e_i = Y_i - \hat{Y}_i \qquad \text{Equation 30}$$

Empirical Algorithm Validation and Transferability

When a strong relationship was obtained between the empirical relationship proposed and analytically measured pigment concentrations, calibration and validation datasets were built to test the algorithms' accuracy in predicting phytoplankton pigment concentration from spectral response across an aggregated dataset. A calibration dataset was created by selecting every other sample site from the aggregated dataset, including both Geist and Morse Reservoir data. The validation dataset included the remaining sites. The retrieved algorithm, including coefficients obtained from the linear least-squares regression of algorithm index values versus analytically measured pigment concentrations from the calibration dataset, was applied to the algorithm index values from the validation dataset to obtain an estimated pigment concentration value. Algorithm accuracy was reported using the RMSE of measured to estimated chlorophyll *a* and phycocyanin concentration values.

Semi-empirical Algorithm Validation and Transferability

Morse and Geist Reservoir data served as a validation dataset for the semi-empirical algorithms introduced by Simis *et al.* (2005) for estimation of chlorophyll *a* and phycocyanin pigment concentration.

RESULTS AND DISCUSSION

Water Quality Data

Water Clarity

The Geist and Morse Reservoir combined dataset yielded an average secchi disk depth of 70 cm. The lowest secchi measurements were collected at Geist Reservoir, with a minimum depth of 30 cm. The low Geist Reservoir average secchi depth of 48 cm coincided with the high total suspended solids (TSS) measurements collected at Geist (average of 20 mg/L) (Table 7). TSS measurements for more than half of the Geist Reservoir sampling sites measured above 20 mg/L (Figure 9a). Geist turbidity measurements were also high, with an average of 10.3 NTU. Over half of the Geist Reservoir sampling sites showed turbidity measurements $\geq$ 11 NTU (Figure 12b).

The lowest TSS and greatest secchi depth measurements were observed at Morse Reservoir (4.4 mg/L and 135 cm, respectively; Table 7). TSS measurements for more than half of the sampling sites on Morse were less than 10 mg/L (Figure 10a). Likewise, turbidity measurements for over half of the Morse sampling sites were low (<5 NTU; Figure 10b). Morse yielded a much larger range of turbidity and TSS values (50 mg/L and 27.7 NTU, respectively) compared to Geist (16 mg/L and 11 NTU, respectively).

Table 7: Summary statistics of water quality parameters for Geist and Morse Reservoirs.

Parameter	Mean	Median	Minimum	Maximum	Σ	N
Geist Reservoir						
Secchi Depth (cm)	48	45	30	75	12	27
Turbidity (NTU)	10.3	9.8	7.0	18.0	2.1	27
TSS (mg/L)	20.4	19.4	13.2	29.2	4.2	27
TDS (g/L)	0.322	0.306	0.300	0.369	0.028	27
DOC (mg C/L)	3.9	4.2	0.5	4.86	1.0	27
TOC (mg C/L)	6.2	5.9	4.4	10.3	1.2	27
Chlorophyll *a* (ppb)	71.3	64.4	34.7	118.9	26.0	27
Phycocyanin (ppb)	96.2	100.4	25.2	185.1	43.8	27
Chl *a*-to-PC Ratio	0.9	0.8	0.4	2.9	0.5	27
Total P (µg P/L)	111.2	113.0	38.0	191.0	39.1	27
Total N (mg N/L)	2.0	2.0	0.6	2.8	0.4	27
Morse Reservoir						
Secchi Depth (cm)	92	90	35	135	36	28
Turbidity (NTU)	6.7	4.6	2.3	30.0	6.4	28
TSS (mg/L)	15.1	8.4	4.4	54.4	15.0	28
TDS (g/L)	0.267	0.268	0.260	0.281	0.005	28
DOC (mg C/L)	4.4	4.2	3.9	5.2	0.4	23
TOC (mg C/L)	5.6	5.1	4.6	7.7	0.9	28
Chlorophyll *a* (ppb)	57.2	35.6	18.0	168.6	42.9	27
Phycocyanin (ppb)	41.8	28.6	2.0	135.1	43.4	24
Chl *a*-to-PC Ratio	4.0	1.6	0.7	12.7	3.8	24
Total P (µg P/L)	64.0	50.0	23.0	204.0	44.3	28
Total N (mg N/L)	1.5	1.5	0.6	2.3	0.3	28
Aggregated Dataset						
Secchi Depth (cm)	70	57	30	135	35	55
Turbidity (NTU)	8.5	9.1	2.3	30.0	5.2	55
TSS (mg/L)	18.1	17.2	4.4	54.4	11.7	55
TDS (g/L)	0.294	0.281	0.260	0.369	0.034	55
DOC (mg C/L)	4.1	4.2	0.5	5.2	0.8	50
TOC (mg C/L)	5.9	5.8	4.4	10.3	1.1	55
Chlorophyll *a* (ppb)	64.7	57.2	18.0	168.6	36.5	54
Phycocyanin (ppb)	71.3	73.2	2.1	185.1	50.3	51
Chl *a*-to-PC Ratio	2.0	1.0	0.4	12.1	2.7	50
Total P (µg P/L)	88.1	72.0	23.0	204.0	49.0	55
Total N (mg N/L)	1.7	1.7	0.6	2.8	0.4	55

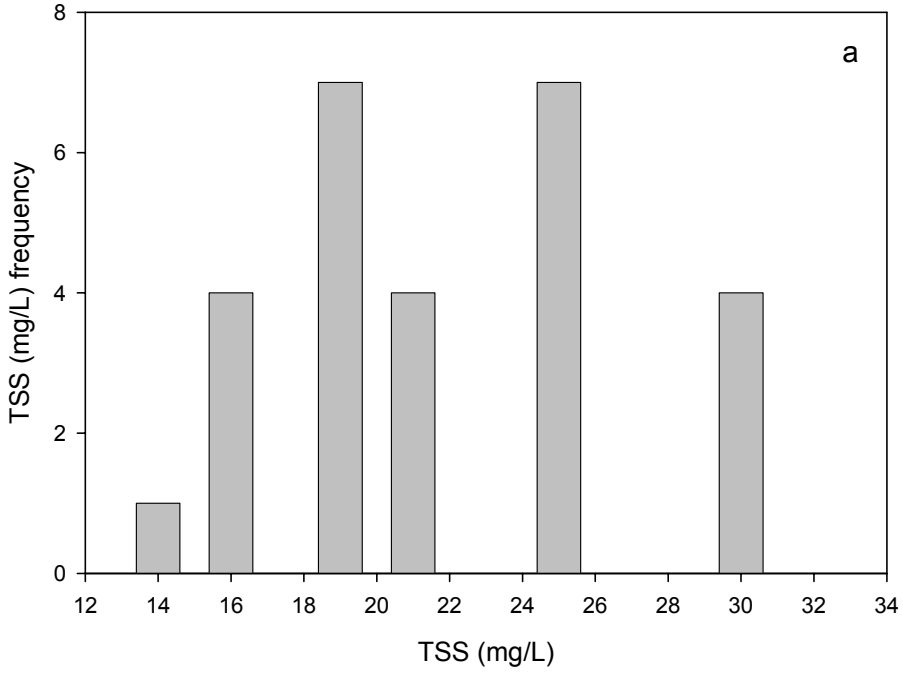

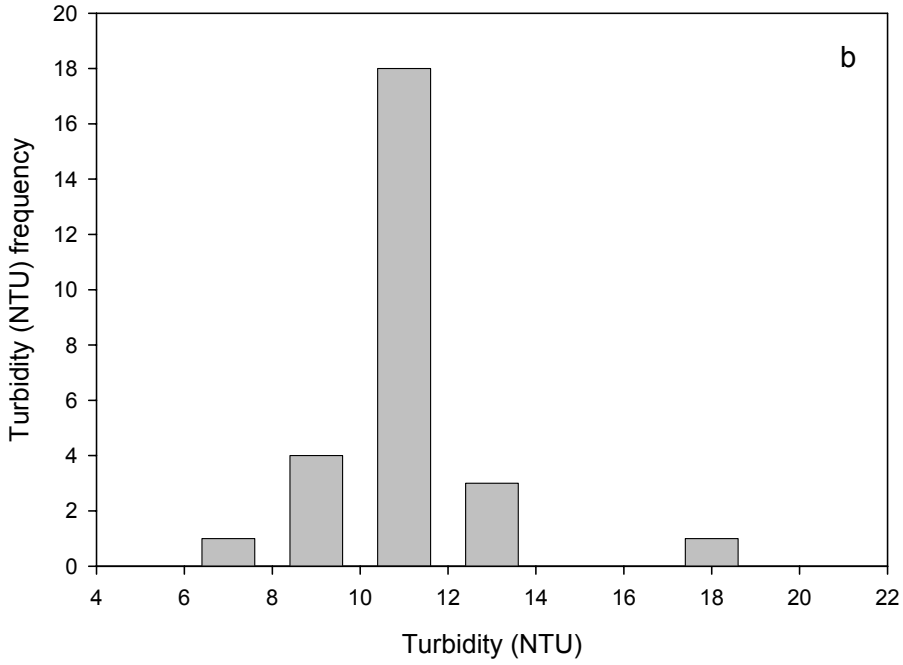

Figure 9a and b: Distribution of optically active constituents (a) total suspended solids (TSS; mg/L; n=28) and (b) turbidity (NTU; n=27) measured in Geist
Reservoir.

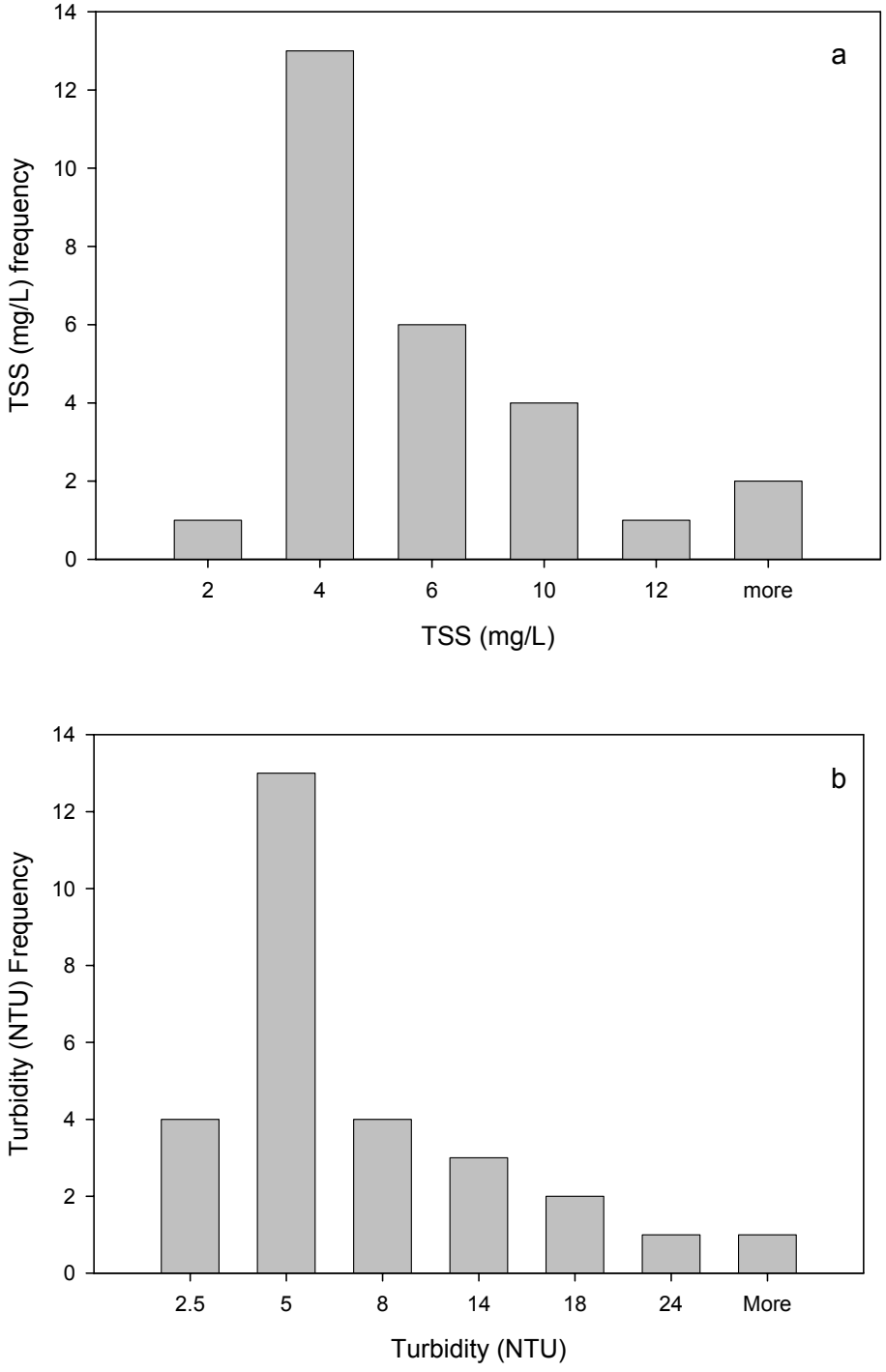

Figure 10a and b: Distribution of (a) total suspended solids (TSS; mg/L; n=27) and (b) turbidity (NTU; n=28) measured in Morse Reservoir.

Dissolved Substances

Average total dissolved solids (TDS) and dissolved organic carbon (DOC) measurements for a combined dataset were 0.294 g/L and 4.1 mg C/L, respectively. The highest TDS measurement was collected at Geist Reservoir (0.369 g/L) while the highest DOC measurement was collected at Morse Reservoir (5.2 mg C/L; Table 7). Samples from Geist showed higher overall concentrations of TDS and lower overall concentrations of DOC compared to Morse samples.

Pigments (Chlorophyll a and phycocyanin)

The combined Morse-Geist dataset showed a large range in both phycocyanin (2 to 135 ppb) and chlorophyll *a* concentration (25-185 ppb). The highest concentration of chlorophyll *a* was recorded in Morse Reservoir and the highest phycocyanin concentration in Geist Reservoir. The range of phycocyanin and chlorophyll *a* pigment concentrations collected from Morse Reservoir were large (151 and 133 ppb, respectively; Figure 12). Ten sampling sites at Morse Reservoir showed phycocyanin concentrations of less than 10 ppb (Figure 12a). These sites also showed low concentrations of chlorophyll *a*, ranging from 18 to 32 ppb (Figure 12b). The range of phycocyanin concentrations was also large for Geist (160 ppb, Figure 11a); however, Geist chlorophyll *a* analysis yielded the lowest range in pigment concentration of 84 ppb (Figure 11b). Morse Reservoir showed a much higher average chlorophyll *a*-to-phycocyanin ratio (4.0) compared to Geist reservoir (0.9), suggesting that four times more chlorophyll *a* is present in the water column at Morse compared to phycocyanin. The low chlorophyll *a*-to-phycocyanin ratio obtained from Geist suggests that phycocyanin is more prevalent than chlorophyll *a* in the water column (Table 7).

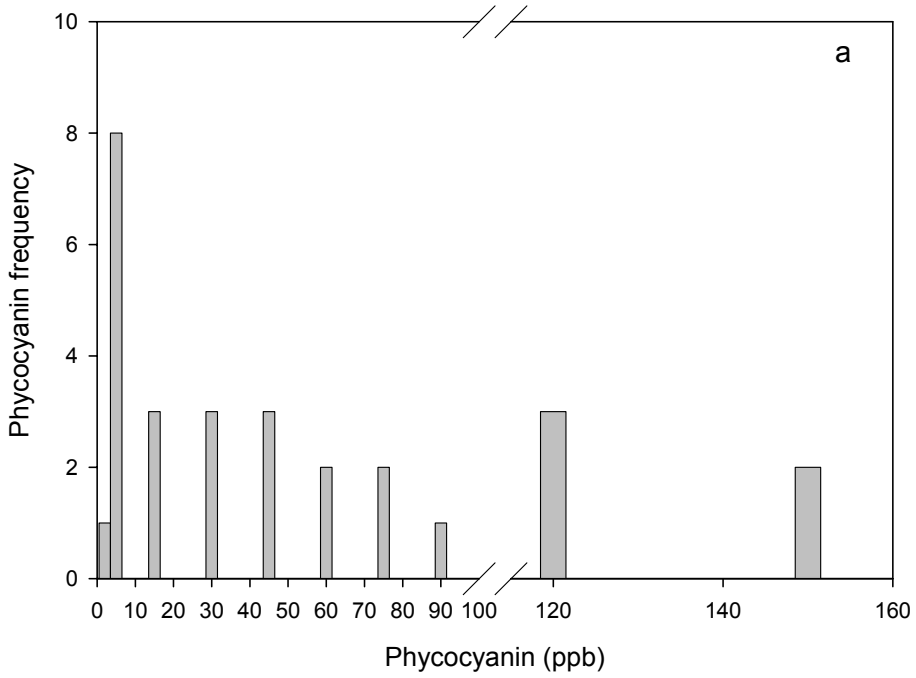

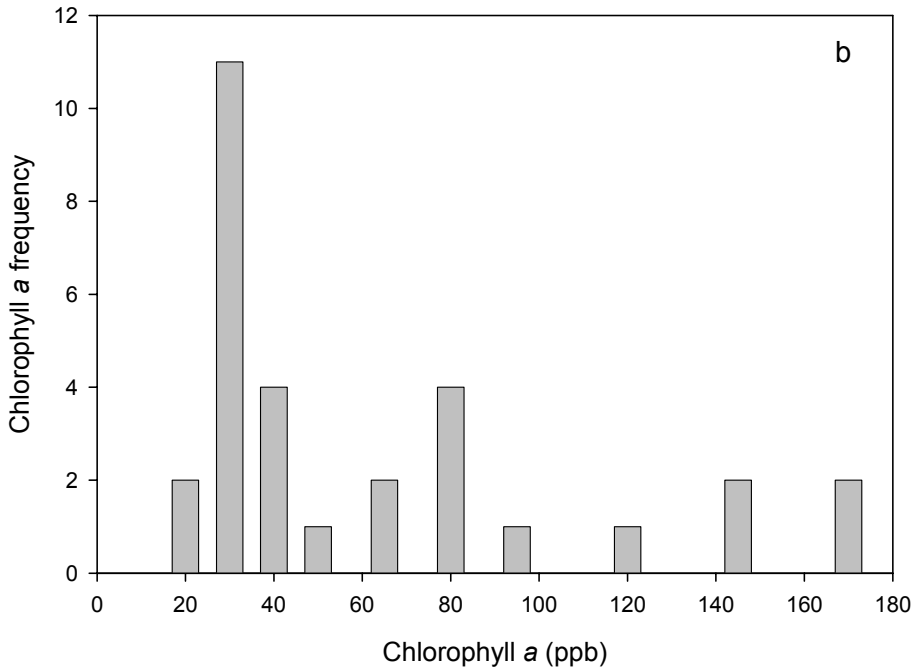

Figure 11a and b: Distribution of (a) phycocyanin (ppb; n=24) and (b) chlorophyll *a* concentrations (ppb; n=27) measured in Morse Reservoir.

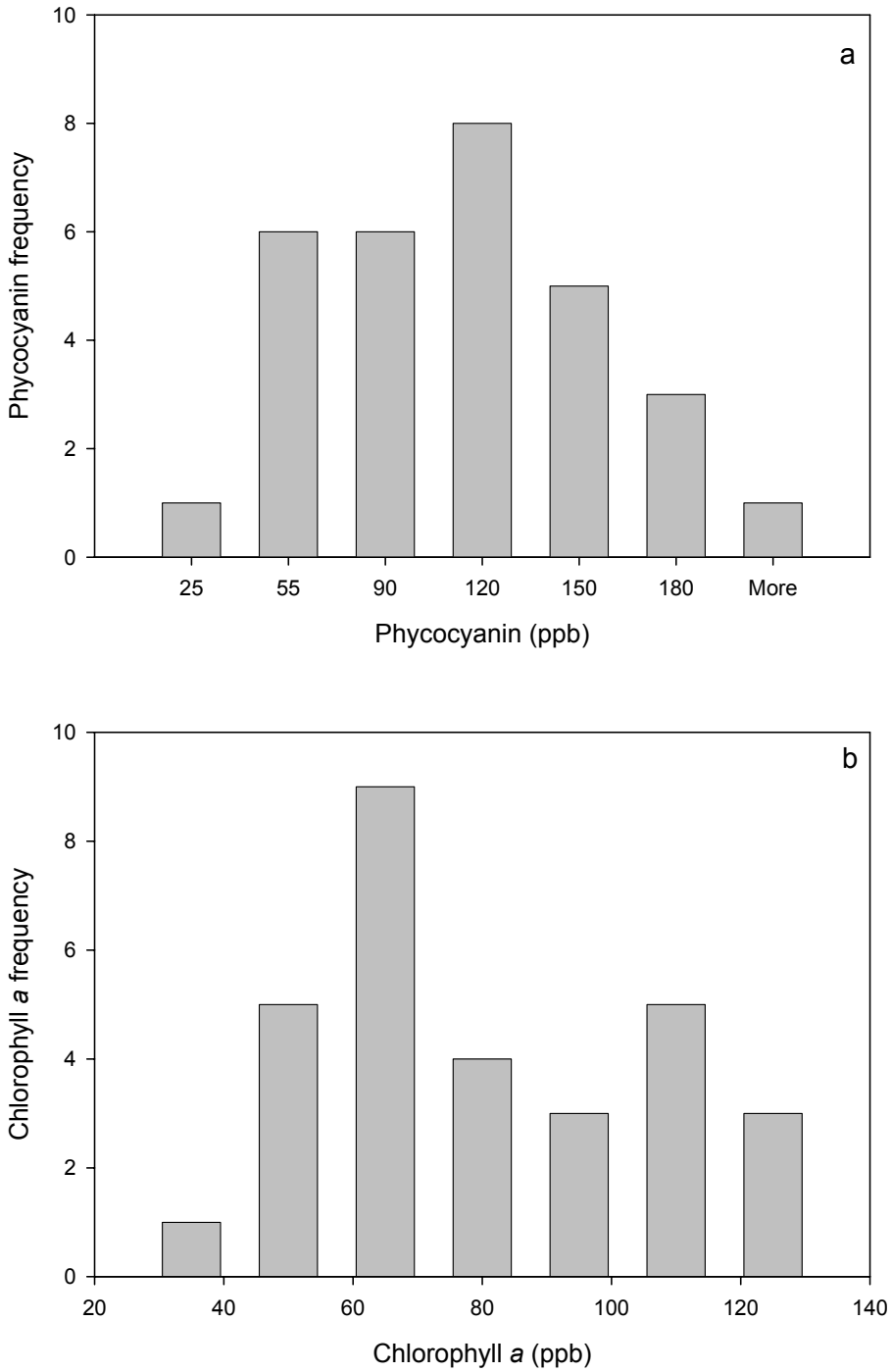

Figure 12a and b: Distribution of (a) phycocyanin (ppb, n=27) and (b) chlorophyll *a* concentrations (ppb; n=27) measured in Geist Reservoir.

Pigment Extraction Accuracy Analysis

Calibration Accuracy

Extracted chlorophyll *a* and phycocyanin, measured flourometrically using a TD-700 Flourometer (Turner Designs, Inc.) were calibrated with chlorophyll *a* from spinach and C-phycocyanin from *Spirulina sp*. standards, respectively (Sigma-Aldrich 10865 and Sigma-Aldrich P6161).

When compared to chlorophyll *a* calibration standards from spinach, prepared to measure 0 (90% buffered acetone only), 5, 20, 40, 100, and 150 ppb, the concentrations measured flourometrically yielded errors ranging from 0-3.8 ppb. Flourometric measurements of chlorophyll *a* were consistently lower than known calibration standards. Highest error was obtained at the ends of the calibration curve, where 1.4%, 2.1%, and 1.8% error was calculated for 5, 100, and 150 ppb, respectively.

Slightly higher errors were measured when calibrating for phycocyanin. Overall, phycocyanin concentrations measured flourometrically were lower than the known calibration standards prepared to measure 0 (phosphate buffer only), 20, 40, 60, 80, and 100 ppb, from *Spirulina sp*. Error between known and flourometrically measured phycocyanin concentrations were 0-5.3 ppb. The highest error value of 5.3 ppb was obtained for the 100 ppb standard, suggesting higher error will result when measuring high concentrations of phycocyanin.

Precision between Samples and Replicates

Pigment extraction precision was assessed by calculating percent error between samples and their replicates. Samples with extraction error greater than 30% were not

used in algorithm testing or validation. For most samples, an extraction error of less than 20% was measured, average error was 11% and 8% for phycocyanin and chlorophyll *a*, respectively (Figure 13; Figure 14). Two sampling sites, GR 238 and MR 297, were not used in further analysis due to high error (39% error for chlorophyll *a* and 66% error for phycocyanin, respectively). High error between replicate phycocyanin samples was also calculated for Morse Reservoir site 275 (40% error obtained from phycocyanin extraction). This site was included in further analysis since the concentration of phycocyanin in the sample was very low. For extraction of both pigments, error was higher for lower concentrations.

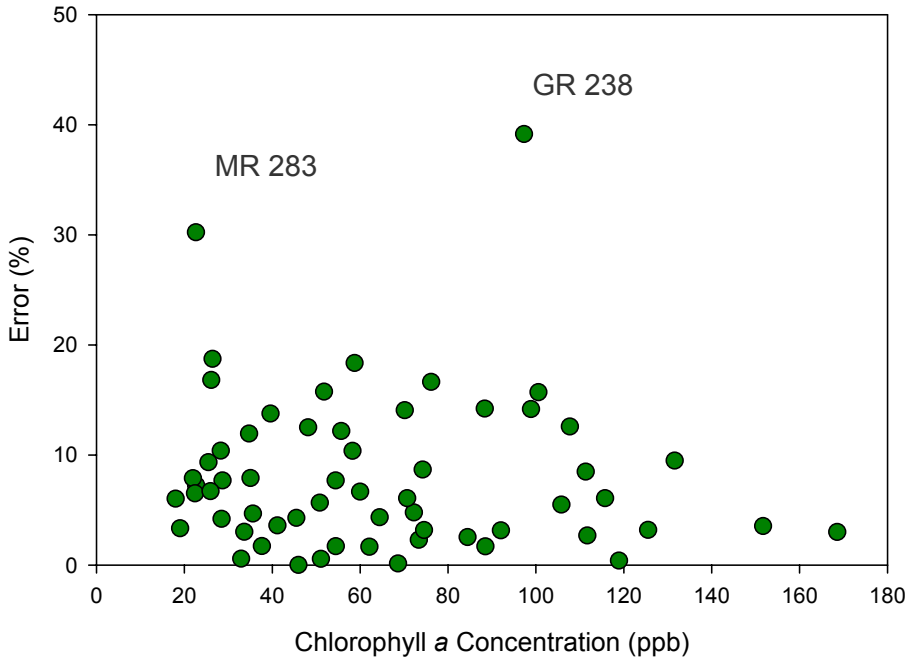

Figure 13: Relationship between flourometrically measured chlorophyll *a* and error (%) between samples and their replicates. Mean error is 8% (n=60).

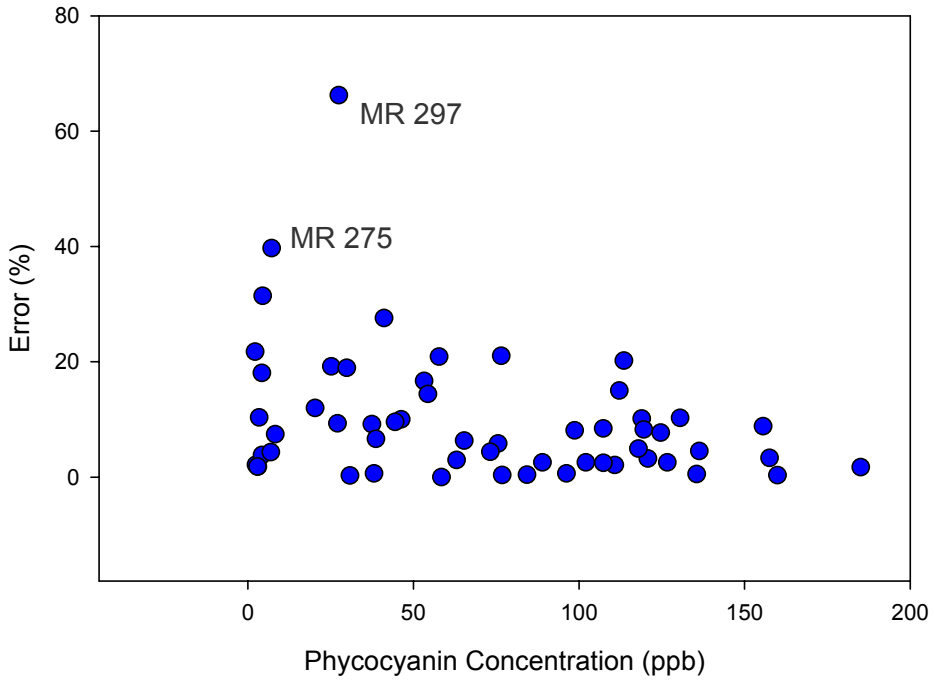

Figure 14: Relationship between flourometrically measured phycocyanin and error (%) between samples and their replicates. Mean error is 11% (n=57).

Relationships between Optically Active Constituents

Strong relationships between phytoplankton pigments and other optically active constituents (OACs), (*i.e*., turbidity and TSS) were observed in Morse Reservoir. The relationship observed from Morse data between the measured phytoplankton pigments, chlorophyll *a* and phycocyanin yielded an r^2 of 0.81 when a single outlier was removed (Figure 15a). The relationship between phycocyanin and turbidity and TSS in Morse also yielded r^2 values of 0.80 for both, with the same single outlier removed (Figure 16a and d). Likewise, a strong relationship exists between chlorophyll *a* concentration and turbidity and TSS, yielding r^2 values of 0.74 and 0.83, respectively (Figure 16b and c). A strong relationship between TSS and turbidity was also observed for Morse Reservoir, yielding an r^2 value of 0.93 (Figure 18a; Table 8). The strong relationships observed between pigment concentration and TSS measurements at Morse Reservoir suggest that turbidity is mostly a function of phytoplankton in the water column.

Unlike Morse Reservoir, concentrations of optically active constituents in Geist Reservoir do not appear to co-vary. The strongest relationship between any two OACs at Geist was observed between chlorophyll *a* and phycocyanin, yielding an r^2 value of 0.53 (Figure 15b). The relationship between phycocyanin and turbidity and TSS at Geist Reservoir yielded r^2 values of 0.01 and 0.21 (Figure 17a and b). Weak relationships also exist between chlorophyll *a* concentration and turbidity and TSS, yielding r^2 values of 0.04 and 0.16, respectively (Figure 17c and d). A weak relationship also exists between and turbidity and TSS with an r^2 value of 0.43 (Figure 18b, Table 9). Weak relationships among pigment concentrations and TSS values suggest higher amounts of non-algal turbidity in the Geist water column.

Table 8: Correlation Matrix of water quality parameters for Morse Reservoir. Strong relationships between optically active constituents are highlighted.

	Secchi Depth (m)	TDS (g/L)	Chla (ppb)	PC (ppb)	Turbidity (NTU)	DOC (mg C/L)	TOC (mg C/L)	TSS
Secchi Depth (m)	–	-0.201	-0.870	-0.826	-0.781	-0.808	-0.864	-0.841
Total Dissolved Solids (TDS) (g/L)	-0.201	–	0.465	0.036	0.633	0.376	0.177	0.596
Chlorophyll *a* (ppb)	-0.870	0.465	–	**0.810**	**0.740**	**0.793**	**0.821**	**0.830**
Phycocyanin (ppb)	-0.826	0.036	**0.810**	–	**0.820**	0.655	**0.876**	**0.880**
Turbidity (NTU)	-0.781	0.633	**0.740**	**0.820**	–	**0.783**	**0.826**	**0.930**
Dissolved Organic Carbon (DOC) (mg C/L)	-0.808	0.376	**0.793**	**0.655**	**0.783**	–	0.684	**0.787**
Total Organic Carbon (TOC) (mg C/L)	-0.864	0.177	**0.821**	**0.876**	**0.826**	0.684	–	**0.864**
Total Suspended Solids (TSS) (mg/L)	-0.841	0.596	**0.830**	**0.880**	**0.930**	**0.787**	**0.864**	–

Table 9: Correlation Matrix of water quality parameters for Geist Reservoir. Strong relationships between optically active constituents are highlighted.

	Secchi Depth (m)	TDS (g/L)	Chla (ppb)	PC (ppb)	Turbidity (NTU)	DOC (mg C/L)	TOC (mg C/L)	TSS (mg/L)
Secchi Depth (m)	–	0.854	-0.583	-0.727	-0.305	0.052	-0.545	-0.674
Total Dissolved Solids (TDS) (g/L)	0.854	–	-0.565	-0.865	0.002	-0.085	-0.652	-0.453
Chlorophyll *a* (ppb)	-0.583	-0.565	–	0.530	0.090	0.047	0.505	0.378
Phycocyanin (ppb)	-0.727	-0.865	0.530	–	-0.060	0.095	0.650	0.418
Turbidity (NTU)	-0.305	0.002	0.090	-0.060	–	-0.048	0.142	0.699
Dissolved Organic Carbon (DOC) (mg C/L)	0.052	-0.085	0.047	0.095	-0.048	–	0.109	-0.115
Total Organic Carbon (TOC) (mg C/L)	-0.545	-0.652	0.505	0.650	0.142	0.109	–	0.488
Total Suspended Solids (TSS) (mg/L)	-0.674	-0.453	0.460	0.210	0.480	-0.115	0.488	–

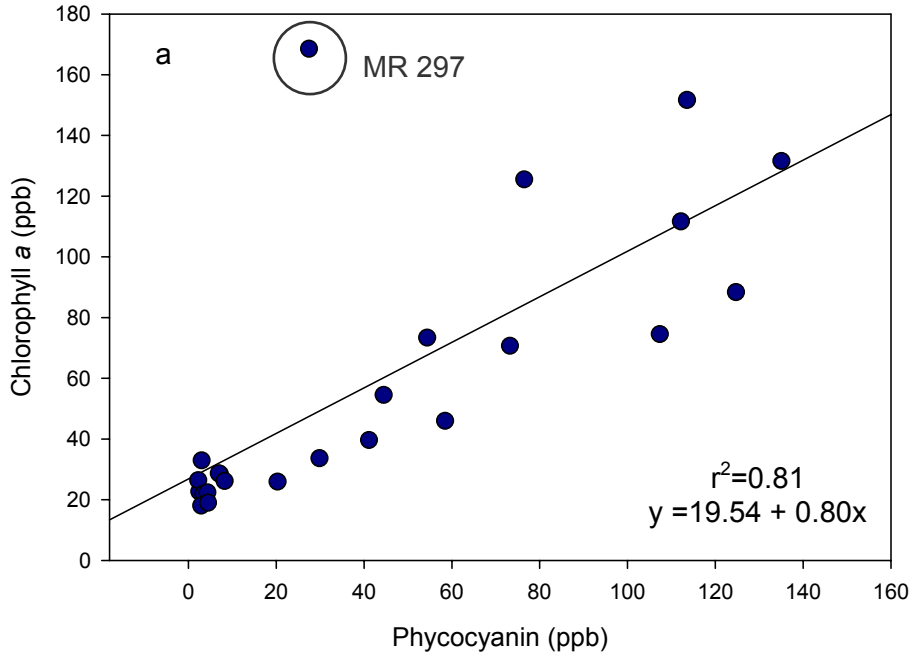

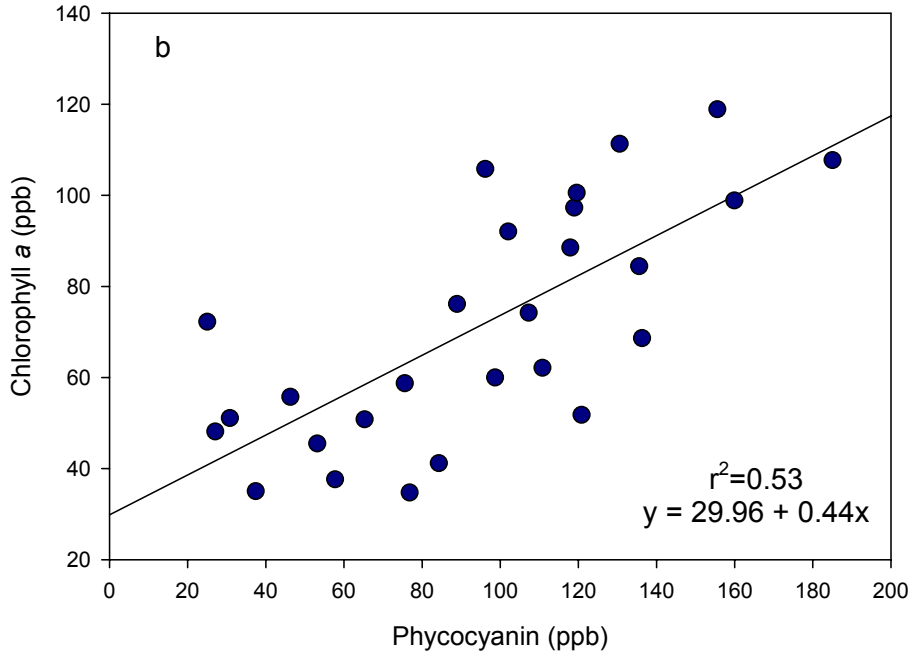

Figure 15a and b: Relationship between phytoplankton pigment concentrations, phycocyanin and chlorophyll *a*, for (a) Morse Reservoir (r^2=0.81), excluding outlying site MR297 (n=26) and (b) Geist reservoir (r^2=0.53, n=26).

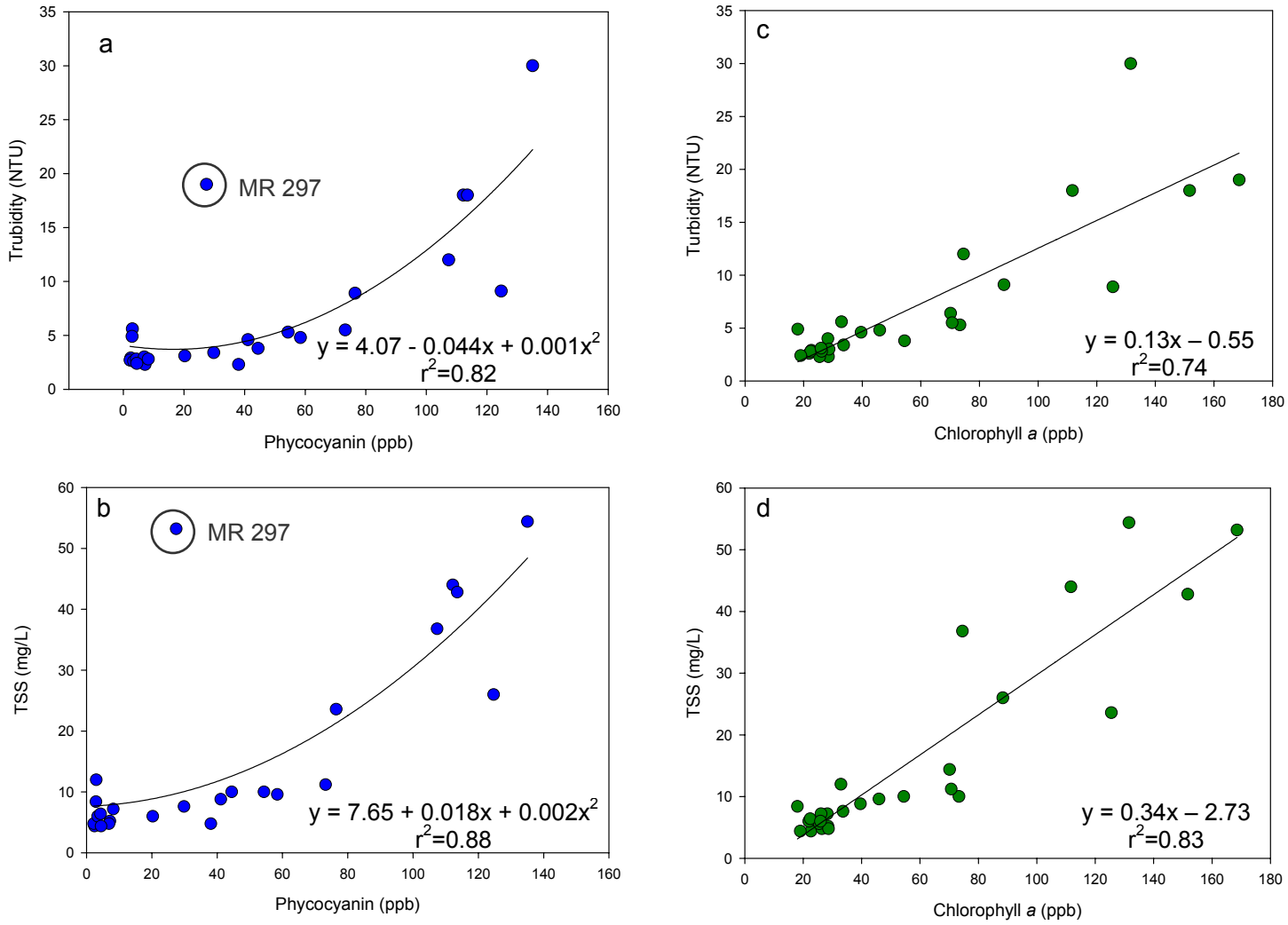

Figure 16a, b, c and d: Morse Reservoir relationships between optically active constituents, turbidity and total suspended solids, and phytoplankton pigment concentration chlorophyll *a* (n=27) and phycocyanin (n=24).

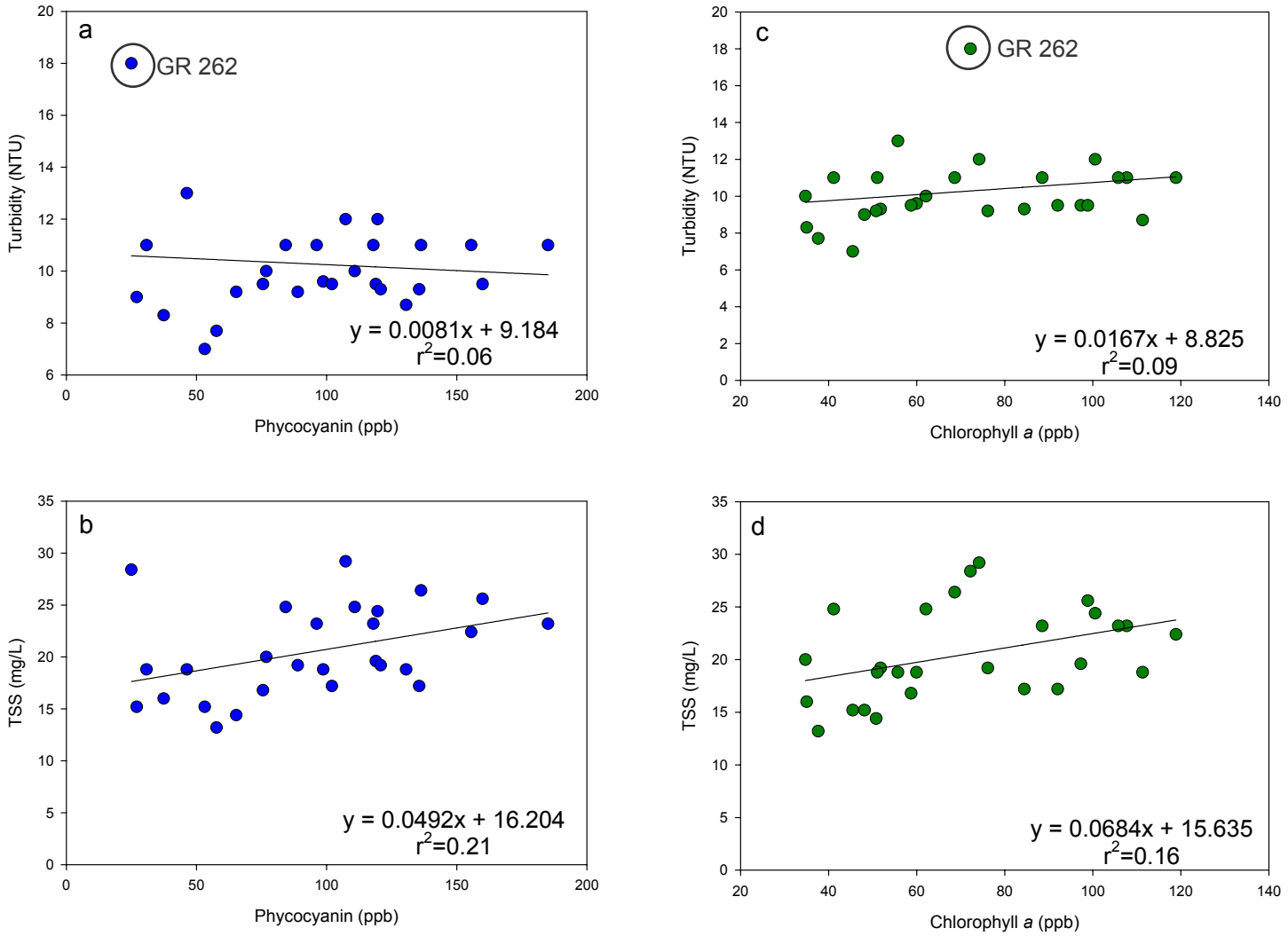

Figure 17a, b, c and d: Geist Reservoir relationships between optically active constituents, turbidity and total suspended solids, and phytoplankton pigment concentration chlorophyll *a* (n=26) and phycocyanin (n=26).

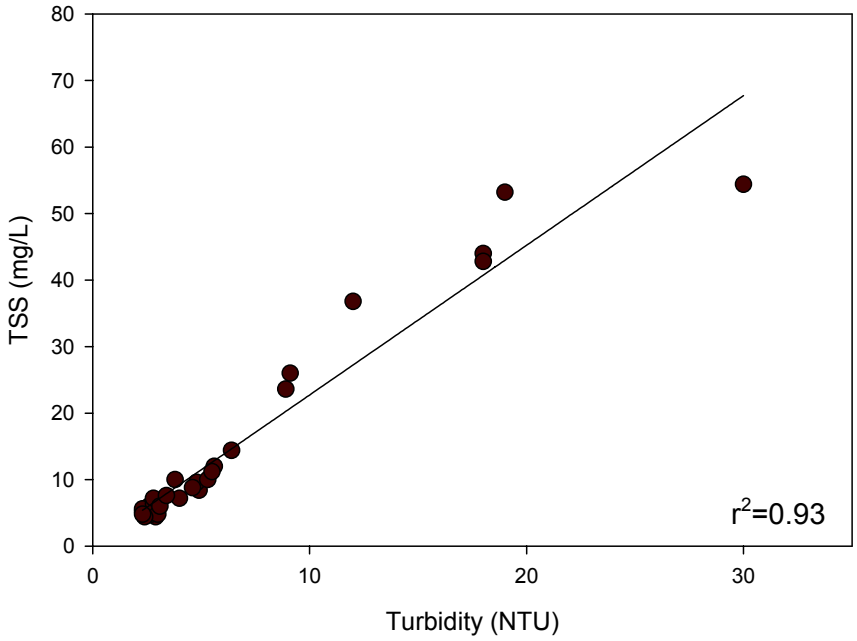

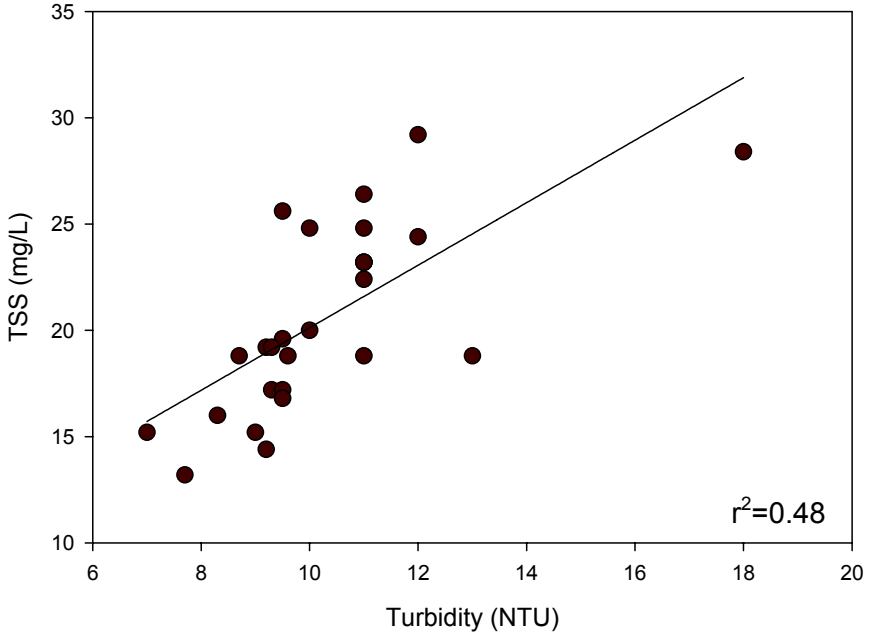

Figure 18a and b: Relationship between total suspended solids (mg/L) and turbidity (NTU) measurements from (a) Morse Reservoir (r^2=0.93) and (b) Geist reservoir (r^2=0.48).

Algorithm Application

Color ratio and band combination algorithms for estimation of chlorophyll a concentration

The color ratio and band combination algorithms for estimation of chlorophyll *a* concentration were applied using two methods. The first method required selection of the reflectance value at a specified band. The second method required the extraction of a peak or trough value within a feature of interest. The first method proved to be consistently less successful than the second; therefore results using the first method are not reported.

The most successful of the NIR_{peak}:red_{trough} band combination algorithms, including variations of the form $R(\lambda_2)/ R(\lambda_1)$, where $R(\lambda_2)$ was chosen as $R_{max}\lambda_{(695-715)}$ and $R(\lambda_1)$ as $R_{min}\lambda_{(665-685)}$, to Geist and Morse Reservoirs yielded r^2 values of 0.44 (Table 10a; Figure 19a) and 0.80 respectively (Table 10b; Figure 20a). Application of the variations on the NIR_{peak}:red_{trough} algorithm yielded lower coefficients of determination compared to the original, two band ratio (Table 10a and b). Derivation of chlorophyll *a* concentration, [Chla], required the application of the regression equation obtained from the linear least-squares regression of the index value from $[R_{max}\lambda_{(695-715)}][R_{min}\lambda_{(665-685)}^{-1}]$ and the analytically measured chlorophyll *a* concentration, where:

$[Chla] = 87.01x + 105.05$ (Geist) and Equation 31

$[Chla] = 76.23x - 70.69$ (Morse) Equation 32

Table 10a and b: Performance summary of band combination algorithms for prediction of chlorophyll *a* concentration for (a) Geist Reservoir ($p<0.001$, $n=27$) and (b) Morse Reservoir ($p<0.0001$, $n=27$), including the slope and intercept of the regression equation for determining [Chla] Estimated, slope and intercept of the linear relationship between [Chla] Measured and [Chla] Estimated with standard errors of estimation (STE), RMSE of [Chla] Estimated, and the linear least-squares fit (r^2) of the model to [Chla] Measured.

(a) Geist	Chlorophyll *a* Empirical Algorithm	Peak reflectance location	Trough reflectance location	Slope, Intercept	Intercept (STE)	Slope (STE)	RMSE	r^2	Figure
NIR:Red band combination algorithms	$R_{max}\lambda_{(695-715)}][R_{min}\lambda_{(665-685)}{}^{-1}]$	700<R(λ2)<707	670<R(λ_2)<676	87.01 105.05	39.86 (7.53)	0.44 (0.09)	19.67	0.44	Figure 19
	$[R_{max}\lambda_{(695-715)}]-[R_{min}\lambda_{(665-685)}][R_{min}\lambda_{(540-570)}{}^{-1}]$			180.14 8.90	44.33 (7.35)	0.38 (0.10)	20.74	0.38	–
	$\{[R_{max}\lambda_{(695-715)}]-[R_{min}\lambda_{(665-685)}]\}\{[R_{min}\lambda_{(540-570)}{}^{-1}]-[R_{min}\lambda_{(665-685)}{}^{-1}]\}$			84.85 4.37	49.64 (6.89)	0.31 (0.09)	21.95	0.31	–
	$\{[R_{max}\lambda_{(695-715)}]-[R_{min}\lambda_{(665-685)}]\}\{[R_{min}\lambda_{(540-570)}{}^{-1}]-[R_{min}\lambda_{(665-685)}{}^{-1}]\}$			81.15 19.06	49.03 (7.03)	0.31 (0.09)	21.81	0.31	–

(b) Morse	Chlorophyll *a* Empirical Algorithm	Peak reflectance location	Trough reflectance location	Slope, Intercept	Intercept (STE)	Slope (STE)	RMSE	r^2	Figure
NIR:Red band combination algorithms	$R_{max}\lambda_{(695-715)}][R_{min}\lambda_{(665-685)}{}^{-1}]$	688<R(λ_2)<706	668<R(λ_2)<675	76.23 -70.69	10.72 (5.5)	0.80 (0.08)	19.34	0.80	Figure 26
	$[R_{max}\lambda_{(695-715)}]-[R_{min}\lambda_{(665-685)}][R_{min}\lambda_{(540-570)}{}^{-1}]$			163.13 -7.34	12.43 (5.8)	0.77 (0.08)	20.82	0.77	–
	$\{[R_{max}\lambda_{(695-715)}]-[R_{min}\lambda_{(665-685)}]\}\{[R_{min}\lambda_{(540-570)}{}^{-1}]-[R_{min}\lambda_{(665-685)}{}^{-1}]\}$			86.17 9.02	14.03 (6.0)	0.74 (0.09)	22.12	0.74	–
	$\{[R_{max}\lambda_{(695-715)}]-[R_{min}\lambda_{(665-685)}]\}\{[R_{min}\lambda_{(540-570)}{}^{-1}]-[R_{min}\lambda_{(665-685)}{}^{-1}]\}$			80.00 18.34	14.97 (6.1)	0.72 (0.09)	22.85	0.72	–

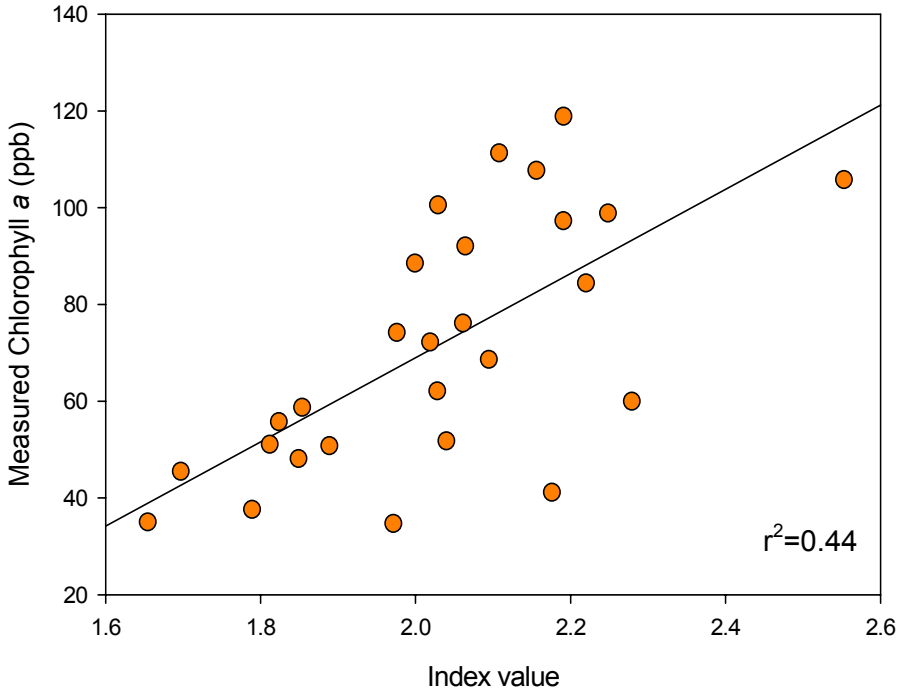

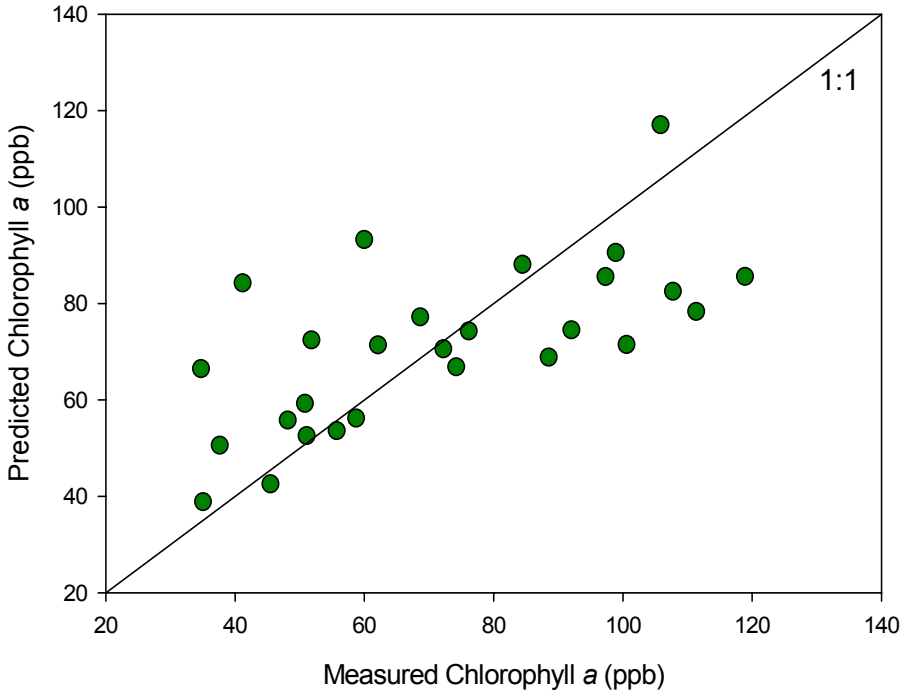

Figure 19a and b: (a) Geist Reservoir NIR:red algorithm index values versus analytically measured chlorophyll *a* concentrations (r^2=0.44; n=27) and (b) analytically measured chlorophyll *a* concentrations versus NIR:red algorithm estimated chlorophyll *a* concentrations (RMSE=19.67).

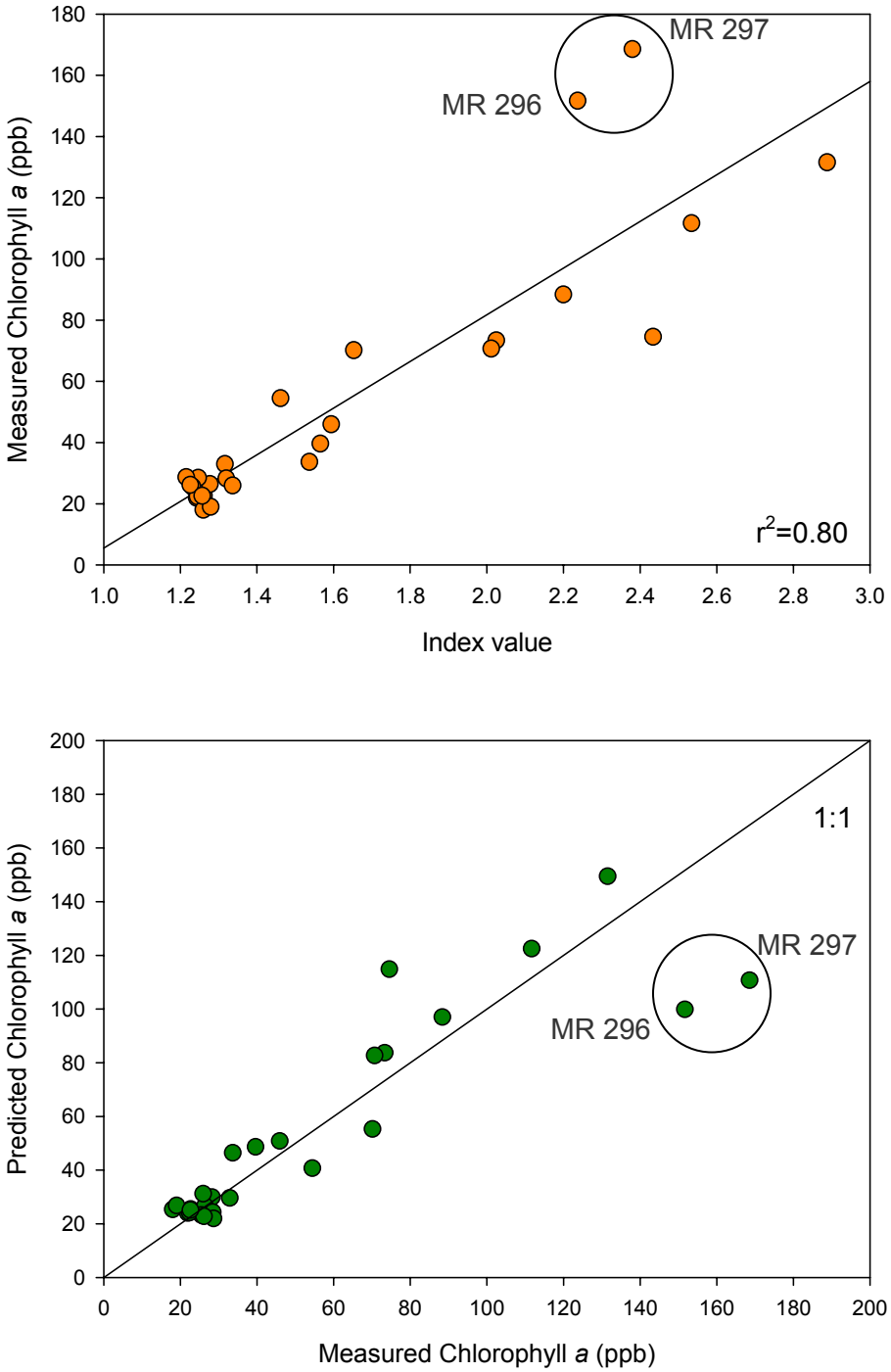

Figure 20 a and b: (a) Morse Reservoir NIR:red algorithm index values versus analytically measured chlorophyll *a* concentrations (r^2=0.80; n=27; outliers indicated by circle) and (b) analytically measured chlorophyll *a* concentrations versus NIR:red algorithm estimated chlorophyll *a* concentrations (RMSE=19.84 ppb).

Though the relationship between analytically measured chlorophyll *a* concentrations and the NIR:red algorithm application to Geist Reservoir data was weak (r^2=0.44; Figure 19a), application of the regression equation yielded a RMSE of only 19.67 ppb (Figure 19b), the result of a lack in extreme outliers in the Geist Reservoir dataset. The small range in chlorophyll *a* concentrations measured at Geist (84 ppb) also explains the weak relationship resulting from the linear least-squares regression and the low RMSE resulting from algorithm application. The relationship between Morse Reservoir analytically measured chlorophyll *a* concentrations and the values produced by the application of the NIR:red algorithm however, yielded a much stronger relationship (r^2=0.80; Figure 20a), but produced nearly the same RMSE of 19.34 ppb (Figure 20b), a discrepancy due to the inclusion of two extreme outliers. Also, unlike Geist Reservoir, chlorophyll *a* measurements collected from Morse Reservoir span a much larger range of values (151 ppb), thus providing a more robust model and stronger relationship.

Morse Reservoir sampling sites 296 and 297 are the only two sites with chlorophyll *a* concentrations greater than 150 ppb (152 and 169 ppb). Residuals of measured to estimated chlorophyll *a* concentrations proved to have a strong positive correlation with TSS and turbidity, yielding an r^2 values of 0.72 and 0.80, respectively (Figure 21a and b). For both outlying sampling sites, the model underestimated chlorophyll *a* concentration by 52 and 58 ppb, respectively. Omission of the outliers from the dataset yielded an r^2 value of 0.93 and RMSE of 8.57 ppb ($p<0.0001$, n=25; Figure 22a and b). The results of the Morse Reservoir residual analysis lends explanation for the low predictive power of the NIR:red ratio on Geist Reservoir. Predictive power was high for sampling sites with turbidity measurements from 2 to 10 NTU. Turbidity in Geist Reservoir was typically greater than 10 NTU. The results suggest that the NIR:red ratio is highly effected by scattering in the water column from colored non-algal material. Attempting to correct for

this effect by employing a band in the spectral region beyond the NIR peak resulted in a low r^2 value (0.31) using the $[R(705) - R(670)] \times [R(550)^{-1} - R(760)^{-1}]$ model.

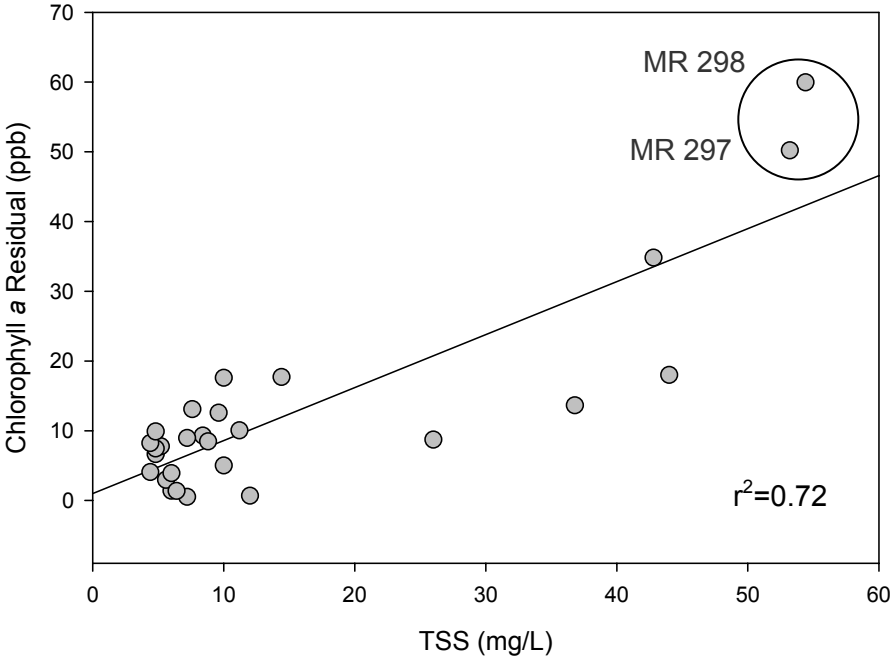

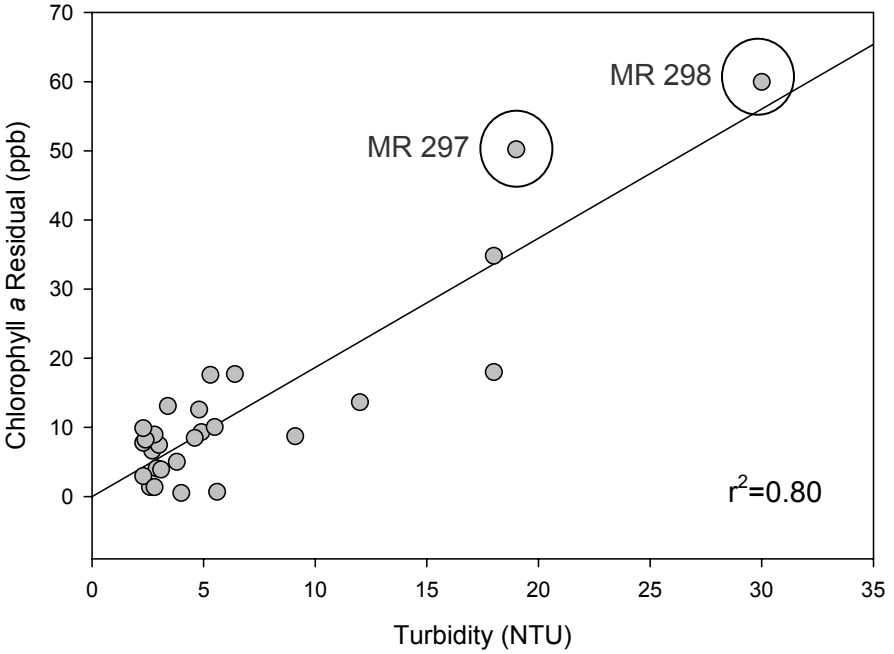

Figure 21a and b: The relationship between (a) TSS (mg/L) (r^2=0.72) and (b) turbidity (NTU) (r^2=0.80) and residual values from the application of the NIR:red algorithm to Morse Reservoir for derivation of chlorophyll *a* concentration.

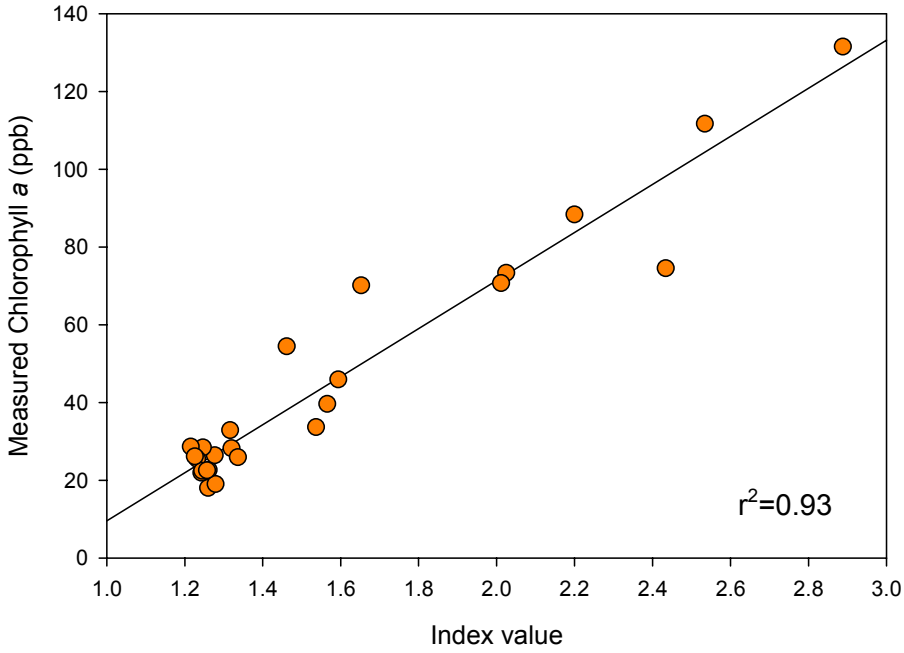

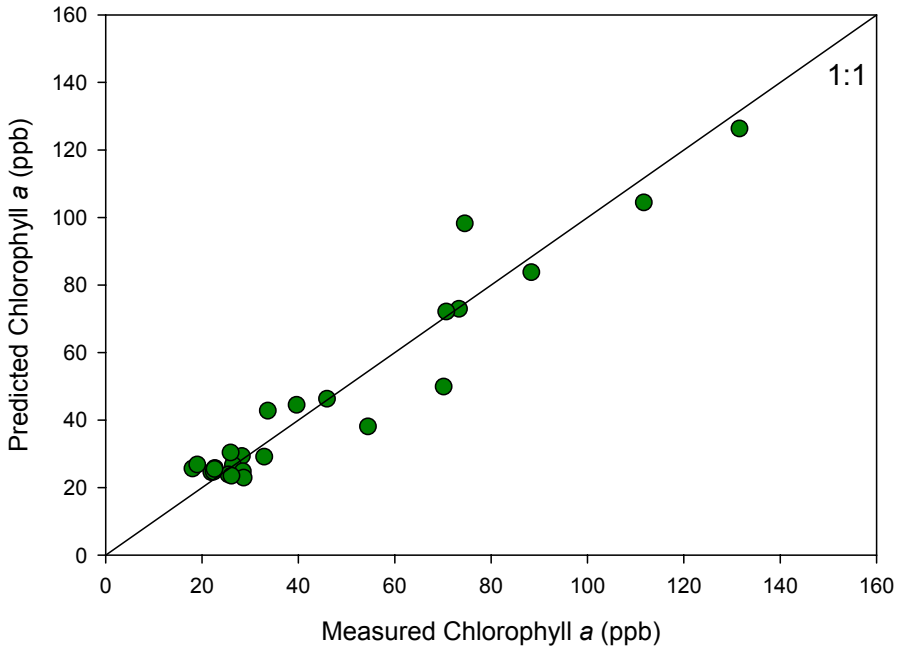

Figure 22a and b: (a) Morse Reservoir NIR:red algorithm index values versus analytically measured chlorophyll *a* concentrations (r^2=0.93) and (b) analytically measured chlorophyll *a* concentrations versus NIR:red algorithm estimated chlorophyll *a* concentrations excluding two outliers (RMSE=8.57).

The relationship between the NIR:red color ratio and analytically measured chlorophyll *a* concentrations for the combined dataset yielded an r^2 value of 0.71 ($p<0.0001$, $n=54$). To test the robustness of the algorithm, the data was divided into two sets, including a calibration set and a validation set. An aggregated dataset, including sampling sites from Morse and Geist Reservoirs, was divided in half by selecting every other sampling site, resulting in the calibration set. The remaining sites were used for validation. Each dataset was comprised of 26 sampling sites. A linear least-squares regression was used to relate the index values resulting from the empirical algorithm application to analytically measured chlorophyll *a* concentration (r^2 =0.71, $p<0.0001$, $n=26$; Figure 23a). Chlorophyll *a* concentration, [Chla], was derived for the validation set by the application of the regression equation obtained from the linear least-squares regression of the index value from $[R_{max}\lambda_{(695-715)}][R_{min}\lambda_{(665-685)}^{-1}]$ and the measured chlorophyll *a* concentration from the calibration dataset:

$$[Chla] = 78.71x - 81.33 \qquad \text{Equation 33}$$

Regression of measured to estimated chlorophyll *a* yielded slope and intercept values of 0.85 and 9.70 respectively (RMSE=20 ppb; Figure 23b). Omission of the two outliers from the Morse Reservoir dataset, sites 296 and 297, improved algorithm performance, yielding an r^2 value of 0.75 and reducing the RMSE to 16 ppb ($p<0.0001$, $n=24$).

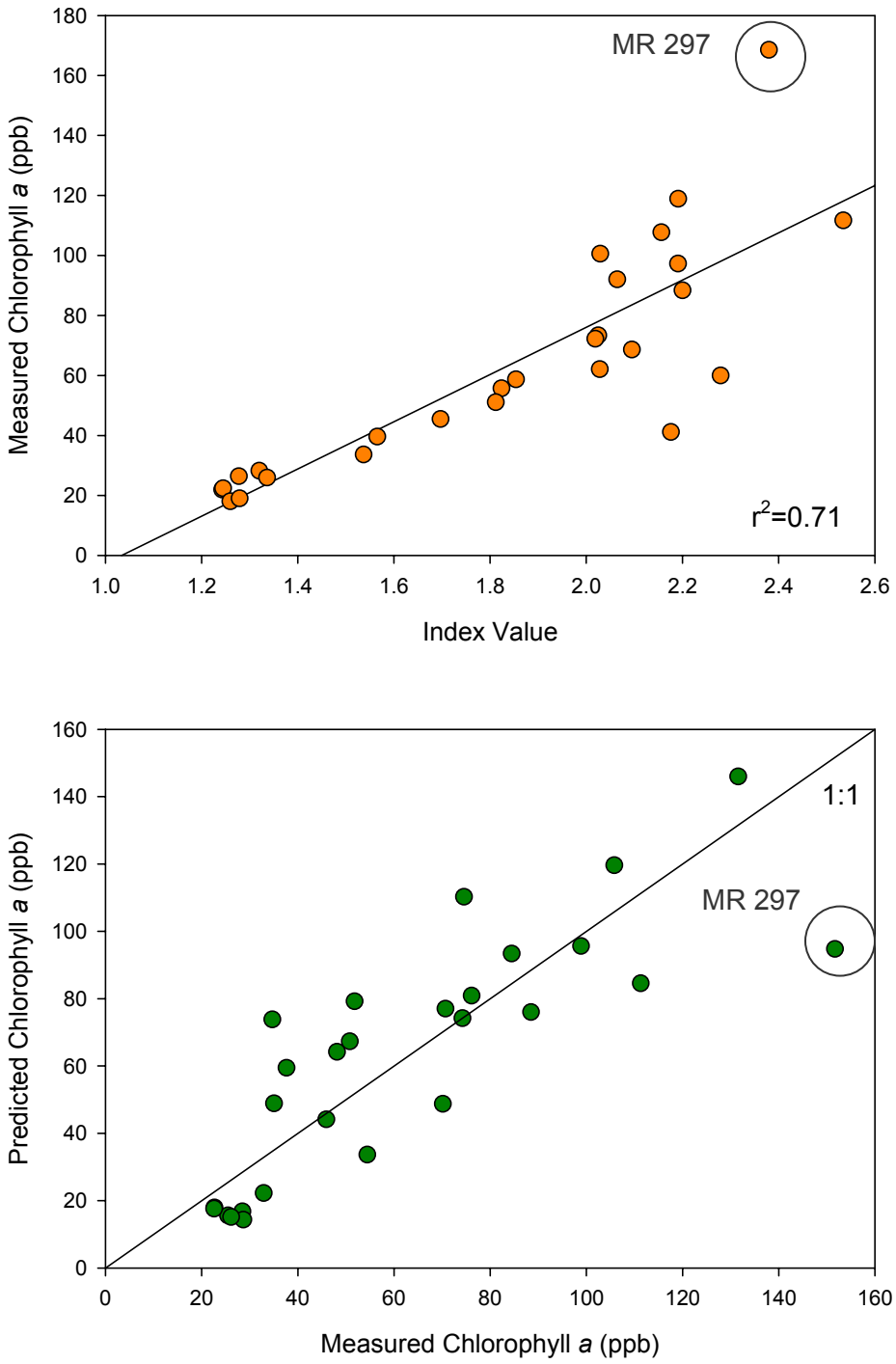

Figure 23a and b: (a) NIR:red algorithm index values from the training dataset (n=26) versus analytically measured chlorophyll *a* concentrations (r^2=0.71) and (b) analytically measured chlorophyll a concentrations versus NIR:red algorithm estimated chlorophyll *a* concentrations for the validation dataset (n=26).

Near-infrared Peak Algorithms

Estimation of chlorophyll *a* concentration using only the near-infrared peak feature was accomplished by utilizing the Reflectance Height (RH) and Sum (SUM) algorithms (Gitelson *et al.*, 2000). To employ the Reflectance Height algorithm ($RH_{670-730}$), the height of the NIR peak was measured from a baseline from 670 to 730 nm. The $SUM_{670-730}$ algorithm required the summation of all reflectance values within the NIR peak using the aforementioned baseline (Gitelson *et al.*, 2000). Two variations on the RH algorithm, $R_{(maxred)}/R_{max}\lambda_{(540-570)}$ and $R_{(maxred)}/R_{min}\lambda_{(665-685)}$, were applied to Geist and Morse data (Gitelson, 1992).

The strength of the relationship between $RH_{670-730}$ algorithm and analytically measured Geist and Morse Reservoir chlorophyll *a* concentrations yielded r^2 values of 0.41 (RMSE=20.15; Table 11; Figure 24) and 0.80 (RMSE=19.34; Table 11, Figure 25), respectively, nearly equal to those obtained using the NIR:red ratio. Reflectance Height algorithm variations, $R_{(maxred)}/R_{max}\lambda_{(540-570)}$ and $R_{(maxred)}/R_{min}\lambda_{(665-685)}$, consistently yielded weaker relationships between algorithm index values and measured pigments for both reservoirs and were not pursued further in the analysis (Table 11). Chlorophyll *a* concentration, [Chla], was obtained using coefficients from the linear least-squares regression of the index values from $RH_{670-730}$ and the measured chlorophyll *a* concentration, where:

$[Chla] = 102.42x - 47.33$ (Geist) and Equation 34

$[Chla] = 83.87x - 10.91$ (Morse) Equation 35

Table 11a and b: Performance summary for the NIR peak algorithms for prediction of chlorophyll *a* concentrations for (a) Geist ($p<0.001$, $n=27$) and (b) Morse Reservoirs ($p<0.0001$, $n=27$) including the slope and intercept of the regression equation for determining [Chla] Estimated, the slope and intercept of the linear relationship between [Chla] Measured and [Chla] Estimated with their corresponding standard errors of estimation (STE), the root mean square error (RMSE) of [Chla] Estimated, and the linear least-squares fit (r^2) of the model to [Chla] Measured.

(a) Geist	Chlorophyll *a* Empirical Algorithm	Slope, Intercept	Intercept (STE)	Slope (STE)	RMSE	r^2	Figure
NIR peak algorithms	$RH_{670-730}$	102.42 -47.33	41.85 (7.47)	0.41 (0.09)	20.15	0.41	Figure 24
	$R_{(maxred)}/R_{max}\lambda_{(540-570)}$	1.40 21.25	52.41 (6.70)	0.27 (0.09)	22.55	0.27	–
	$R_{(maxred)}/R_{min}\lambda_{(665-685)}$	0.60 21.91	51.72 (6.78)	0.28 (0.09)	22.40	0.28	–
	$SUM_{670-730}$	3.71 61.88	32.39 (7.54)	0.54 (0.09)	17.73	0.55	Figure 27

(b) Morse	Chlorophyll *a* Empirical Algorithm	Slope, Intercept	Intercept (STE)	Slope (STE)	RMSE	r^2	Figure
NIR peak algorithms	$RH_{670-730}$	83.87 -10.91	11.07 (5.52)	0.80 (0.08)	19.68	0.80	Figure 25
	$R_{(maxred)}/R_{max}\lambda_{(540-570)}$	2.27 -8.41	23.84 (6.80)	0.56 (0.10)	28.84	0.56	–
	$R_{(maxred)}/R_{min}\lambda_{(665-685)}$	1.12 -14.96	21.33 (6.69)	0.61 (0.10)	27.28	0.61	–
	$SUM_{670-730}$	2.83 -18.04	11.00 (5.51)	0.80 (0.08)	19.60	0.80	Figure 26

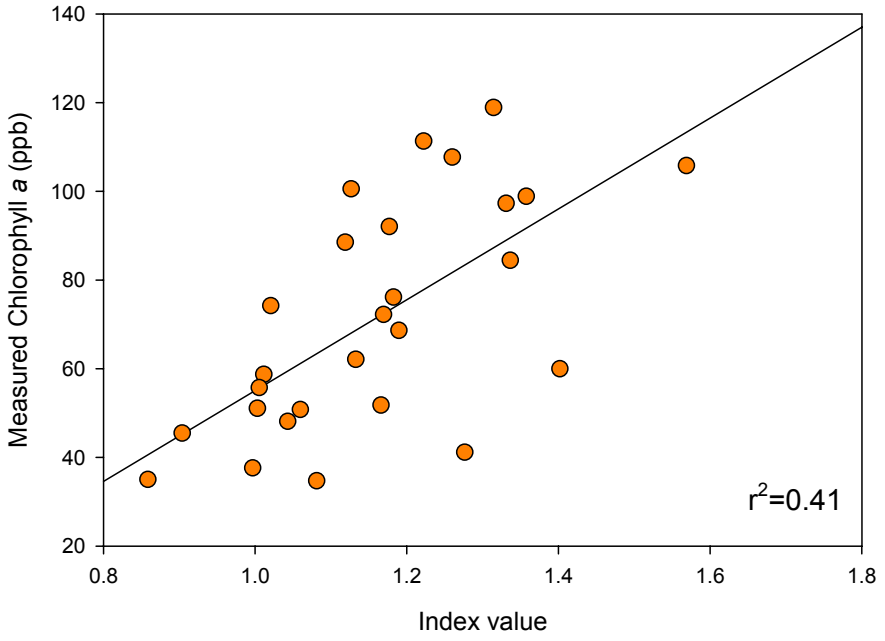

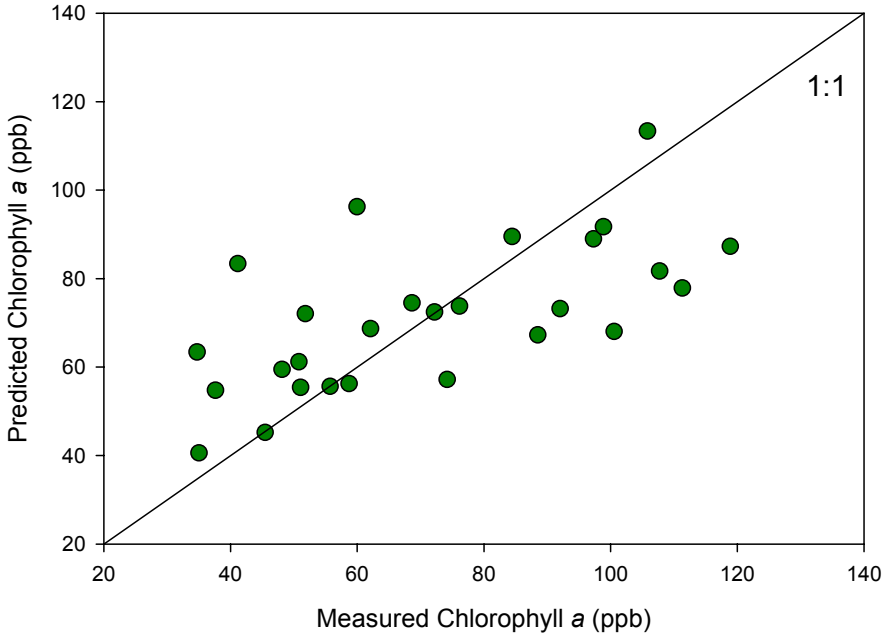

Figure 24a and b: (a) Geist Reservoir $RH_{670\text{-}730}$ algorithm index values versus analytically measured chlorophyll *a* concentrations (r^2=0.41) and (b) analytically measured chlorophyll *a* concentrations versus $RH_{670\text{-}730}$ algorithm estimated chlorophyll *a* concentrations (RMSE=20.15 ppb).

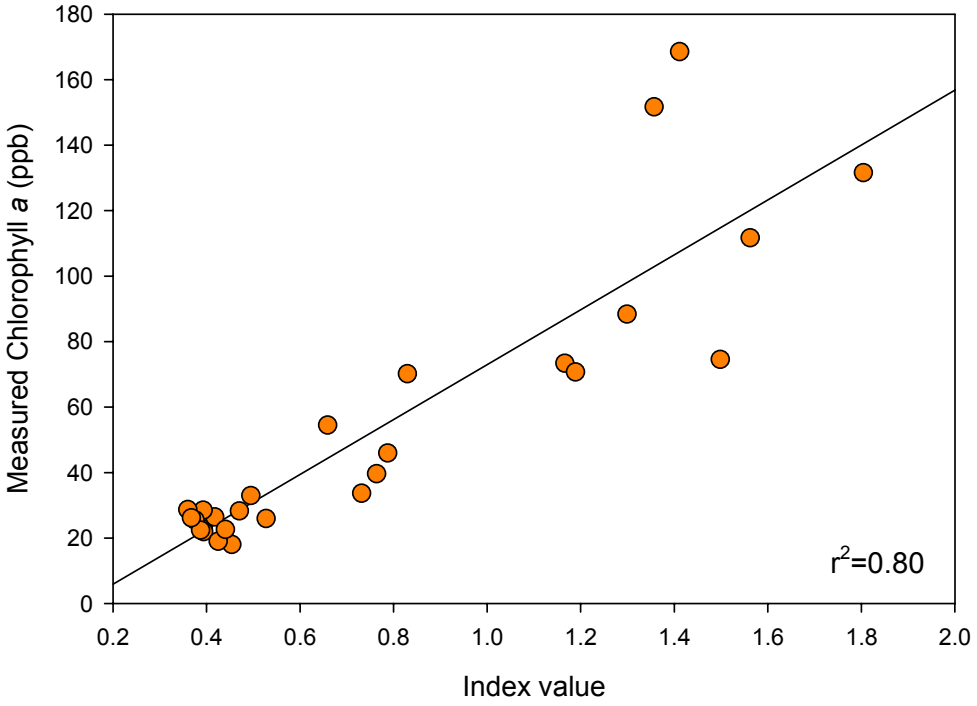

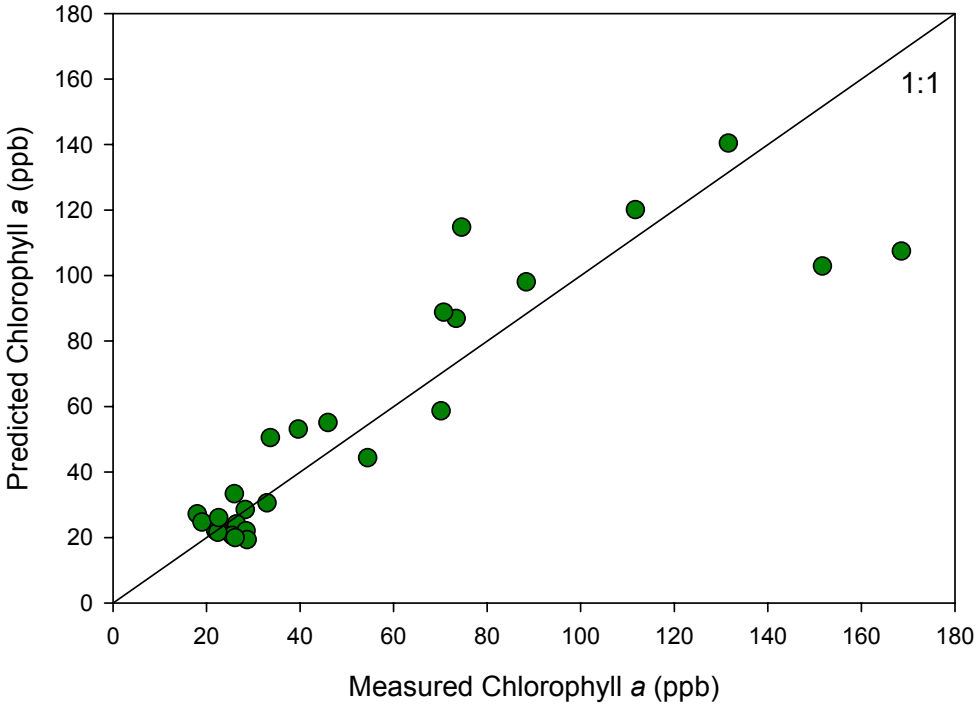

Figure 25a and b: (a) Morse Reservoir $RH_{670\text{-}730}$ algorithm index values versus analytically measured chlorophyll *a* concentrations (r^2=0.80) and (b) analytically measured chlorophyll *a* concentrations versus $RH_{670\text{-}730}$ algorithm estimated chlorophyll *a* concentrations (RMSE=19.68 ppb).

For Morse Reservoir, the Reflectance Height and Sum algorithms performed equally well, both yielding a relatively strong relationship between measured chlorophyll *a* concentration and algorithm indices (r^2=0.80; Table 11; Figure 25a; Figure 26a) and nearly equal RMSE between measured and estimated chlorophyll *a* concentrations (19.68 and 19.60 ppb, respectively; Table 11; Figure 25b; Figure 26b). Concentration of chlorophyll *a* in Geist Reservoir however, was most accurately estimated using the SUM algorithm, yielding the strongest relationship between the algorithm index and measured chlorophyll *a* concentrations (r^2=0.55; Table 11; Figure 27a) and the lowest RMSE (RMSE=17.73; Table 11; Figure 27b) for the Geist dataset. These results suggest that the Sum algorithm, compared to the Reflectance Height algorithm, more efficiently accounts for small variability in chlorophyll *a* pigment concentration, likely because it utilizes information about the NIR feature as a whole, rather than only in a single band. More extreme differences in concentrations of chlorophyll *a,* as seen in the Morse dataset (Figure 28), can be deciphered using only peak height since change in peak height is also significant between samples. The only slight height differences in the spectra of Geist Reservoir, yet more significant change in width of the NIR feature lend explanation for the improved performance of the Sum algorithm (Figure 29).

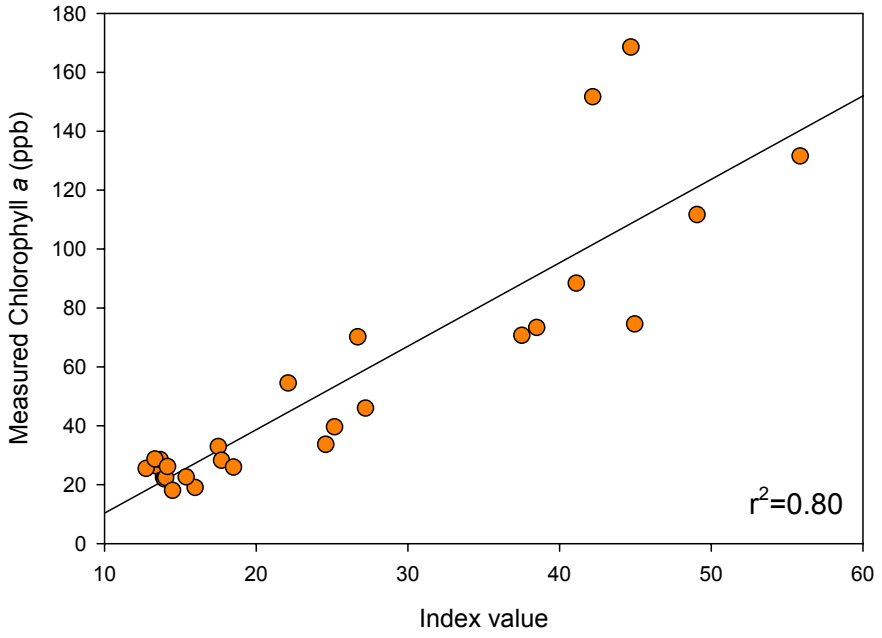

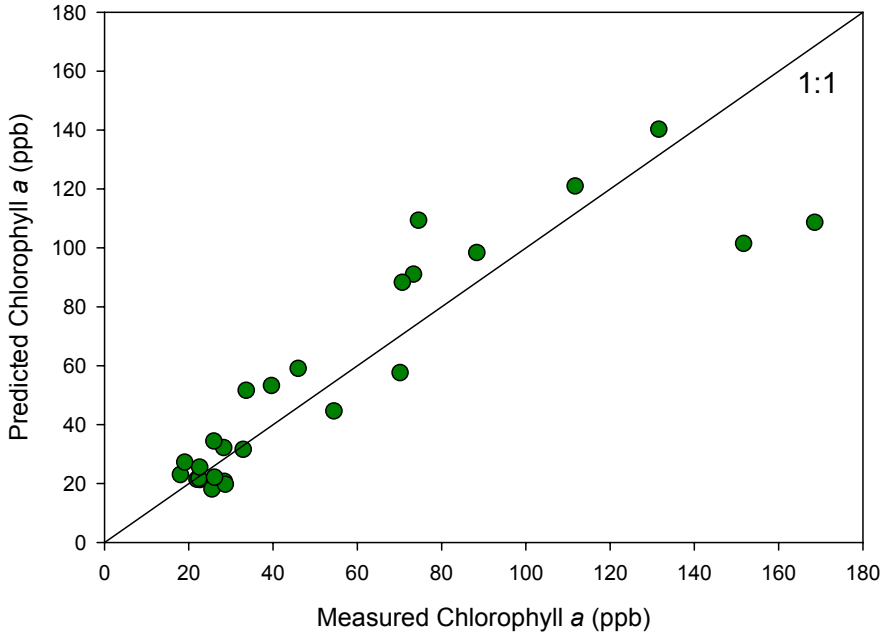

Figure 26a and b: (a) Morse Reservoir $SUM_{670-730}$ algorithm index values versus analytically measured chlorophyll *a* concentrations (r^2=0.80) and (b) analytically measured chlorophyll *a* concentrations versus $SUM_{670-730}$ algorithm estimated chlorophyll *a* concentrations (RMSE=19.60 ppb).

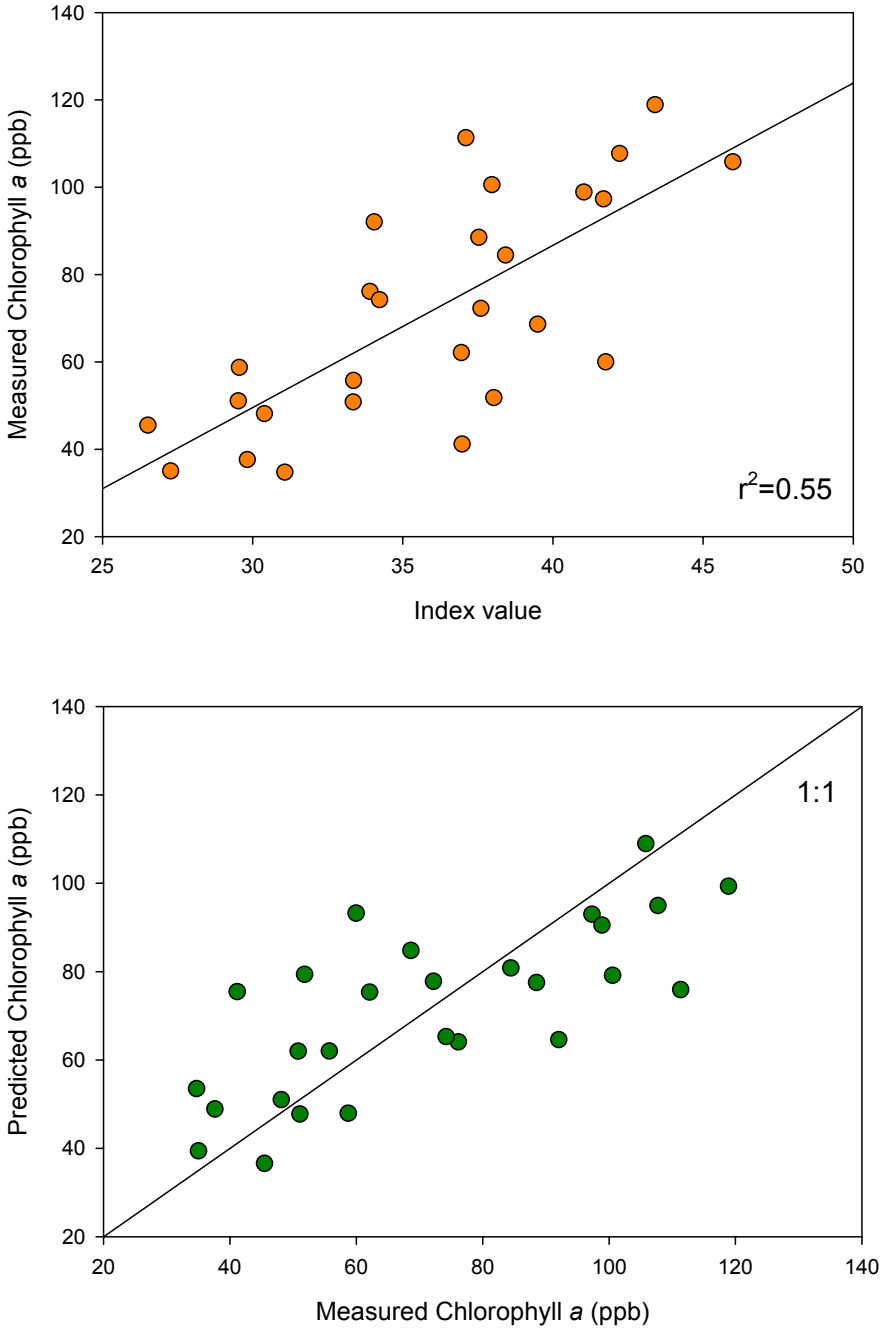

Figure 27a and b: (a) Geist Reservoir $SUM_{670-730}$ algorithm index values versus analytically measured chlorophyll *a* concentrations (r^2=0.55) and (b) analytically measured chlorophyll *a* concentrations versus $SUM_{670-730}$ algorithm estimated chlorophyll *a* concentrations (RMSE=17.73 ppb).

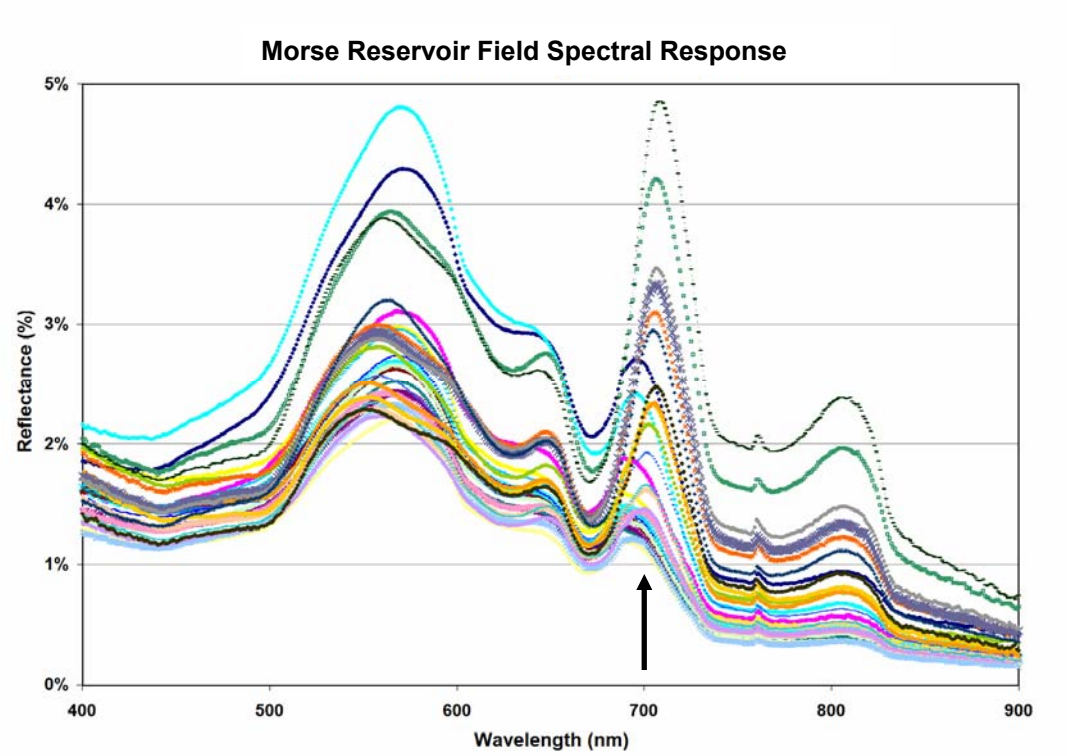

Figure 28: Morse Reservoir spectral responses show significant variability in NIR peak height. (NIR feature indicated by arrow.)

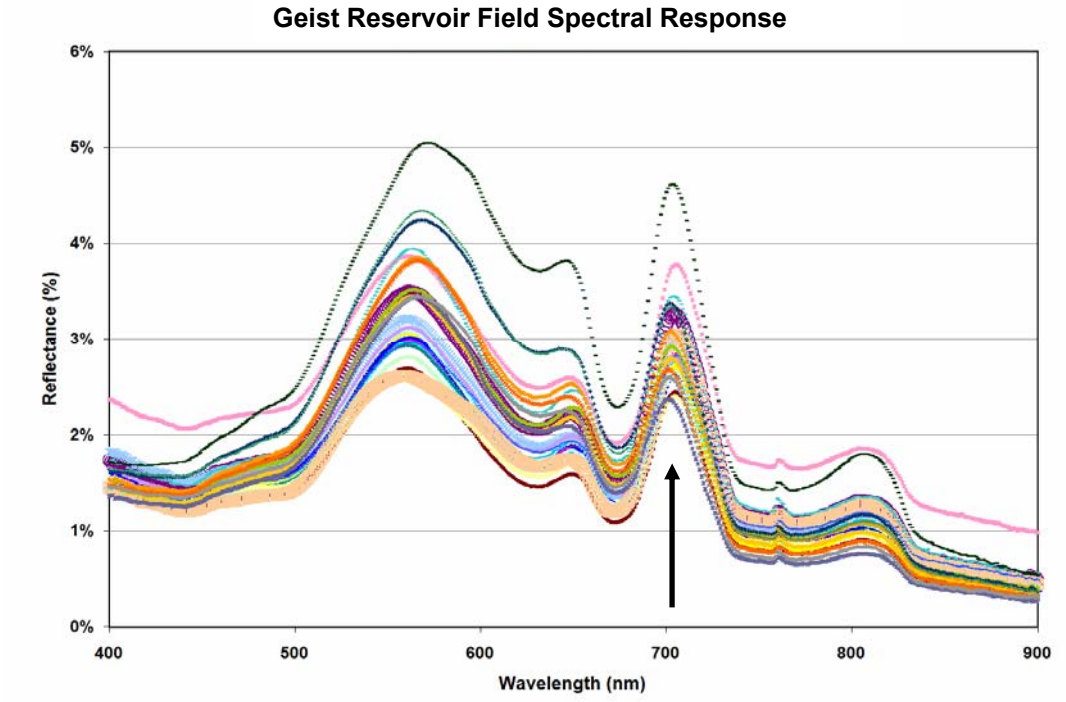

Figure 29: Geist Reservoir spectral response shows little variability in NIR peak height. (NIR feature indicated by arrow.)

Residuals of observed to SUM and Reflectance Height estimated chlorophyll *a* concentrations for Morse Reservoir showed strong positive correlations with TSS and turbidity, yielding a r^2 values of 0.70 and 0.80 respectively, as was seen in the NIR:red residual analysis for Morse data. Again, the models underestimated chlorophyll *a* concentration for the two outlying sites, sites 296 and 297, by more than 50 ppb. The results of the residual analysis indicate high algal turbidity and low non-algal turbidity at Morse, as was seen with the strong relationship between pigment concentration and turbidity and TSS measurements (Figure 16b and d).

To test the robustness of the Reflectance Height and SUM algorithms, the combined reservoir data was divided into a calibration set (n=26) and a validation set (n=26). A linear least-squares regression was used to relate the index values resulting from the empirical algorithm application to analytically measured chlorophyll *a* concentrations, resulting in r^2 values of 0.68 and 0.72 for the Reflectance Height and SUM algorithms respectively ($p<0.0001$, n=26; Figure 30a; Figure 31a). Chlorophyll *a* concentration, derived for the validation set by the application of the regression equation obtained from the linear least-squares regression of the index value from $RH_{670\text{-}730}$ and $SUM_{670\text{-}730}$ and the measured chlorophyll *a* concentration from the calibration dataset, yielded RMSE of 22 and 20 ppb, respectively.

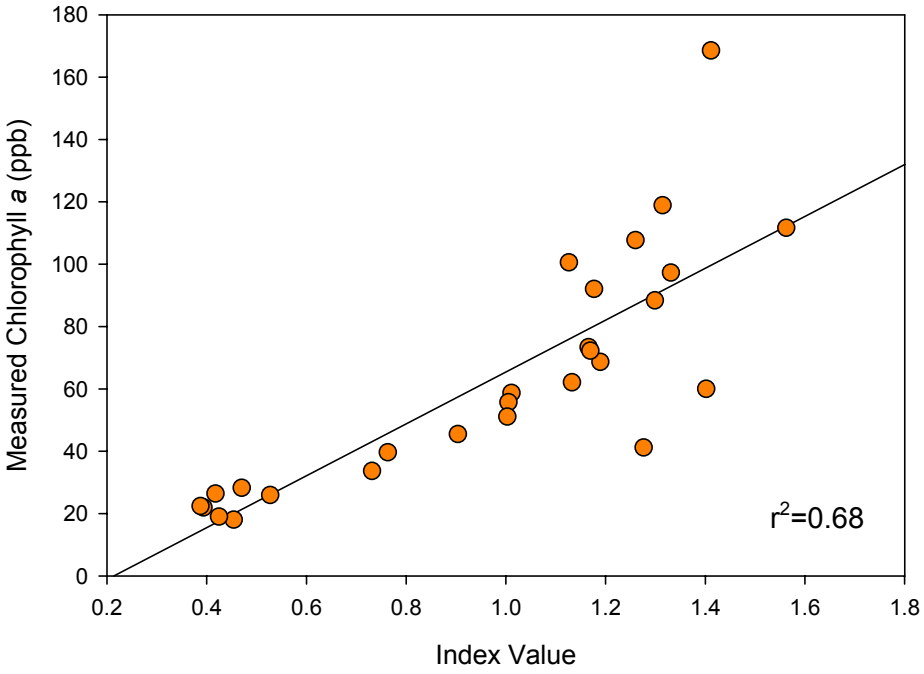

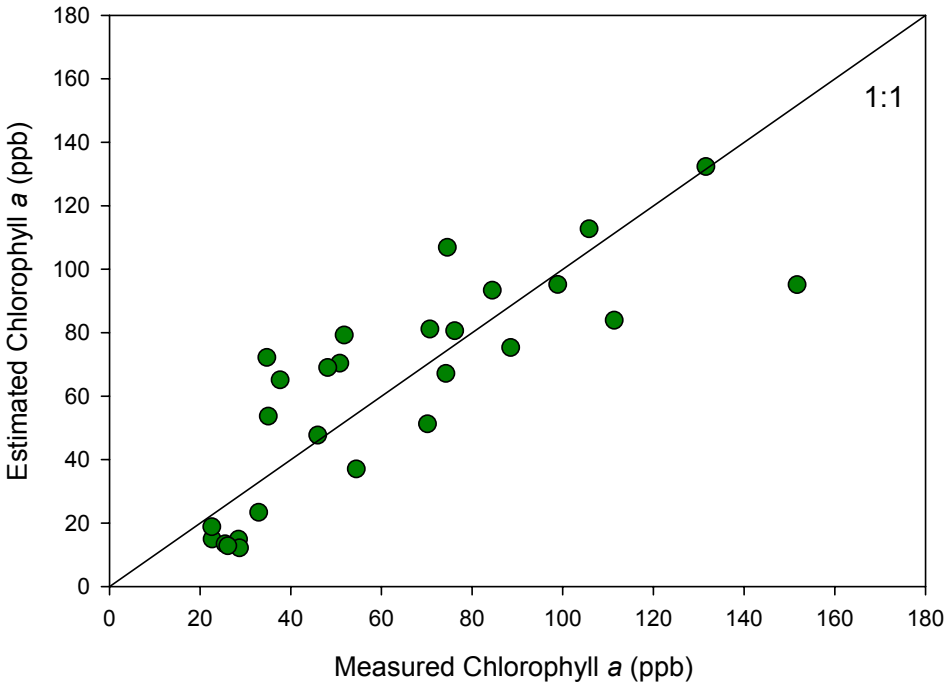

Figure 30a and b: (a) $RH_{670\text{-}730}$ algorithm index from the Morse and Geist training dataset (n=26) versus analytically measured chlorophyll *a* concentrations (ppb) (r^2=0.68) and (b) analytically measured chlorophyll a concentrations versus $RH_{670\text{-}730}$ algorithm estimated chlorophyll a concentrations for a validation dataset (RMSE 22 ppb, n=26).

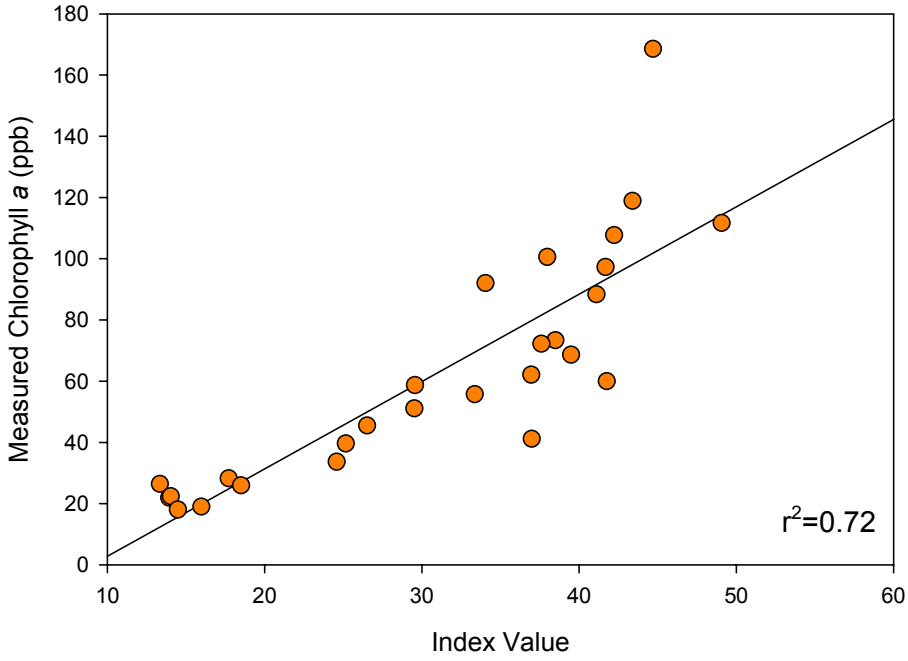

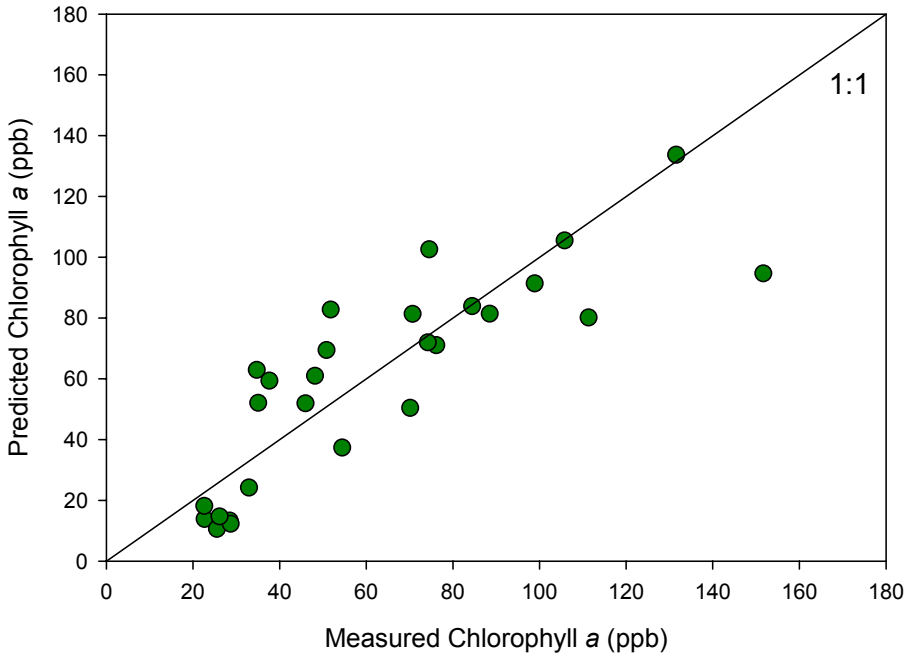

Figure 31a and b: (a) $SUM_{670\text{-}730}$ algorithm index from the Morse and Geist training dataset (n=26) versus analytically measured chlorophyll *a* concentrations (ppb) (r^2=0.72) and (b) analytically measured chlorophyll *a* concentrations versus $SUM_{670\text{-}730}$ algorithm estimated chlorophyll *a* concentrations for a validation dataset (RMSE 20 ppb, n=26).

Color ratio and band combination algorithms for estimation of Phycocyanin concentration

Phycocyanin estimation was completed through the implementation of a band ratio, introduced by Schalles and Yacobi (2000), and three-band combination method by Dekker (1993). Both utilize the bands of maximum absorption (at approximately 620 nm) and fluorescence (at approximately 645 nm) for phycocyanin.

Implementation of the Schalles and Yacobi (2000) color ratio algorithm of the form $R(\lambda_2)/ R(\lambda_1)$, where $R(\lambda_2)$ was chosen as $R_{max}\lambda_{(640\text{-}660)}$ and $R(\lambda_1)$ as $R_{min}\lambda_{(615\text{-}635)}$, to Geist and Morse Reservoirs yielded a r^2 values of 0.67 and 0.51, respectively (Table 12; Figure 32a; Figure 33a). For both Geist and Morse, the Dekker (1993) algorithm proved to have the lowest predictive power, yielding r^2 values of 0.10 (RMSE=39 ppb) and 0.32 (RMSE=21 ppb), respectively (Table 12). The Dekker (1993) algorithm was not pursued for further analysis.

Derivation of phycocyanin concentration, [PC], using the Schalles and Yacobi (2000) algorithm, required application of the equation obtained from the linear least-squares regression of the index value from $[R_{max}\lambda_{(695\text{-}715)}][R_{min}\lambda_{(665\text{-}685)}{}^{-1}]$ and the measured phycocyanin concentration, where:

$[PC] = 1035.7x - 1021.0$ (Geist) and Equation 36

$[PC] = 932.67x - 908.83$ (Morse) Equation 37

Root-mean-square error of the measured to Schalles and Yacobi (2000) algorithm estimated pigment concentrations for Geist and Morse Reservoirs was 24 and 32 ppb, respectively (Table 12; Figure 32b; Figure 33b).

Table 12a and b: Performance summary for the Schalles and Yacobi (2000) band ratio and Dekker (1993) band combination algorithms for prediction of phycocyanin concentration for (a) Geist Reservoir (n=25) and (b) Morse Reservoir (n=24) including the slope and intercept of the regression equation for estimating [PC], the slope and intercept of the linear relationship between [PC] Measured and [PC] Estimated with their corresponding standard errors of estimation (STE), RMSE of the [PC] Estimated value, and linear least-squares fit of the model to [PC] Measured (r^2).

(a) Geist	Phycocyanin empirical algorithm	Peak reflectance location	Trough reflectance location	Slope Intercept	Intercept (STE)	Slope (STE)	RMSE	r^2	figure
Band ratio and Combination Algorithms	$[R_{max}\lambda_{(640-660)}][R_{min}\lambda_{(615-635)}^{-1}]$	$646<R(\lambda_2)<651$	$626<R(\lambda_2)<633$	1035.7 -1021.0	30.17 (9.76)	0.66 (0.09)	23.72	0.67	Figure 32a
	0.5[R(600)+R(648)]-R(624)	–	–	32657.9 193.3	81.8 (6.34)	0.10 (0.06)	39.05	0.10	–

(b) Morse	Phycocyanin empirical algorithm	Peak reflectance location	Trough reflectance location	Slope Intercept	Intercept (STE)	Slope (STE)	RMSE	r^2	figure
Band ratio and Combination Algorithms	$[R_{max}\lambda_{(640-660)}][R_{min}\lambda_{(615-635)}^{-1}]$	$649<R(\lambda_2)<653$	$626<R(\lambda_2)<640$	932.67 -908.83	20.76 (6.52)	0.51 (0.11)	31.94	0.51	Figure 33
	0.5[R(600)+R(648)]-R(624)	–	–	99235.79 -39.8851	29.16 (0.32)	0.31 (0.09)	37.85	0.32	–

Algorithm application to Geist data yielded two outliers, sampling sites 241 and 249 (Figure 32a). For these sites, residuals of measured to estimated phycocyanin concentrations did not yield a strong relationship to TSS or turbidity, however both sites measured higher than average TSS concentrations of 26 and 29 mg/L respectively. The model underestimated phycocyanin concentration by more than 47 ppb for both sampling sites. Omission of the outliers from the dataset yielded an r^2 value of 0.78 and RMSE of 19 ppb ($p<0.0001$, $n=23$; Figure 34).

When applied to Morse Reservoir data the algorithm resulted in one extreme outlier, sampling site 298, with a residual of 97 ppb (Figure 33a). Site 298 showed the highest measured turbidity recorded for Morse reservoir of 30 NTU and the highest TSS concentration overall of 54 mg/L. Omission of this site improves the predictive power of the Schalles and Yacobi (2000) algorithm, resulting in an r^2 value of 0.66, with a RMSE of 19.96 ppb ($p<0.0001$, $n=24$; Figure 35).

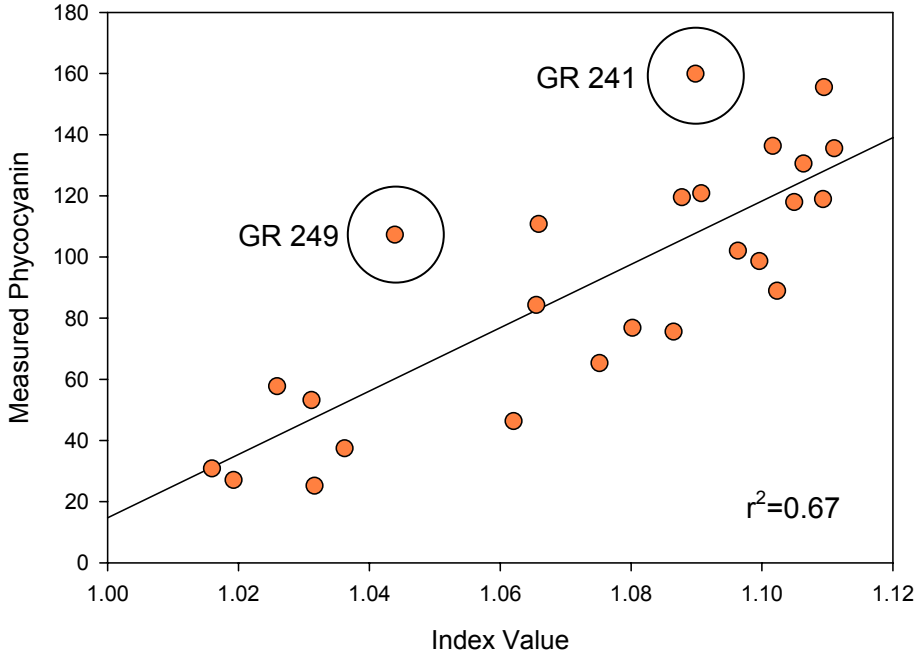

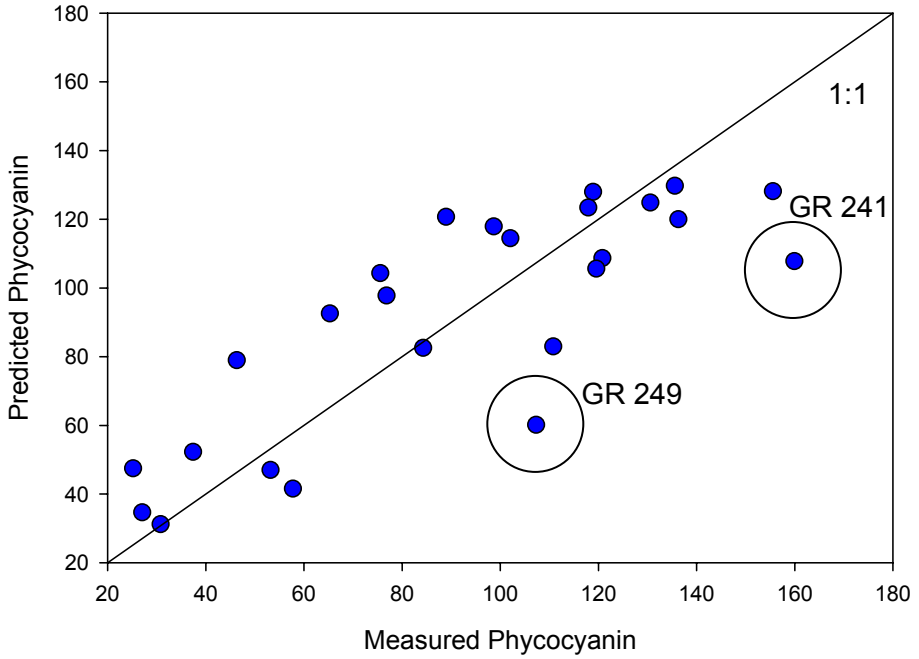

Figure 32a and b: (a) Geist Reservoir Schalles and Yacobi (2000) algorithm index values versus measured phycocyanin concentrations (r^2=0.67, n=25) and (b) measured phycocyanin concentrations versus the Schalles and Yacobi (2000) algorithm estimated phycocyanin concentrations (RMSE=24 ppb).

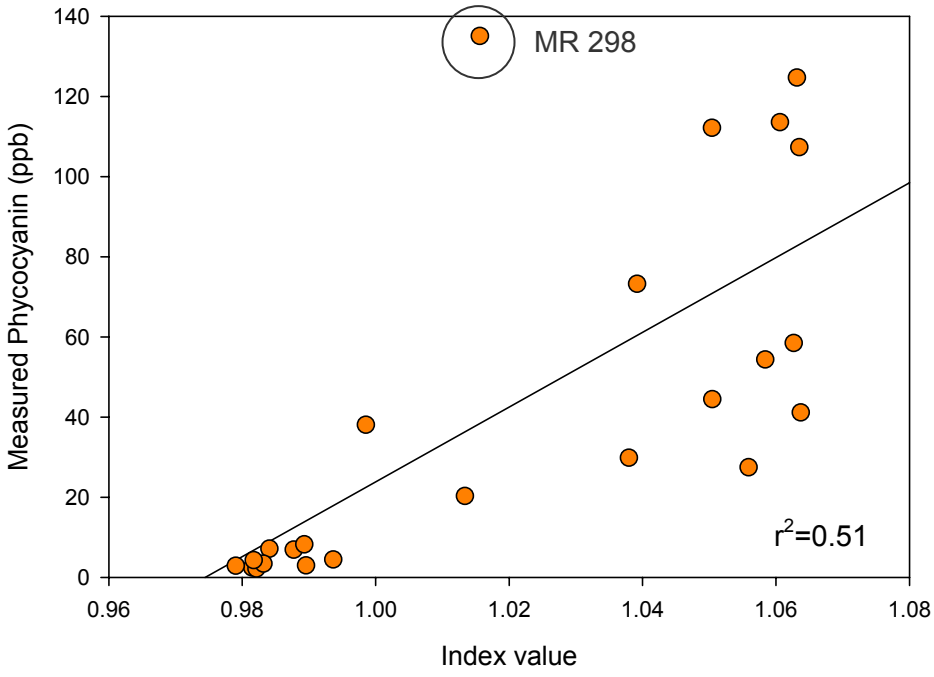

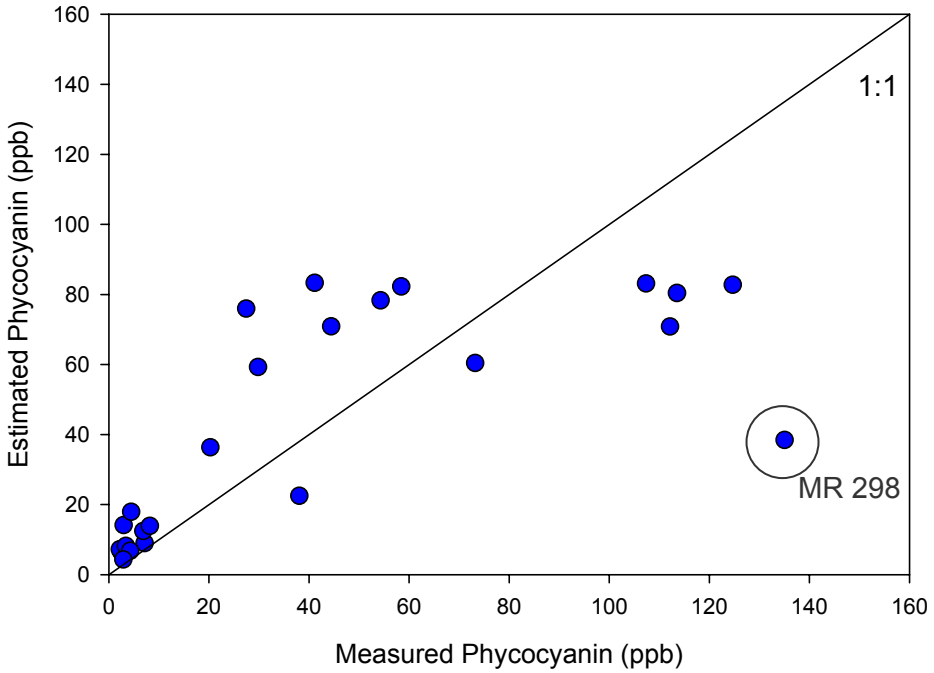

Figure 33a and b: (a) Morse Reservoir Schalles and Yacobi (2000) algorithm index values versus measured phycocyanin concentrations (r^2=0.67, n=24) and (b) measured phycocyanin concentrations versus the Schalles and Yacobi (2000) algorithm estimated phycocyanin concentrations (RMSE=23.72 ppb).

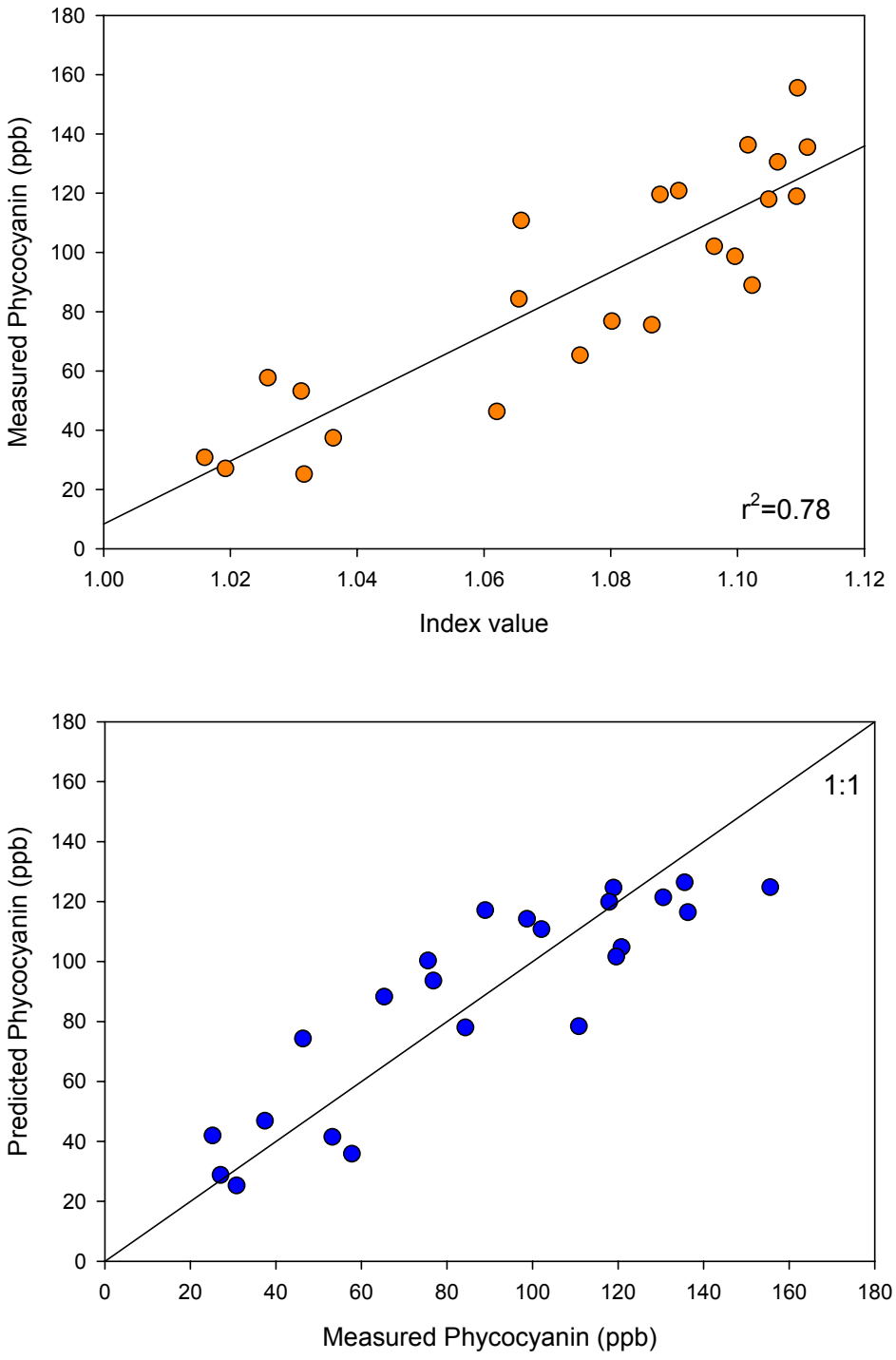

Figure 34a and b: (a) Geist Reservoir Schalles and Yacobi (2000) algorithm index values versus measured phycocyanin concentrations (ppb) (r^2=0.78; n=23) and (b) measured phycocyanin concentrations versus Schalles and Yacobi (2000) algorithm estimated phycocyanin concentrations excluding two outliers (RMSE=19 ppb).

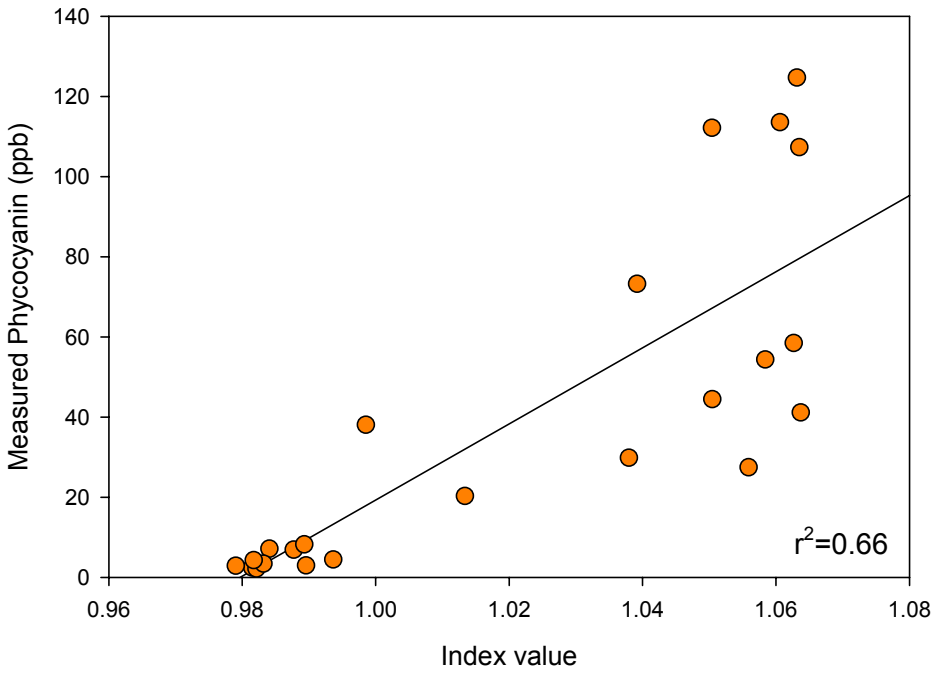

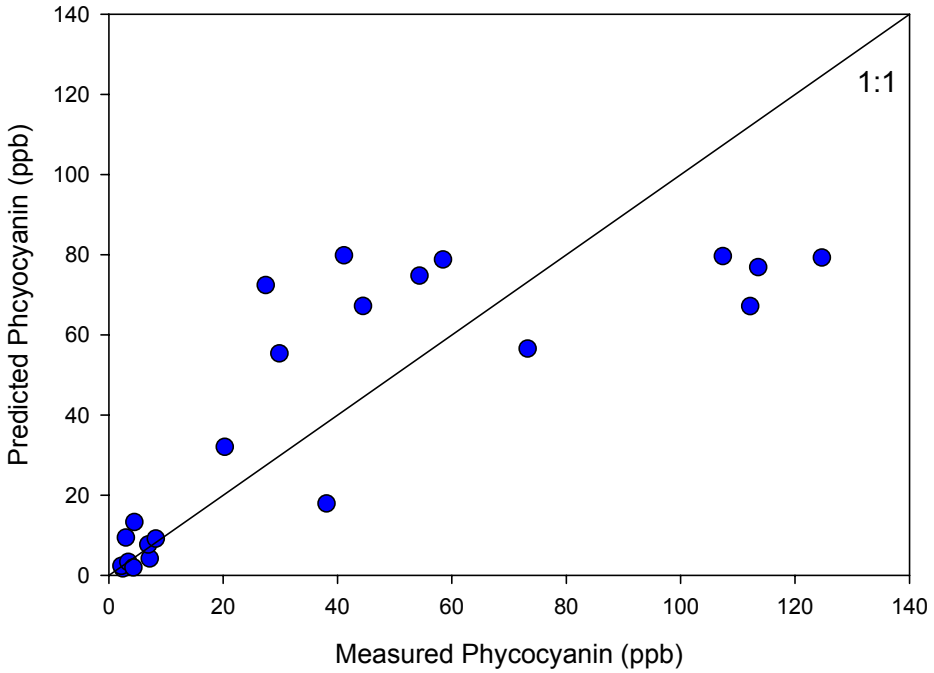

Figure 35a and b: (a) Morse Reservoir Schalles and Yacobi (2000) algorithm index values versus measured phycocyanin concentrations (ppb) (r^2=0.66, n=23) and (b) measured phycocyanin concentrations versus Schalles and Yacobi (2000) algorithm estimated phycocyanin concentrations excluding one outlier (RMSE=19.96 ppb).

When applied to a combined dataset, the relationship between the Schalles and Yacobi (2000) color ratio and analytically measured phycocyanin concentration (ppb) was relatively good, yielding an r^2 value of 0.70 ($p<0.0001$, $n=48$). To test the robustness of the algorithm, the data was divided into a calibration and validation set, both comprised of 24 sampling sites. The linear least-squares regression used to relate the index values resulting from the empirical algorithm application to analytically measured phycocyanin concentration resulted in an r^2 value of 0.74 ($p<0.0001$, $n=26$; Figure 36a). Phycocyanin concentration, [PC], was derived for the validation set by the application of the regression equation obtained from the linear least-squares regression of the index value from $[R_{max}\lambda_{(640-660)}][R_{min}\lambda_{(615-635)}^{-1}]$ and the measured phycocyanin concentration from the calibration dataset:

$$[PC] = 1013.76x - 995.25 \qquad \text{Equation 38}$$

Application of the Schalles and Yacobi (2000) color ratio algorithm to an aggregated dataset resulted in the same Morse Reservoir extreme outlier, sampling site 298, with a residual of 82 ppb. Omission of this site improved the predictive power of the Schalles and Yacobi (2000) algorithm for the validation dataset, yielding a RMSE of 18.91 ppb ($p<0.0001$, $n=23$).

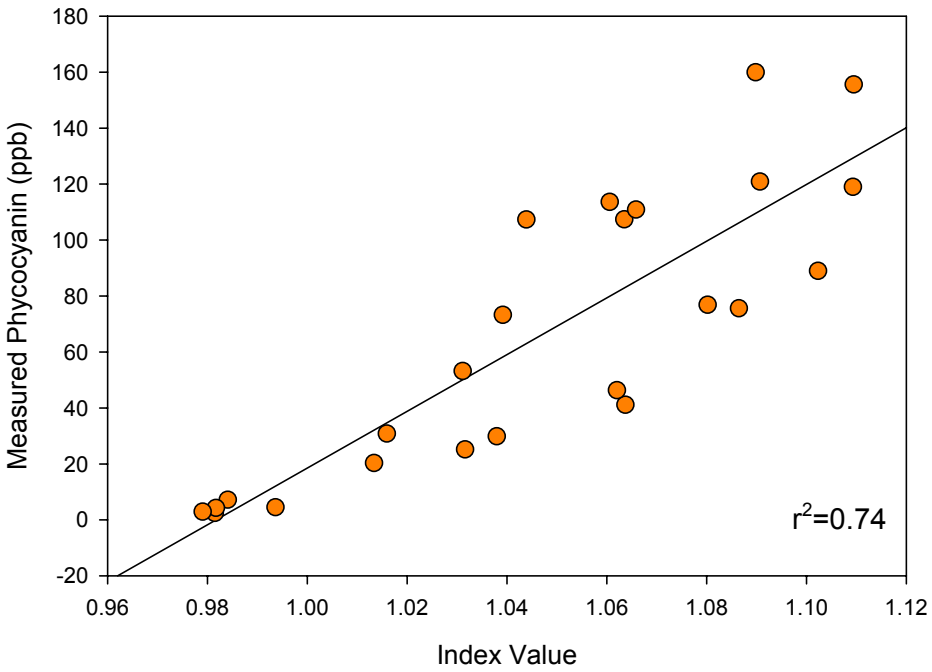

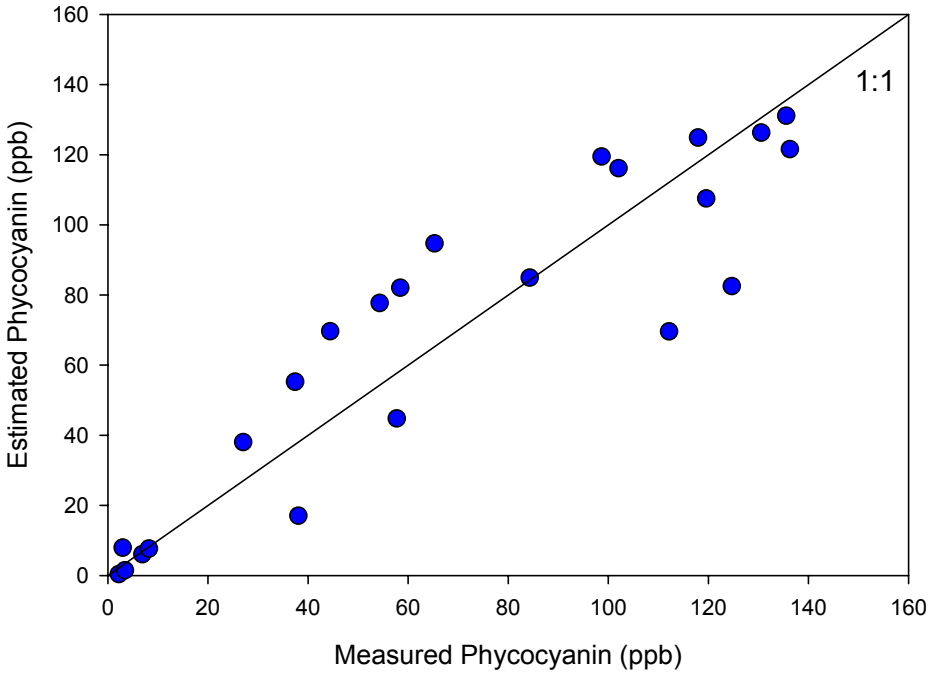

Figure 36and b: (a) Schalles and Yacobi (2000) algorithm index values from the training dataset (n=24) versus measured phycocyanin concentrations (ppb) (r^2=0.74) and (b) measured phycocyanin concentrations versus Schalles and Yacobi (2000) algorithm estimated phycocyanin concentrations for a validation dataset (RMSE=26 ppb, n=24 including outlying site).

Semi-empirical Algorithms

Chlorophyll a

A modified version of the Simis *et al.* (2005) algorithm was implemented for estimation of the chlorophyll *a* absorption coefficient at 665 nm, $a_{chl}(665)$ and ultimately the concentration of chlorophyll *a* for Geist and Morse Reservoir data:

$a_{chl}(665) = (\{[R(709)/R(665)] \times [a_w(709) + b_b]\} - b_b - a_w(665))$

Where:

b_b = $[a_w(778)\ \alpha\ R(778)] \times [(\gamma' - R(778))^{-1}]$
(Gordon, 1988; Gons, 1999; Astoreca *et al.,* 2006)

$a_w(778)$ = 2.71 m^{-1} (Buitevled *et al.*, 1994)

α = 0.60, constant accounting for refraction and reflection at the water's surface (Gordon, 1988; Astoreca *et al.*, 2006)

γ' = 0.082, accounts for the reflectance-IOP model, taken from Astoreca *et al.*, 2006 (based on Gordon, 1988)

Adapted from Simis *et al.* (2005)

Application of the Simis *et al.* (2005) algorithm for retrieval of the chlorophyll *a* absorption coefficient $a_{chl}(665)$ to Geist Reservoir data yielded a low r^2 value of 0.41 from the linear least-squares regression of $a_{chl}(665)$ to measured chlorophyll *a* (Table 13; Figure 37a). Estimated chlorophyll *a* concentration, [Chla], was obtained using the chlorophyll *a* specific absorption coefficient at 665 nm, $a^*_{chl}(665)$, as reported by Simis *et al.* (2005) for Lake Loosedrect data. Concentration of chlorophyll *a* was then determined from:

$$[Chla] = a_{chl}(665)(m^{-1})/a^*_{chl}(665)(m^2\ mg\ pigment^{-1}) \quad \text{Equation 39}$$

Where:

$a^*_{chl}(665)$ = 0.0153, specific absorption coefficient of chlorophyll *a* at 665 nm (taken from Simis *et al.* (2005) Lake Loosedrect data)

Simis *et al.* (2005) estimated chlorophyll *a* yielded a RMSE of 21 ppb (n=27, p<0. 001; Table 13; Figure 37b). The average residual value of measured to estimated chlorophyll *a* concentration for Geist Reservoir was 15.71 ppb, with minimum and maximum residuals of 1.27 and 45.56 ppb, respectively (Table 13; Figure 37). No strong relationship was determined between the Geist Reservoir residual values and other optically active constituents; however the two outlying sites with the highest residual values (sites 236 and 239) also proved to have the highest analytically measured chlorophyll *a* concentrations. For both sites, the model underestimated chlorophyll *a* concentration.

The Simis *et al.* (2005) algorithm proved more successful for retrieval of the chlorophyll *a* absorption coefficient $a_{chl}(665)$ from Morse Reservoir data, yielding a higher r^2 value of 0.79 from the linear least-squares regression of $a_{chla}(665)$ to analytically measured chlorophyll *a* concentration (Table 13; Figure 38a).

Morse Reservoir measured to estimated chlorophyll *a* yielded RMSE of 20 ppb (p<0.0001, n=27; Table 13; Figure 38b). The average residual value of measured to estimated chlorophyll *a* concentration for Morse Reservoir was 13.63 ppb, with minimum and maximum residuals of 1.99 and 59.15 ppb, respectively (Table 13; Figure 38). Like Geist, no strong relationships were found between the Morse Reservoir residual values and other optically active constituents and, yet again, two outlying sites with the highest residual values (sites 296 and 297) also proved to have the highest analytically measured chlorophyll *a* concentrations. The Simis *et al.* (2005) algorithm underestimated the chlorophyll *a* concentrations for both sampling sites.

When applied to a combined dataset, an r^2 value of 0.69 was obtained from the linear least-squares regression of Simis *et al.* (2005) estimated $a_{Chla}(665)$ to analytically measured chlorophyll *a* (Table 13; Figure 39a). The combined dataset yielded a RMSE of 21 ppb ($p<0.0001$, $n=54$) (Table 13; Figure 39b).

Table 13: Performance summary for the Simis *et al.* (2005) algorithm for estimation of chlorophyll *a* concentration for Geist and Morse Reservoirs and for a combined dataset, including the slope and intercept of the linear relationship between [Chla] Measured and [Chla] Estimated with their corresponding standard errors of estimation (STE), the root-mean-square error (RMSE) of [Chla] Estimated, and the linear least-squares fit (r^2) of $a_{chl}(665)$ to [Chla] Measured.

	Reservoir	Intercept (STE)	Slope (STE)	RMSE (ppb)	r^2 (p-value)	min/max residuals (ppb)	Average Residual (ppb)	n	figure
Simis *et al.* (2005) Semi-empirical algorithm	Geist	41.67 (6.07)	0.33 (0.08)	21.49	0.41 p<0.001	1.27 45.56	15.71	27	Figure 37
	Morse	17.60 (5.19)	0.74 (0.07)	20.32	0.79 p<0.0001	1.99 59.15	13.63	27	Figure 38
	Combined	22.61 (4.16)	0.62 (0.06)	20.51	0.69 p<0.0001	–	–	54	Figure 39

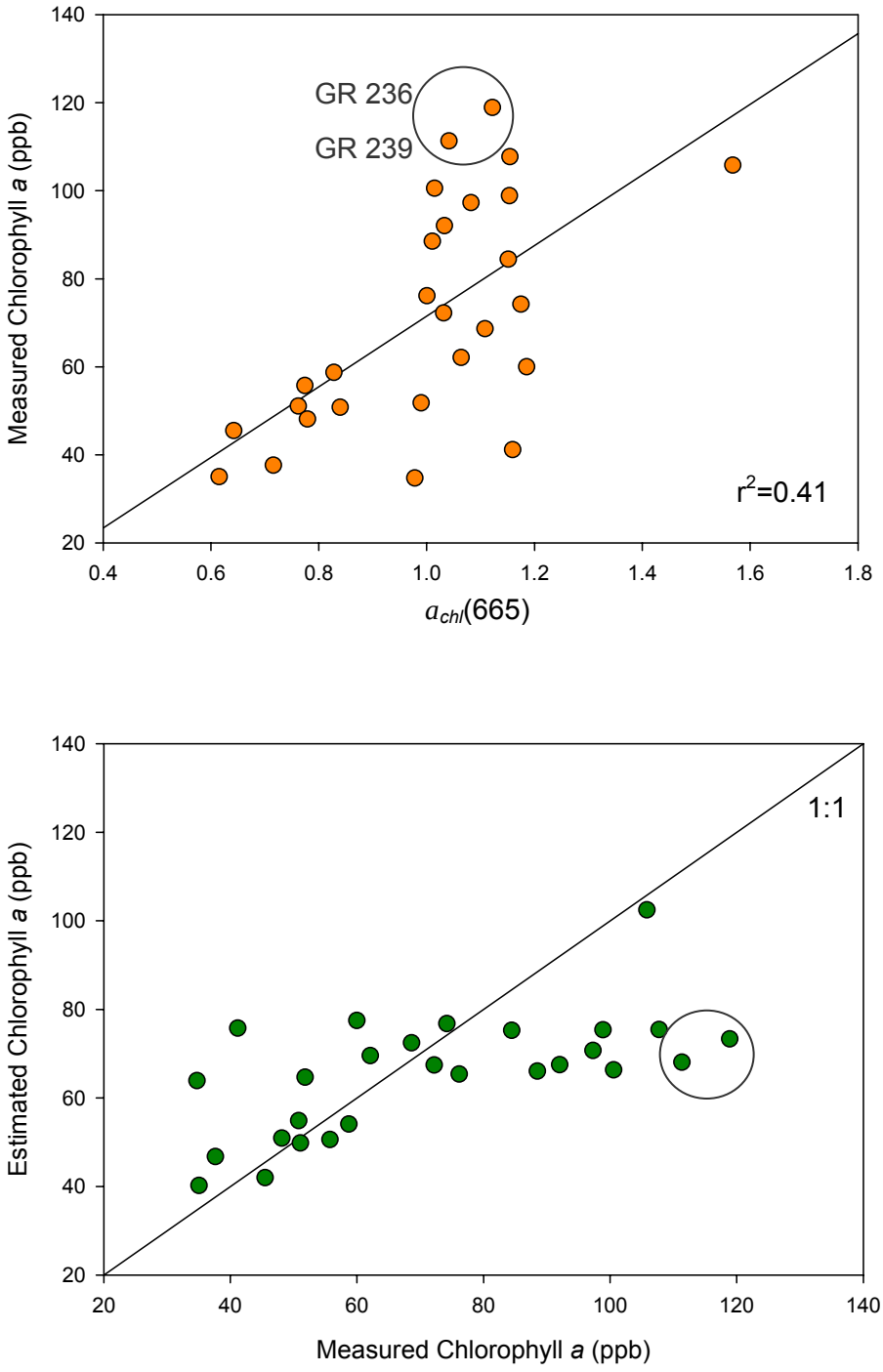

Figure 37and b: (a) Geist Reservoir Simis *et al.* (2005) algorithm derived absorption coefficients for chlorophyll *a* at 665 nm, a_{chl}(665) versus analytically measured chlorophyll *a* concentrations (r^2=0.41) and (b) analytically measured chlorophyll *a* concentrations versus estimated concentrations using a^*_{Chl}(665) (RMSE=21.49 ppb). The circle identifies the site with the largest residual.

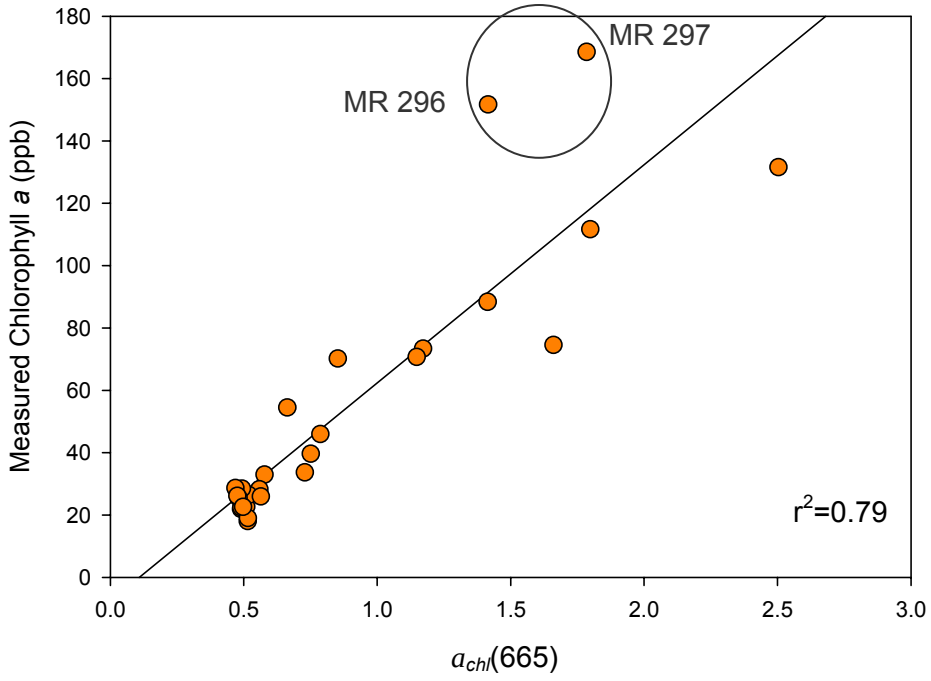

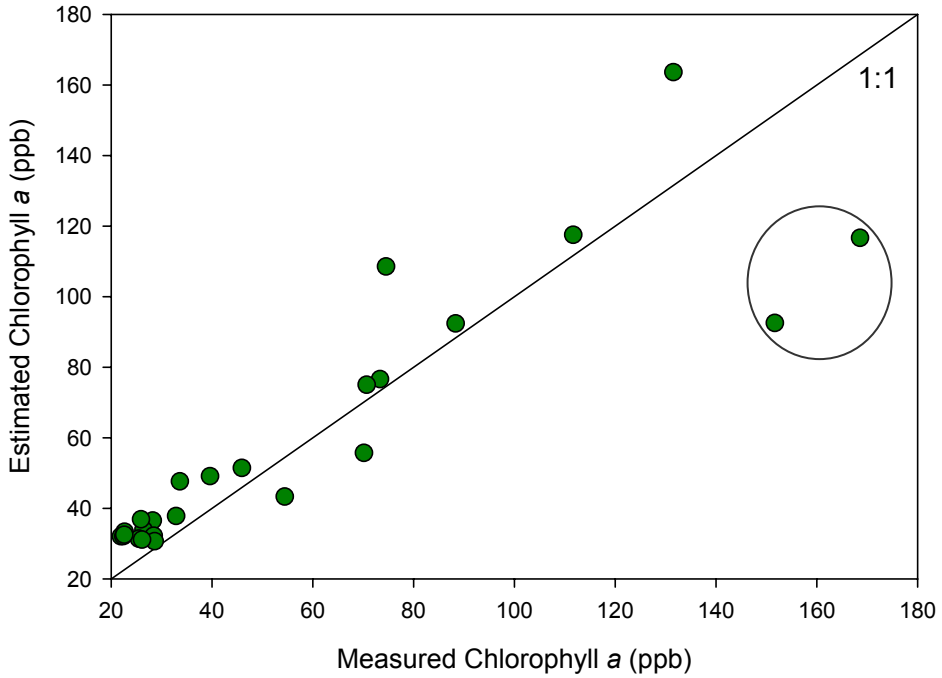

Figure 38a and b: (a) Morse Reservoir Simis *et al.* (2005) algorithm derived absorption coefficients for chlorophyll *a* at 665 nm, $a_{chl}(665)$ versus analytically measured chlorophyll *a* concentrations (r^2=0.79) and (b) analytically measured chlorophyll *a* concentrations versus estimated concentrations using $a^*_{chl}(665)$ (RMSE=20.32 ppb).

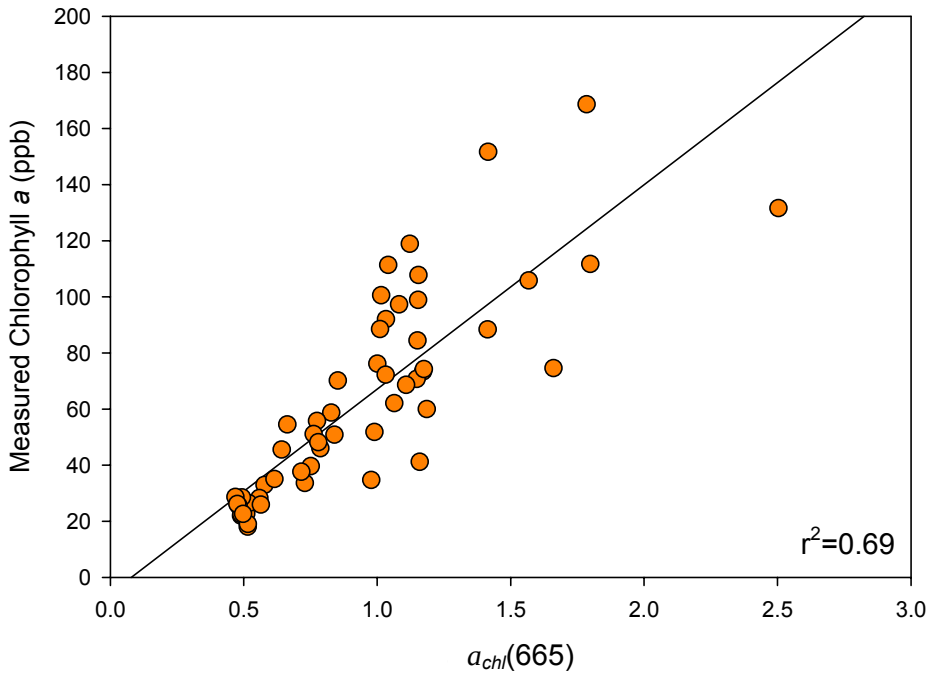

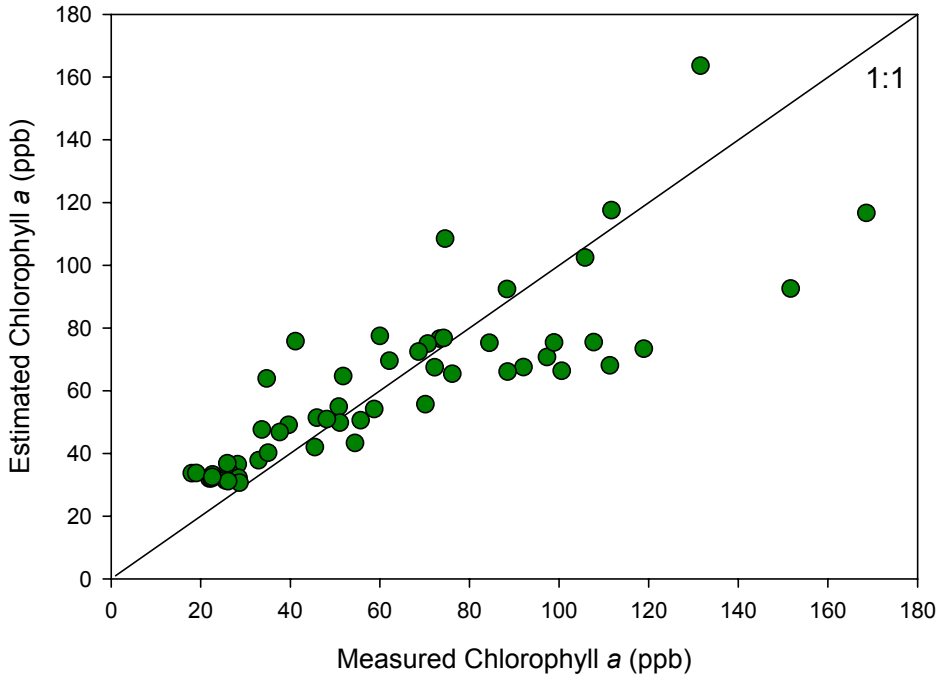

Figure 39a and b: Combined dataset, including both Morse and Geist Reservoirs, Simis *et al.* (2005) algorithm derived absorption coefficients for chlorophyll *a* at 665 nm, $a_{chl}(665)$ versus analytically measured chlorophyll *a* concentrations (r^2=0.69) and (b) analytically measured chlorophyll *a* concentrations versus estimated concentrations using $a^*_{chl}(665)$ (RMSE=20.51 ppb).

Phycocyanin

The following modified Simis *et al.* (2005) algorithm was implemented to obtain the phycocyanin absorption coefficient at 620 nm, $a_{PC}(620)$, and ultimately the estimated phycocyanin concentration from Geist and Morse Reservoir data:

$$a_{pc}(620) = (\{[R(709)/R(620)] \times [a_w(709) + b_b]\} - b_b - a_w(620)) - [\varepsilon \times a_{chl}(665)] \quad \text{Equation 40}$$

Where:

b_b = backscattering coefficient obtained from $b_b = [a_w(778)\ \alpha\ R(778)] \times [(\gamma' - R(778))^{-1}]$ (Gons, 1999; Astoreca *et al.,* 2006)

$a_w(778)$ = 2.71 m^{-1} (Buitevled *et al.*, 1994)

α = 0.60, constant accounting for refraction and reflection at the water's surface (Gordon *et al.*, 1988; Astoreca *et al.*, 2006)

γ' = 0.082, accounts for the reflectance-Inherent Optical Property model, taken from Astoreca, 2006 (based on Gordon *et al.*, 1988)

Adapted from Simis *et al.* (2005)

Concentration of phycocyanin was then determined from:

$$[PC] = a_{PC}(620)\ (m^{-1}) / a^*_{PC}(620)\ (m^2\ mg\ pigment^{-1}) \quad \text{Equation 41}$$

Where:

$a^*_{PC}(620)$ = 0.0049, the minimum specific absorption coefficient of phycocyanin at 620 nm (taken from Simis *et al.* (2005) Lake Loosedrect data)

Application of the Simis *et al.* (2005) algorithm for retrieval of the phycocyanin absorption coefficient $a_{PC}(620)$ from Geist and Morse Reservoir data yielded r^2 values of 0.74 and 0.91, respectively from the linear least-squares regression of $a_{PC}(620)$ to analytically measured phycocyanin (Table 14; Figure 40a, Figure 41a). Estimated phycocyanin concentration, [PC], was obtained using the phycocyanin specific absorption coefficient at 620 nm, $a^*_{PC}(620)$, as reported by Simis *et al.* (2005) for Lake Loosedrect data.

Table 14: Performance summary for the Simis *et al.* (2005) algorithm for estimation of phycocyanin concentration for Geist (n=26) and Morse Reservoirs (n=23) and for a combined dataset (n=49) including the slope and intercept of the linear relationship between measured phycocyanin and estimated phycocyanin with their corresponding standard errors of estimation (STE), the root mean square error (RMSE) of the estimated [PC] value, and the linear least squares fit (r^2) of the phycocyanin absorption coefficient at 620 nm to analytically measured phycocyanin concentration.

	Reservoir	Intercept (STE)	Slope (STE)	RMSE (ppb)	r^2	|min/max Residuals| (ppb)	n (p-value)	figure
Simis *et al.* (2005) Semi-empirical algorithm	Geist	30.87 (6.14)	0.51 (0.06)	27.59	0.74	0.23 66.07	26 p<0.0001	Figure 40
	Morse	25.96 (2.81)	0.66 (0.05)	22.04	0.91	1.11 34.68	23 p<0.0001	Figure 41
	Combined	27.99 (2.89)	0.56 (0.03)	24.61	0.85	–	49 p<0.0001	Figure 42

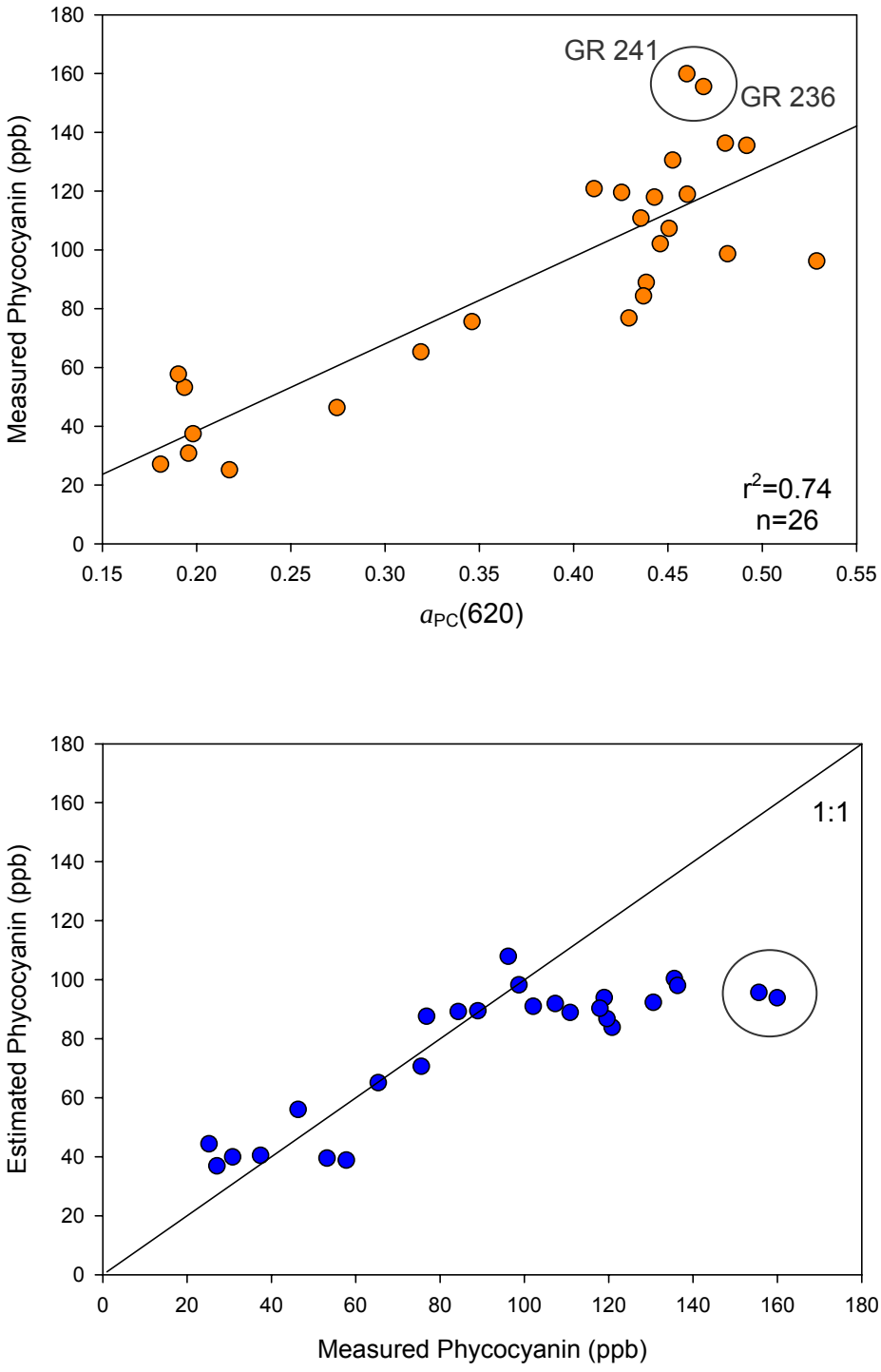

Figure 40a and b: (a) Geist Reservoir Simis *et al.* (2005) algorithm derived absorption coefficients for phycocyanin at 620 nm, $a_{PC}(620)$ versus analytically measured phycocyanin concentrations (r^2=0.74, n=26, p<0.0001) and (b) analytically measured phycocyanin concentrations versus estimated concentrations using $a^*_{PC}(620)$ (RMSE=27.59 ppb).

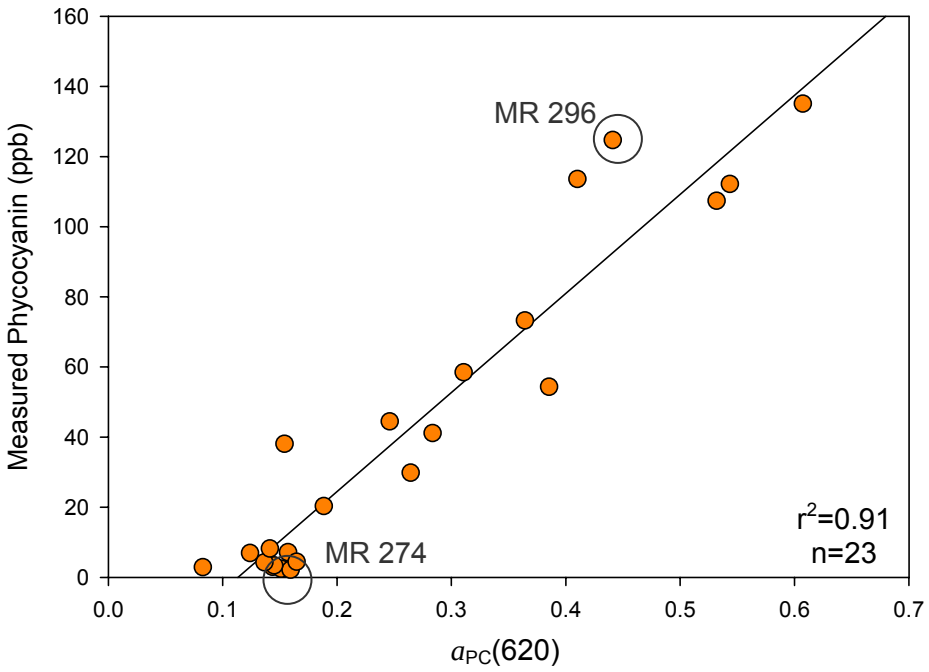

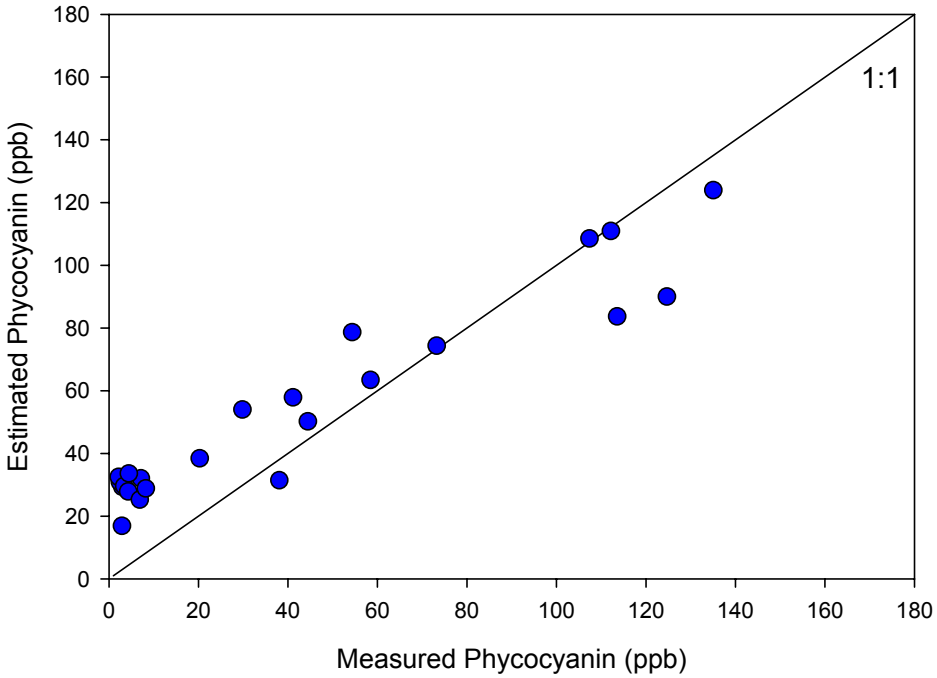

Figure 41a and b: (a) Morse Reservoir Simis *et al.* (2005) algorithm derived absorption coefficients for phycocyanin at 620 nm, $a_{PC}(620)$ versus analytically measured phycocyanin concentrations (r^2=0.91, n=23, p<0.0001) and (b) analytically measured phycocyanin concentrations versus estimated concentrations using $a^*_{PC}(620)$ (RMSE=22.04 ppb)

Geist Reservoir measured to Simis *et al.* (2005) estimated phycocyanin yielded a RMSE of 28 ppb ($p<0.0001$, n=26; Table 14; Figure 40b). The average residual value of observed to Simis *et al.* (2005) estimated phycocyanin concentration for Geist Reservoir was 20.20 ppb, with minimum and maximum residuals of 0.23 and 66.07 ppb, respectively. The linear least-squares relationship between measured phycocyanin concentration and residual values showed a relatively strong positive correlation (r^2=0.55, n=26). The two outlying sites (sites 241 and 236) with the highest residual values also proved to have high analytically measured phycocyanin concentrations (156 and 160 ppb, respectively; Figure 40a). The model underestimated phycocyanin concentrations at these sites by approximately 60 ppb (Figure 40b).

Morse Reservoir Simis *et al.* (2005) estimated phycocyanin concentrations were closer to a one-to-one relationship than those retrieved using Geist data, with a RMSE of 22 ppb ($p<0.0001$, n=23; Table 14; Figure 41b). The average residual value of observed to Simis *et al.* (2005) estimated chlorophyll *a* concentration for Morse Reservoir was 18.34 ppb, with minimum and maximum residuals of 1.11 and 34.68 ppb, respectively. The sites yielding the largest residual values (sites 274 and 293) resulting from the algorithm estimation also served as the most extreme values found in the measured phycocyanin dataset (2 ppb and 125 ppb, respectively; Figure 41a). The algorithm produced an overestimation of phycocyanin greater than 30 ppb for site 274, with a very low measured concentration (2.19 ppb). The sampling site 296, with a high measured phycocyanin concentration (114 ppb) was underestimated by the algorithm by greater than 30 ppb (Figure 41b).

When applied to a combined dataset, an r^2 value of 0.85 was obtained from the linear least squares regression of Simis *et al.* (2005) estimated $a_{PC}(620)$ to analytically

measured phycocyanin (Figure 42a). The combined dataset yielded a RMSE of 21 ppb ($p<0.0001$, $n=54$; Figure 42b).

A potential explanation for the consistent underestimation of phycocyanin for Geist Reservoir sampling sites with measured phycocyanin concentrations greater than 120 ppb could simply be that the Simis *et al.* (2005) algorithm assumes that the absorption by phytoplankton pigments at 709 nm is negligible, thus absorption at this location is attributed only to pure water. It is therefore possible to underestimate the absorption coefficient of phycocyanin at 620 nm if phycocyanin is also absorbing energy at 709 nm. An underestimation of $a_{PC}(620)$ will cause an underestimation in retrieved pigment concentration that will increase with increasing concentration (Simis *et al.*, 2005).

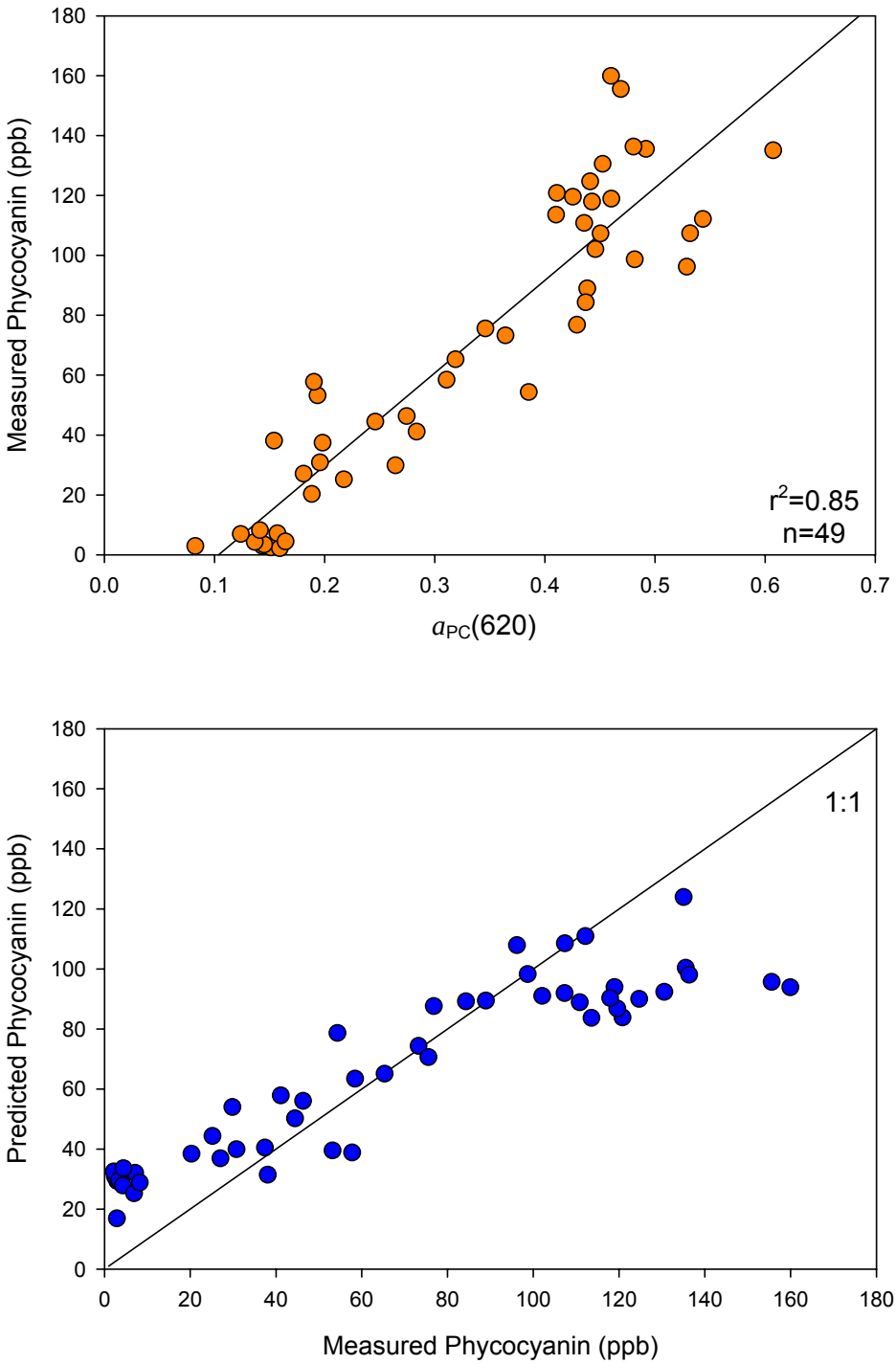

Figure 42a and b: (a) Combined dataset including both Morse and Geist Simis *et al.* (2005) algorithm derived absorption coefficients for phycocyanin at 620 nm, $a_{PC}(620)$ versus analytically measured phycocyanin concentrations (r^2=0.85, n=49, p<0.0001) and (b) analytically measured phycocyanin concentrations versus estimated concentrations using $a^*_{PC}(620)$ (RMSE=24.61 ppb).

Evaluation of Phycocyanin Pigment Concentration as a Measure of Blue-green Algal Abundance

To ensure that the remote sensing of optically active pigments, phycocyanin and chlorophyll *a*, is an accurate method for estimating *in-vitro* phytoplankton pigment concentrations, the relationship between ground spectral response and extracted phycocyanin and chlorophyll *a* was determined. It is the relationship between *in-vitro* phytoplankton pigment concentration and measures of blue-green algal biomass and biovolume, however that ultimately determined the effectiveness of remote sensing of phytoplankton pigments as a proxy for blue-green algal abundance. A subset of 25 samples were randomly selected from an aggregated dataset and analyzed for phytoplankton identification, enumeration, and biovolume, a density measure of blue-green cell biomass. A strong correlation between measured phycocyanin concentrations and biovolume measurements was observed (r^2=0.9460, p<0.0001; Figure 43). Measures of blue-green algal biovolume and natural units can be determined using the equations obtained from the linear least squares regression of measured phycocyanin concentration to blue-green biovolume and natural units from the 25 sample subset:

Blue-green Biovolume (mm^3/m^3) = 110.1 + (3.56 x [PC] (ppb)) Equation 42

Blue-green Natural Units / mL = 3,629 + (67 x [PC] (ppb)) Equation 43

Variation in the size and shape of algal cells cannot be accounted for when performing phytoplankton counts, but can when measuring algal biovolume. Sampling sites with high algal counts could have low algal biovolume if the taxa present are small in size. For Morse Reservoir, sampling site 274 was often seen as an outlier, where small taxa accounted for 77% of the natural units but only 21% of the biovolume. Algorithms consistently overestimated phycocyanin concentration at this site. The disparity was caused by the prevalence of small blue-green taxa such as *Merismopedia minima* and

Pseudanabaena limnetica, which contribute little to overall biovolume and phycocyanin concentrations but can dominate counts. The strong relationship observed between *in-vitro* pigment concentration and blue-green algal biovolume suggests measurements of pigment concentration are an accurate measure of blue-green algal abundance.

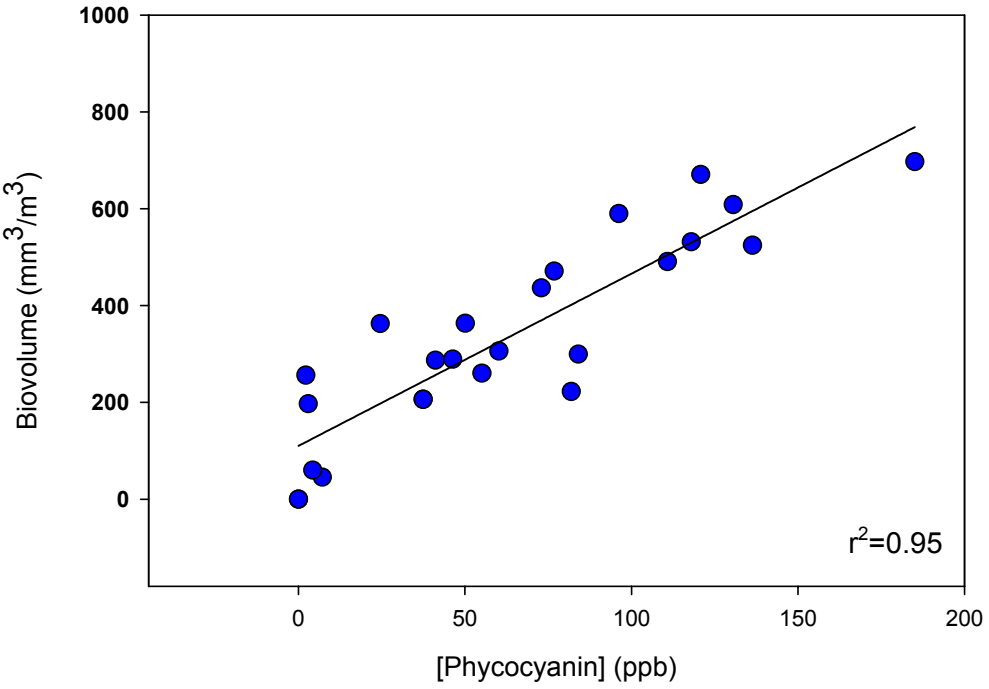

Figure 43: Relationship between phycocyanin concentrations and measures of blue-green algal biovolume (r^2=0.95, p<0.0001, n=25).

CONCLUSIONS

The data presented suggests that hyperspectral remote sensing, coupled with the established empirical and semi-empirical algorithms for inland, turbid waters, is an effective method for rapid cyanobacteria bloom assessment.

Application of the Gitelson *et al.* (1986) NIR:red and SUM and the Schalles and Yacobi (2000) empirical algorithms for retrieval of chlorophyll *a* and phycocyanin, respectively proved to be accurate and robust when applied to a combined dataset. Coefficients obtained from the linear least-squares regression of empirical algorithm index values, obtained using above surface remote sensing reflectance, and analytically measured phycocyanin concentration need to be further validated through algorithm application to spectra collected over the entire bloom season and under varying conditions. For increased predictive power, empirical algorithms need to be modified further to account for the influence of non-algal turbidity on reflectance spectra, potentially by including a third band in the NIR portion of the spectrum, as described by Dall'Olmo and Gitelson (2005).

The Simis *et al*. (2005) semi-empirical models for estimation of chlorophyll *a* and phycocyanin concentrations also proved to be robust. When applied to a combined dataset, a strong relationship resulted from the linear least-squares regression of chlorophyll *a* absorption coefficients and analytically measured pigment concentrations. When applied to Geist Reservoir data only, the Simis *et al.* (2005) algorithm yielded a relatively weak relationship (r^2=0.41) between the chlorophyll *a* absorption coefficient at 665 nm, $a_{chla}(665)$, and measured chlorophyll *a*, the result of model application to a low range of chlorophyll *a* values. Ultimately, the model performed well in estimating

chlorophyll *a* concentration, yielding a low root-mean-square error of 21 ppb between measured and estimated pigment concentrations.

A strong relationship also resulted from the linear least-squares regression of the Simis *et al.* (2005) phycocyanin absorption coefficients, obtained from remote sensing reflectance, and analytically measured pigment concentrations (r^2=0.85, RMSE=24.61 ppb). Algorithm error in concentration estimation could be attributed to several potential sources including error in the estimation of pigment specific absorption coefficients, change in pigment absorption efficiency, the presence of non-algal particles, and error in prediction for non-cyanobacteria- dominated waters.

Error Associated with Algorithm Application

The specific absorption coefficients used for retrieval of pigment concentrations in this study were measured by Simis *et al.* (2005), where absorption coefficients obtained from Lake Loosdrecht data were divided by extracted pigment concentrations. Several sources of error could be attributed to the estimation of specific absorption coefficients, and the application of the Lake Loosdrecht coefficients to Indianapolis reservoir data. According to Simis *et al.* (2005), high variability exists in phycocyanin specific absorption coefficients, as was seen in data obtained from Lakes Loosedrect and IJsselmeer. Therefore, applying a fixed specific absorption coefficient, as was done in this study, has a tendency to produce error in the estimation of phycocyanin concentration. Simis *et al.* (2005) suggested that the application of a fixed $a^*_{PC}(620)$ to sites exhibiting low phycocyanin concentration consistently produced an overestimation of pigment concentration. This effect was observed in Morse Reservoir data, where phycocyanin concentrations measuring 2-10 ppb where estimated to have 20-30 ppb phycocyanin.

Pigment absorption efficiency is suggested to be a function of the season, environmental conditions, nutrient and light availability, phytoplankton composition and species competition (Tandeau de Marsac, 1977; Metsamaa *et al*., 2005). Different strains of cyanobacteria also exhibit different absorption efficiencies per mass unit (Ahn *et al.* 1992; Metsamaa *et al*., 2005). This identified source of error could be one potential explanation for the underestimation of phycocyanin concentrations for Geist Reservoir sites, where measured pigment concentrations were greater than 120 ppb. It is possible that, at high concentrations, pigments no longer absorb energy proportional to the concentration, rather absorption efficiency of the cyanobacterial cell decreases. A non-linear relationship appears to exist between the phycocyanin estimated using the absorption coefficient at 620 nm and *in-vitro* phycocyanin with measured concentrations greater than 120 ppb.

Simis *et al.* (2005) also described two major simplifications employed in the semi-empirical algorithm: the assumption that absorption by phytoplankton pigments at 709 nm is insignificant or absent (absorption here is attributed to pure water only) and absorption by non-algal material is not quantified. The first simplification is said to cause an underestimation of phycocyanin. Absorption at 709 nm by phytoplankton pigments will increase as concentration increases, resulting in a miscalculation of the absorption coefficient. To correct for the simplification, Simis *et al.* (2005) proposed the use of a correction factor (δ) obtained by relating laboratory measured to algorithm derived phycocyanin absorption coefficients. The correction factor calculated and employed by Simis *et al.* (2005) was applied for this study. Application of these simplifications was successful for Morse Reservoir, where concentrations of non-algal material was low, however the correction proved less successful for Geist, where concentrations of non-

algal material were high. This simplification could also have been the cause of an underestimation of phycocyanin concentrations for Geist Reservoir by 30-66 ppb.

The semi-empirical algorithm introduced by Simis *et al.* (2005) is suggested to function best in cyanobacteria-dominated systems. This assumption was supported by this study. As was suggested, the highest error in Indianapolis data occurred at sites dominated by chlorophyll *a*, indicative of the presence of green-algae. For sites where Chla:PC > 2, a consistent underestimation of phycocyanin resulted and errors of greater than 14 ppb occurred (Figure 44).

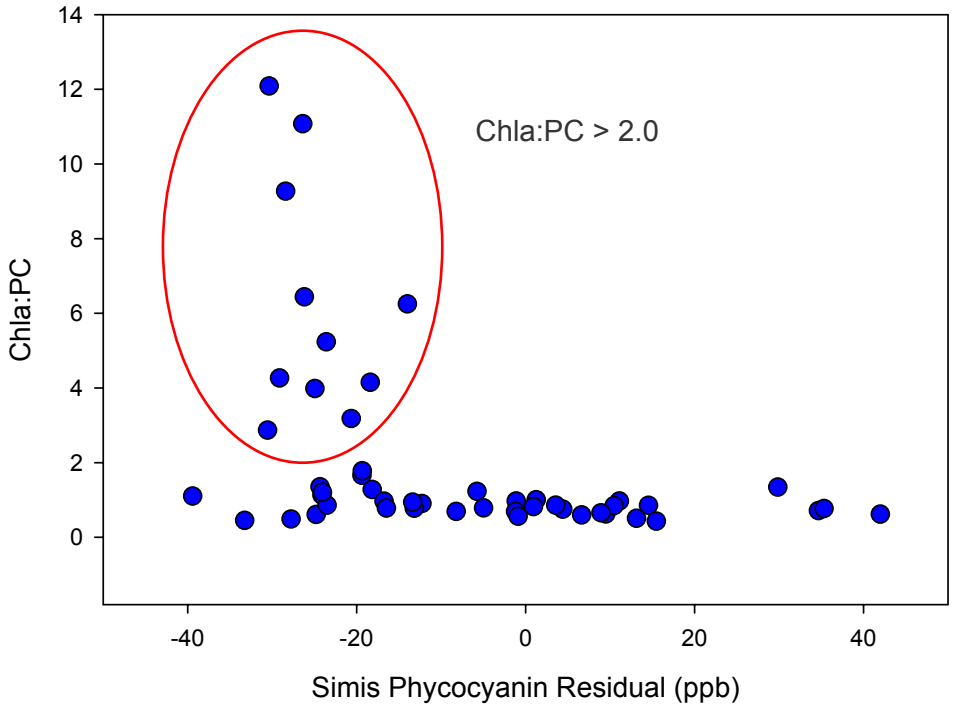

Figure 44: Relationship between residual values from measured to Simis et al. (2005) estimated phycocyanin concentrations and the Chla:PC ratio, with Chla:PC >2 identified by red circle.

As the ratio of phycocyanin-to-chlorophyll *a* decreases, error in the estimation of phycocyanin concentration is likely to occur. Simis *et al.* (2005) specifically identifies an

acute increase in estimation error for waters with PC:Chla of less than 0.4. This threshold was observed in Indianapolis reservoir data. For sites with PC:Chla $\geq$ 0.5, percent error between measured and estimated phycocyanin concentration was less than 40% (Figure 45).

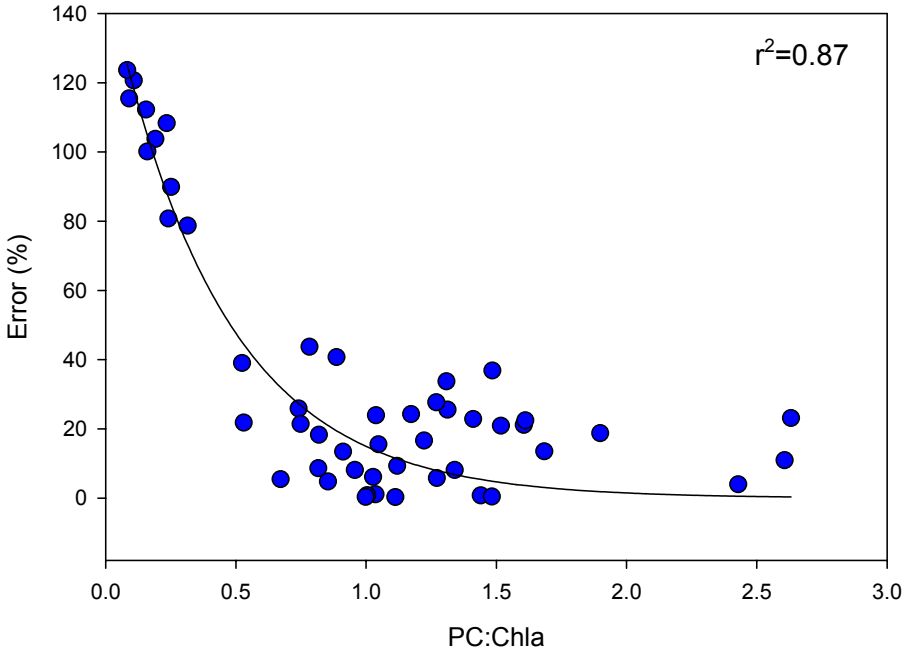

Figure 45: Relationship of PC:Chla for Indianapolis reservoir sites and percent error between measured and estimated phycocyanin concentrations (r^2=0.87).

Simis *et al.* (2005) identified an inverse relationship between the phycocyanin-to-chlorophyll *a* ratio and the specific absorption coefficient for cyanobacteria at 620 nm. Thus, for low concentrations of phycocyanin, low $a_{PC}(620)$, $a^*_{PC}(620)$ should be higher compared to that of cyanobacteria dominated waters. The fixed specific absorption coefficient would therefore result in an overestimation of phycocyanin concentrations, also observed in Indianapolis reservoir data.

Error Related to Data Collection

Errors introduced by data collection rather than algorithm application also exist. To minimize effects of atmospheric interference, data were collected under cloudless, dry sky conditions where intensity of solar irradiance was constant. A total of 15 spectra were averaged for each site, reducing the signal-to-noise ratio and, thus error induced by *in-situ* reflectance collection. The optic was positioned at nadir on a mount extending 1 m from the boat to reduce the influence of reflectance off of the vessel on collected spectra. Though the water was placid, the potential for error due to surface refraction also exists. Some researchers suggest a viewing geometry where the optic is positioned at a 45^{o} angle from the water's surface to avoid noise attributed to surface refraction. The empirical relationships employed likely reduce error resulting from skylight surface reflection since this error is likely to affect reflectance along the spectral range of interest similarly.

Error Introduced in Analytical Analysis

Error in the estimated values obtained using the phycocyanin empirical and semi-empirical algorithms mentioned could have arisen from the analytical method used for pigment extraction. Though several methods for phycocyanin extraction have been tested, adequate validation for these methods has not yet been provided, thus no method is widely accepted. Simis *et al.* (2005) suggested that low extraction efficiency would result in an overestimation of the phycocyanin specific absorption coefficient and a corresponding underestimation of phycocyanin concentration. It is possible that, because the average specific absorption coefficient obtained from Lakes Loosdrecht and Ijsselmer data was too high, the phycocyanin extraction efficiency for this study was better than that of Simis *et al.* (2005).

Though elimination of or reduction in the aforementioned sources of error has potential to increase algorithm predictive power, overall the empirical and semi-empirical algorithms for retrieval of blue-green algal abundance performed well, are robust and transferable. The use of remote sensing as a rapid assessment tool for the spatial distribution and concentration of blue-green algae can provide an efficient method for tracking blue-green algal occurrence over time and relative to management strategies indicating areas for treatment and mitigation. The effectiveness of management strategies for controlling algal abundance can also be efficiently measured using remote sensing methods. Most importantly, coupled with physical and chemical data from the reservoir, remote sensing of cyanobacteria can aid in understanding bloom formation and can facilitate bloom prediction.

FUTURE WORK

Bio-optical modeling has been pursued for water quality assessment to eliminate the need for gathering water samples to provide statistical analysis linking phytoplankton concentration to reflectance, thus improving the accuracy of algorithms extended to air and space-borne systems. However, both semi-empirical and bio-optical models require the specific absorption coefficients for algal pigments to be known or to be constant. Unfortunately, the specific absorption coefficient of phycocyanin is highly variable Simis *et al.* (2005) suggest that the absorption coefficient should be adjusted for cell size, intracellular pigment content, and environmental conditions. Dall'Olmo and Gitelson (2005) suggested that certain spectral regions are highly affected by variability in the chlorophyll *a* specific absorption coefficient (a_{chla}*) and chlorophyll *a* fluorescence quantum yield (η), the efficiency at which a cell will emit absorbed light (photons emitted: photons absorbed), introducing high error to the prediction of chlorophyll *a* from remote sensing reflectance. To resolve this issue, Dall'Olmo and Gitelson (2006) suggested a band tuning method, reducing the requirement for parameterization of the optical properties of natural water constituents by selecting bands that are least affected by a_{chla}* and η. Based on the hypothesis that bands used in a semi-empirical model for determination of chlorophyll *a* concentration can be tuned to reduce the sensitivity of the model to variation in the phytoplankton specific absorption coefficient and chlorophyll *a* fluorescence quantum yield, Dall'Olmo and Gitelson (2005) presented the following three-band algorithm for chlorophyll *a* estimation, reducing the standard error of estimation to less than 30%:

$$[\,pigment\,] \propto (R^{-1}(\lambda_1) - R^{-1}(\lambda_2)) \times R(\lambda_3) \qquad \text{Equation 44}$$

Where:

$R(\lambda_1)$ = reflectance value at wavelength location λ_1 most sensitive to pigment absorption (chlorophyll *a* or phycocyanin), but also affected by particulate material induced scattering and absorption of accessory pigments

$R(\lambda_2)$ = reflectance value at wavelength location λ_2 that is least sensitive to absorption by the pigment of interest and is most sensitive to absorption by other constituents (correcting for the absorption by other pigments at λ_1)

$R(\lambda_3)$ = reflectance value at wavelength location λ_3 least affected by absorption of all pigments and therefore used to quantify scattering

The Dall'Olmo and Gitelson (2005) algorithm is based on the absorbance of chlorophyll *a*, thus the reciprocal of the remote sensing reflectance to inherent optical property (IOP) relationship proposed by Gordon *et al.* (1975).

The following three-band optical model for obtaining the phytoplankton absorption coefficient (by utilizing the band in the red region which is proportional to chlorophyll *a* concentration) in natural waters requires the selection of three specific wavelength locations based on the sensitivity of that wavelength region on the constituent properties of interest:

$$a_{phy}(\lambda_1)=m(\lambda_1, \lambda_2, \lambda_3) \times (\lambda_1, \lambda_2, \lambda_3) + b(\lambda_1, \lambda_2, \lambda_3) \quad \text{Equation 45}$$

Where:

a_{phy}	=	phytoplankton absorption coefficient
m	=	coefficient obtained from regression analysis
x	=	value obtained from the reflectance index to assess the absorption of a pigment of interest
b	=	coefficient obtained from regression analysis

The first band location (λ_1), is selected as the spectral feature most sensitive to chlorophyll *a* pigment absorption:

$$R_{rs}^{-1}(\lambda_1) \propto \frac{Q}{f}\frac{a_{Chla}(\lambda_1) + a_{TD}(\lambda_1) + a_w(\lambda_1) + b_b}{b_b} \quad \text{Equation 46}$$

Where:

R_{rs}^{-1}	=	the reciprocal of the remote sensing reflectance function as defined by Gordon *et al.* (1975)
(λ_1)	=	spectral region chosen as most sensitive to chlorophyll *a* absorption
a_{Chla}	=	chlorophyll *a* absorption coefficient
a_{TD}	=	total absorption coefficient for the non-algal particles (tripton) and colored dissolved organic matter (a_{CDOM}) combined (sometimes called a_{NAP})
$a_w(\lambda_1)$	=	pure water absorption coefficient at the specified wavelength location
b_b	=	total backscattering coefficient
$f:Q$	=	a function of the sun and viewing angles

The second spectral region is selected as the wavelength where absorption of non-algal particles is equal to that of the first spectral region and absorption by chlorophyll *a* is minimized. Because the absorption efficiency of CDOM and inorganic suspended matter (ISM) decreases as wavelength increases, then $\lambda_2 > 700$ nm. Tuning for λ_2 is written as:

$$R_{rs}^{-1}(\lambda_1) - R_{rs}^{-1}(\lambda_2) \propto \frac{Q}{f}\frac{a_{Chla}(\lambda_1) + a_w(\lambda_1) - a_w(\lambda_2)}{b_b} \quad \text{Equation 47}$$

Where:

a_{Chla}	=	chlorophyll *a* absorption coefficient
a_{TD}	=	total absorption coefficient for the non-algal particles colored dissolved organic matter (a_{CDOM}) and tripton ($a_{tripton}$) combined (sometimes called a_{NAP})

Wavelength location λ_3 is selected according to the location least affected by absorption of all pigments, therefore absorption at λ_3 can be attributed solely to that of pure water and can be used to quantify scattering. Reflectance at λ_3 is proportional to the product of *f:Q* ratio and total backscattering, written as:

$$[R_{rs}^{-1}(\lambda_1) - R_{rs}^{-1}(\lambda_2)]R_{rs}(\lambda_3) \propto a_{Chla}(\lambda_1) \qquad \text{Equation 48}$$

In the case that the absorption of CDOM and tripton is far less than that of chlorophyll *a* at location λ_1 and the backscattering coefficient is far less than the total absorption at λ_1, then λ_2 can be removed from the equation so that:

$$[R_{rs}^{-1}(675) - R_{rs}^{-1}(710)]R_{rs}(750) \propto a_{Chla}(\lambda_1)$$

$$[R_{rs}^{-1}(\lambda_1)R_{rs}(\lambda_3) \propto a_{Chla}(\lambda_1)$$

The following steps are employed for adoption of the initial spectral regions:

(1) Tuning of λ_1 by use of the initial band locations λ_2=710nm and λ_3=750 nm and a moving location for λ_1 between 400 and 800 nm, thus: $[R_{rs}^{-1}(400 < \lambda_1 < 800) - R_{rs}^{-1}(710)]R_{rs}(750) \propto a_{Chla}(\lambda_1)$ regressed against chlorophyll *a* concentration to obtain the lowest standard error of estimation

(2) Tuning of λ_2 by use of the tuned λ_1 location (λ_1=671 nm from step 1) and initial λ_3=750 nm and a moving location for λ_2 between 700 and 750 nm, thus: $[R_{rs}^{-1}(671) - R_{rs}^{-1}(700 < \lambda_2 < 750)]R_{rs}(750) \propto a_{Chla}(\lambda_1)$ regressed against chlorophyll *a* concentration to obtain the lowest standard error of estimation

(3) Tuning of λ_3 by use of the tuned λ_1 location (λ_1=671 nm from step 1), a tuned λ_2 location (λ_2=710 nm from step 2) and a moving location for λ_3 between 730 and 750 nm, thus: $[R_{rs}^{-1}(671) - R_{rs}^{-1}(710)R_{rs}(730 < \lambda_3 < 750) \propto a_{Chla}(\lambda_1)$ regressed against chlorophyll *a* concentration to obtain the lowest standard error of estimation

(4) Verification of λ_1 by use of a tuned λ_2 and λ_3 and a moving λ_1 regressed against chlorophyll *a* concentration to obtain the lowest standard error of estimation, giving the final algorithm: $[R_{rs}^{-1}(671) - R_{rs}^{-1}(710)R_{rs}(740) \propto a_{Chla}(\lambda_1)$

For datasets where the effect of the backscattering (compensated for by the addition of λ_3) on reflectance at λ_1 is greater than that of the combination of tripton and CDOM, the λ_2 can be omitted, resulting in the following two-band algorithm:

$a_{phy}(\lambda_1)=m(\lambda_1, \lambda_3)x(\lambda_1, \lambda_3) + b(\lambda_1, \lambda_3)$

Where:

a_{phy}	=	phytoplankton absorption coefficient
m	=	coefficient obtained from regression analysis
x	=	value obtained from the reflectance index to assess the absorption of a pigment of interest
b	=	coefficient obtained from regression analysis

The following is the tuned algorithm:

$$[R_{rs}^{-1}(671)R_{rs}(740) \propto a_{Chla}(\lambda_1)$$

The final three and two-band algorithms was tuned to variability in η and a_{chla}^* using the same method of adjusting both bands one and three ($650 \leq \lambda_1 \leq 700$ and $700 \leq \lambda_3 \leq 750$) to minimize standard error of estimation by isolating each factor from the dataset used.

The following three algorithms were presented as having the highest predictive power and lowest sensitivity to variability in η and a_{chla}^*:

$$[R_{rs}^{-1}(671) - R_{rs}^{-1}(710)R_{rs}(740) \propto a_{Chla}(\lambda_1)$$
$$[R_{rs}^{-1}(673)R_{rs}(735) \propto a_{Chla}(\lambda_1)$$
$$[R_{rs}^{-1}(665)R_{rs}(725) \propto a_{Chla}(\lambda_1)$$
$$a_{Chla}(\lambda_1) \propto [R_{rs}^{-1}(671) - R_{rs}^{-1}(710)R_{rs}(740)$$

Using simulated data, Dall'Olmo and Gitelson (2006) further investigated bio-optical parameter induced error on estimated chlorophyll *a* as a function of wavelength. It is shown that the bands most sensitive to chlorophyll *a* concentration are also most sensitive to variability in bio-optical parameters. The following observations regarding reduced *Chla* predictive power as a result of variability in bio-optical properties (as a function of wavelength) were made:

(i) Phytoplankton specific absorption coefficient (a_{phy}^*) and chlorophyll *a* fluorescence quantum yield (η) variability decreases as λ_1 moves from 678 nm toward 670 nm and as λ_3 moves from 700 nm toward 750 nm. The two-band algorithm performs better than the three-band in circumstances with high variation in a_{phy}^*.

(ii) The specific absorption coefficient of non-algal particles (a_{nap}^*) mostly effects features in the blue portion of the spectrum and causes only negligible change in *Chla* prediction for a range in a_{nap}^* variability of up to fourfold.

(iii) Total particle specific backscatter coefficient ($b_{b,P}^*$) causes only minimal changes in estimated *Chla*. The three-band algorithm performs better than the two-band in conditions with highly variable $b_{b,P}^*$.

(iv) Concentration of total suspended particles *P* increases error in *Chla* prediction most significantly for low *Chla* concentrations (i.e. 10 ppb), though variation in *P* is said to affect the entire red-NIR region. For low (10 ppb) to medium (36 ppb) concentrations of chlorophyll, the three-band algorithm (with λ_1, λ_2, and λ_3 set at 675, 700, 750 nm respectively) has the best predictive power. For high *Chla* concentrations (100 ppb) the two-band algorithm (with λ_1 and λ_2 set at 675 and 750 nm respectively) reports the lowest error.

Dall'Olmo and Gitelson (2006) suggest that, although the tuning technique and coefficients used in this model are dependent on the optical composition of the water on which it was built, the large range of constituent concentrations and optical properties included in the model derivation suggest that it could be extended to similar systems.

Following Dall'Olmo and Gitelson (2006), a similar band tuning technique could be applied to derive phycocyanin concentration from remote sensing reflectance using the three-band optical model. The phytoplankton absorption coefficient could be obtained

by utilizing a band in the red region which is proportional to phycocyanin concentration in natural waters. Reflectance values at wavelength location λ_2 could be tuned to that is least sensitive to absorption by phycocyanin and potentially most sensitive to absorption by other constituents (correcting for the absorption by other pigments at λ_1). And reflectance value at wavelength location λ_3 least affected by absorption of all pigments and therefore used to quantify scattering.

The following steps should be employed:

(1) Adoption of the following initial spectral regions:
$[R_{rs}^{-1}(620) - R_{rs}^{-1}(710)]R_{rs}(750) \propto a_{Chla}(\lambda_1)$

(2) Tuning of λ_1 by use of the initial band locations λ_2=710nm and λ_3=750 nm and a moving location for λ_1 between 400 and 800 nm, thus:
$[R_{rs}^{-1}(400 < \lambda_1 < 800) - R_{rs}^{-1}(710)]R_{rs}(750) \propto a_{Chla}(\lambda_1)$ regressed against phycocyanin concentration to obtain the lowest standard error of estimation

(3) Tuning of λ_2 by use of the tuned λ_1 location (λ_1≈620 nm from step 1) and initial λ_3=750 nm and a moving location for λ_2 between 700 and 750 nm, thus:
$[R_{rs}^{-1}(620) - R_{rs}^{-1}(700 < \lambda_2 < 750)]R_{rs}(750) \propto a_{Chla}(\lambda_1)$ regressed against chlorophyll *a* concentration to obtain the lowest standard error of estimation

(4) Tuning of λ_3 by use of the tuned λ_1 location (λ_1≈620 nm from step 1), a tuned λ_2 location (λ_2≈710 nm from step 2) and a moving location for λ_3 between 730 and 750 nm, thus: $[R_{rs}^{-1}(620) - R_{rs}^{-1}(710)R_{rs}(730 < \lambda_3 < 750) \propto a_{Chla}(\lambda_1)$ regressed against chlorophyll *a* concentration to obtain the lowest standard error of estimation

(5) Verification of λ_1 by use of a tuned λ_2 and λ_3 and a moving λ_1 regressed against chlorophyll *a* concentration to obtain the lowest standard error of estimation, giving the final algorithm: $[R_{rs}^{-1}(620) - R_{rs}^{-1}(710)R_{rs}(740) \propto a_{Chla}(\lambda_1)$

WORK CITED

Ahn, Y., Bricaud, A., Morel, A. (1992). Light backscattering efficiency and related properties of some phytoplankters. *Deep-Sea Research* 39(11/12): 1835-1855.

American Public Health Association (1998). Standard Methods for the Examination of Water and Wastewater. Washington, D.C., American Public Health Association

Astoreca, R., Ruddick, K., Rousseau, V., Van Mol, B., Parent, J., Lancelot, C. (2006). Variability of the inherent and apparent optical properties in a highly turbid coastal area: impact on the calibration of remote sensing algorithms. EARSel eProceedings.

Backer, L. C. (2002). Cyanobacterial harmful algal blooms: developing a public health response. *Lake and Reservoir Management* 18(1): 20-31.

Behm, D. (2003). Coroner cites algae in teen's death. Milwaukee Journal Sentinel.

Buitevled, H., Hakvoort, J., Donze M. (1994). The optical properties of pure water. Ocean Optics XII Proc Soc Photoopt Eng 2258: 174-183.

Bukata, R., Jerome, J., Kondratyev, K., Pozdnyakov, D. (1991). Estimation of organic and inorganic matter in inland waters: optical cross sections of Lakes Ontario and Ladoga. *Journal of Great Lakes Research* 17: 461-469.

Dall'Olmo, G., Gitelson, A. (2006). Effect of bio-optical parameter variability and uncertainties in reflectance measurements on the remote estimation of chlorophyll-*a* concentration in turbid productive waters: modeling results. *Applied Optics* 45(15): 3577-3592.

Dall'Olmo, G., Gitelson, A. (2005). Effect of bio-optical parameter variability on the remote estimation of chlorophyll *a* concentration in turbid productive waters: experimental results. *Applied Optics* 44(3): 412-422.

Dekker, A. (1993). Detection of the Optical Water Quality Parameters for Eutrophic Waters by High Resolution Remote Sensing. Amsterdam, Free University. Ph.D.

Dekker, A., Malthus, T., Seyhan, E. (1991). Quantitative modeling of inland water-quality for high-resolution MSS-systems. *IEEE Trans. Geosci. Remote Sens*. 29(1): 89-95.

Gitelson, A. (1992). The peak near 700 nm in the reflectance spectra of algae and water: relationships of its magnitude and position with chlorophyll concentration. *International Journal of Remote Sensing* 13: 1367-1373.

Gitelson, A., Garbuzov, G., Szilagyi, F., Mittenzwey, K.-H., Karnieli, A., Kaiser A. (1993). Quantitative remote sensing methods for real-time monitoring of inland water quality. *International Journal of Remote Sensing* 14: 1269-1295.

Gitelson, A., Laorawat, S., Keydan, G., Vonshak, A. (1995). Optical properties of dense algal cultures outdoors and its application to remote estimation of biomass and pigment concentration in spirulina platensis. Journal of Phycology 31(5): 828-834.

Gitelson, A., Mayo, M., Yacobi, Y. (1994). Signature analysis of relfectance spectra and its application for remote observations of phytoplankton distribution in Lake Kinneret. ISPRS 6th International Symposium, Val d' Isere, France.

Gitelson, A., Nikanorov, A., Sabo, G., Szilagyi, F. (1986). Etude de la qualite des eaux de surface par teledetection. *IAHS Publications* 157: 111-121.

Gitelson, A., Schalles, J., Rundquist, D., Schiebe, F., Yacobi, Y. (1999). Comparative reflectance properties of algal cultures with manipulated densities. *Journal of Applied Phycology* 11: 345-354.

Gitelson, A., Yacobi, Y., Schalles, J., Rundquist, D., Han, L., Stark, R., Etzion, D. (2000). Remote estimation of phytoplankton density in productive waters. *Arch. Hydrobiol. Spec. Issues. Advanc. Limnol* 55: 121-136.

Gons, H. (1999). Optical teledetection of chlorophyll *a* in turbid inland waters. *Environmental Science Technology* 33: 1127-1132.

Gons, H., Burger-Wiersma, T., Otten J., Rijkeboer, M. (1992). Coupling of phytoplankton and detritus in a shallow, eutrophic lake (Lake Loosdrecht, The Netherlands). *Hydrobiologia* 233: 51-59.

Gordon, H. (1993). Sensitivity of radiative transfer to small-angle scattering in the ocean: Quantitative assessment. Applied Optics 32(36): 7505-7511.

Gordon, H., Brown, O., Evans, R., Brown, J., Smith, R., Baker, K., Clark, D. (1988). A semi-analytic radiance model of ocean color. *Journal of Geophysical Research* 93D: 10,909-10,924.

Gordon, H., Brown, O., Jacobs, M. (1975). Computed relationships between the inherent and apparent optical properties of a flat homogeneous ocean. *Journal of Applied Optics* 14: 417-427.

Gordon, H., Morel, A. (1983). Remote assessment of ocean color for interpretation of satellite visible imagery: A review. New York and Berlin, Springer-Verlag.

Han, L., Rundquist, D. (1997). Comparison of NIR/RED Ratio and first derivative of reflectance in estimating algal-chlorophyll concentration: A case study in a turbid reservoir. *Remote Sensing of the Environment* 62: 253-261.

Han, L., Rundquist, D., Lui, L., Fraser, R., Schalles, J. (1994). "The spectral response of algal chlorophyll in water with varying levels of suspended sediment." International Journal of Remote Sensing 15: 3707-3718.

Indiana Department of Environmental Management (2002). Indiana Integrated Water Quality Monitoring and Assessment Report. IDEM/34/02/004/2002.

Indiana Department of Environmental Management (2004). Indiana Integrated Water Quality Monitoring and Assessment Report. http://www.in.gov/idem/water/planbr/wqs/quality.html.

Indiana Department of Environmental Management (2006). Indiana Integrated Water Quality Monitoring and Assessment Report. http://www.in.gov/idem/water/planbr/wqs/quality.html.

Jensen, J. (2005). Introductory digital image processing: a remote sensing perspective. Upper Saddle River, NJ, Pearson Education, Inc.

Jupp, D., Kirk, J., Harris, G. (1994). Detection, identification, and mapping of cyanobacteria - using remote sensing to measure the optical quality of turbid inland waters. *Australian Journal of Marine and Freshwater Research* 45: 801-828.

Krijgsman, J. (1994). Optical remote sensing of water quality parameters: interpretation of reflectance spectra. Thesis Delft University of Technology, 198 pp.

Lund, J. W. G., Kipling, C., LeCren, E.D. (1958). The inverted microscope method of estimating algal numbers and the statistical basis of estimations by counting. *Hydrobiologia* 11: 143-170.

Metsamaa, L., Kutser, T., Strombeck, N. (2005). Recognising cyanobacterial blooms based on their optical signature. *Harmful Algae* (submitted).

Mittenzwey, K., Breitwieser, S., Penig, J., Gitelson, A., Dubovitzkii, G., Garbusov, G., Ullrich, S., Vobach, V., Muller, A. (1991). Fluorescence and reflectance for the in-situ determination of some water quality parameters of surface waters. *Acta hydrochim. hydrobiol.* 19(1): 3-15.

Mittenzwey, K., Gitelson, A. (1988). In-situ monitoring of water quality on the basis of spectral reflectance. *Int. Revue Ges. Hydrobiol.* 73: 61-72.

Mittenzwey, K., Ullrich, S., Gitelson, A., Kondratiev, K. (1992). Determination of chlorophyll *a* of inland waters on the basis of spectral reflectance. *American Society of Limnology and Oceanography* 37: 147-149.

Morel, A. (2001). Bio-optical Models. In *Encyclopedia of Ocean Sciences*. Ed. J.H. Steele, K. K. Turekian and S.A. Thorpe (pp. 317-326). New York: Academic Press.

Morel, A., Gentili, B. (1991). Diffuse reflectance of oceanic waters - its dependence on sun angle as influenced by the molecular scattering contribution. *Applied Optics* 30: 4427-4438.

Morel, A., Gordon, H. (1980). Report of the working group on water color. *Boundary-Layer Meteorol.* 18: 343-355.

Morel, A., Prieur, L. (1977). Analysis of variation in ocean color. *Limnol. Oceanogr.* 37: 147-149.

Pitois, S., Jackson, M., Wood, B. (2000). Problems Associated with the presence of cyanobacteria in recreational and drinking waters. *International Journal of Environmental Health Research* 10: 203-218.

Pope, R., Fry, E. (1997). Absorption spectrum (380-700 nm) of pure water. *Applied Optics* 36: 8710-8723.

Rowan, R. (1989). Photosynthetic pigments of algae. Cambridge, Cambridge Univeristy Press.

Rundquist, D., Han, L., Schalles, J., Peake, J. (1996). Remote measurement of algal chlorophyll in surface waters: the case for the first derivative of reflectance near 690 nm. *Photogrammetric Engineering and Remote Sensing* 62: 195-200.

Sarada, R., Pillai, M., Ravishankar, G. (1999). Phycocyanin from spirulina sp: influence of processing of biomass on phycocyanin yield, analysis of efficacy of extraction methods and stability studies on phycocyanin. *Process Biochemistry* 34: 795-801.

Schalles, J., Gitelson, A., Yacobi, Y., Kroenke, A. (1998). Estimation of Chlorophyll *a* from time series measurements of high spectral resolution reflectance in a eutrophic lake. *Journal of Phycology* 34: 383-390.

Schalles, J., Yacobi, Y. (2000). Remote detection and seasonal patterns of phycocyanin, carotenoid and chlorophyll pigments in eutrophic waters. *Arch. Hydrobiol. Spec. Issues. Advanc. Limnol* 55: 153-168.

Simis, S., Peters, S., Gons, S. (2005). Remote sensing of the cyanobacterial pigement phycocyanin in turbid inland water. *American Society of Limnology and Oceanography* 50(11): 237-245.

Tandeau De Marsac, N. (1977). Occurrence and nature of chromatic adaptation in cyanobacteria. *Journal of Bacteriology* 130(1): 82-91.

Tedesco, L., Atekwana, E., Filippelli, G., Licht, K., Shrake, L., Hall, B., Pascual, D., Latimer, J., Raftis, R., Sapp, D., Lindsey, G., Maness, R., Pershing, D., Peterson, D., Ozekin, K., Mysore, C., Prevost, M. (2003). Water Quality and Nutrient Cycling in Three Indiana Watersheds and their Reservoirs: Eagle Creek/Eagle Creek Reservoir, Fall Creek/Geist Reservoir and Cicero Creek/Morse Reservoir. Central Indiana Water Resources Partnership. CEES Publication 2003-01, IUPUI, Indianapolis, IN, 163 pp.

Tedesco, L., Pascual, D., Shrake, L., Casey, L., Hall, B., Vidon, P, Hernly, F., Barr, R., Ulmer, J., Pershing, D. 2005. Eagle Creek Watershed Management Plan: An Integrated Approach to Improved Water Quality. Eagle Creek Watershed Alliance, CEES Publication 2005-07, IUPUI, Indianapolis, IN, 182 pp.

Teixeira, M., Costa, M., Carvalho, V., Pereira, M., Hage, E. (1993). Gastroenteritis epidemic in the area of the Itaparica Dam, Bahia, Brazil. Bulletin of PAHO. Bahia, Brazil: 244-253.

Wilson, J., Morlock, S., Baker, N. (1996). Bathymetric Surveys of Morse and Geist Reservoirs in Central Indiana Made with Acoustic Doppler Current Profiler and Global Positioning System Technology. Retrieved December 12, 2002, from http://in.water.usgs.gov/bathymetry.web/

USEPA (1983). Methods for Chemical Analysis of Water and Wastes. USEPA, EPA 600/4-79-020.

U.S. Geological Survey (2003). Water Resources Division, Monthly Streamflow Statistics for Indiana. http://waterdata.usgs.gov/in/nwis/monthly/ from 7 April 2003.

Yacobi, Y., Gitelson, A., Mayo, M. (1995). Remote Sensing of chlorophyll in Lake Kinneret using high spectral resolution radiometer and Landsat TM: spectral reflectance features of reflectance and algorithm development. *Journal of Plankton Research* 17: 2155-2157.

APPENDIX A

Summary of Analytical Methods

Sample	Analytical Method	Detection Limit	Method Description	Description
Alkalinity (mg/L as CaCO3)	EPA (310.1)	2.0	Titrametric	Alkalinity by titration to pH 4.5. Acid neutralizing capacity (sum of all titratable bases). Primarily a function of carbonate, bicarbonate, and hydroxide content (usually an indicator of the concentration of these consituents).
DOC (mgC/L)	SM (5310C)	0.5	Persulfate	Oxidation-Amount of TOC that passes through a 0.45µm-pore-diam filter.
TOC (mgC/L)	SM (5310C)	0.5	Persulfate	Oxidation-Persulfate and Ultraviolet Oxidation with IR detection. Carbon atoms covalently bonded in organic molecules are broken down to be measured quantitatively. Organic Carbon is oxidized into CO2 by persulfate using UV light. CO2 is removed from the sample, dried, and transferred with a carrier gas to an IR analyzer.
Chloride (mg/L)	EPA (300.0)	8.0	Ion	Method 300.0 is an ion chromatograph method using a Dionex DX-600 system with a conductivity detector. Sample is added to an ion chromatograph. Anions are separated and measured using a gaurd column, analytical column, supressor device, and conductivity detector.
Sulfate (mg/L)	EPA (300.0)	8.0	Ion	Method 300.0 is an ion chromatograph method using a Dionex DX-600 system with a conductivity detector. Sample is added to an ion chromatograph. Anions are separated and measured using a gaurd column, analytical column, supressor device, and conductivity detector.
O-Phos (mg/L)	EPA (300.0)	0.05	Ion	Method 300.0 is an ion chromatograph method using a Dionex DX-600 system with a conductivity detector. Sample is added to an ion chromatograph. Anions are separated and measured using a gaurd column, analytical column, supressor device, and conductivity detector.
Total P (mg/L)	SM (4500-P E.)	0.010	Colorimetric	Ascorbic Acid Colorimetric method-Ammonium molybdate and potassium antimonyl tartrate react in acid with orthophosphate to form phosphomolybdic acid that is reduced to colored moltybdenum blue by ascorbic acid.
Nitrite (mg/L)	EPA (300.0)	0.0	IC	Method 300.0 is an ion chromatograph method using a Dionex DX-600 system with a conductivity detector. Sample is added to an ion chromatograph. Anions are separated and measured using a gaurd column, analytical column, supressor device, and conductivity detector.
Nitrate (mg/L)	EPA (300.0)	0.10	IC	Method 300.0 is an ion chromatograph method using a Dionex DX-600 system with a conductivity detector. Sample is added to an ion chromatograph. Anions are separated and measured using a gaurd column, analytical column, supressor device, and conductivity detector.

Sample	Analytical Method	Detection Limit	Method Description	Description
Silica (mg/L) unfiltered	EPA (370.1)	0.10	Colorimetric	Heteropoly acids are produced by the addition of Ammonium molybdate (at pH 1.3) to sample containing silica and phosphates. Molybdosilicic acid is preserved and molybdphosphoric destroyed with the addtion of oxalic acid. Intensity of yellow color is indicative of concentration of molybdate-reactive silica.
Ca (mg/L)	EPA (300.7)	3.0	IC	Method 300.0 is an ion chromatograph method using a Dionex DX-600 system with a conductivity detector. Sample is added to an ion chromatograph. Anions are separated and measured using a gaurd column, analytical column, supressor device, and conductivity detector.
Mg (mg/L)	EPA (300.7)	1.0	IC	Method 300.0 is an ion chromatograph method using a Dionex DX-600 system with a conductivity detector. Sample is added to an ion chromatograph. Anions are separated and measured using a gaurd column, analytical column, supressor device, and conductivity detector.
K (mg/L)	EPA (300.7)	0.05	IC	Method 300.0 is an ion chromatograph method using a Dionex DX-600 system with a conductivity detector. Sample is added to an ion chromatograph. Anions are separated and measured using a gaurd column, analytical column, supressor device, and conductivity detector.
Na (mg/L)	EPA (300.7)	1.0	C	Method 300.0 is an ion chromatograph method using a Dionex DX-600 system with a conductivity detector. Sample is added to an ion chromatograph. Anions are separated and measured using a gaurd column, analytical column, supressor device, and conductivity detector.
Total Hardness (mg)	SM (2340 B)	12.0	Calculation	Total hardness is calculated from the sum of Calcium and Magnesium Concentrations (mg CaCO3/L).
MIB (*ng*/L)	SM (6040)	3.0	Mass Spectrometric	Organics are extracted from water by closed-loop stripping. Extracted organics are injected into a gas chromatograph/mass spectrometer for identification based on retention time and spectrum comparison. Single-ion current integration is used to quantify MIB.
Geosmin (*ng*/L)	SM (6040)	3.0	Mass Spectrometric	Organics are extracted from water by closed-loop stripping. Extracted organics are injected into a gas chromatograph/mass spectrometer for identification based on retention time and spectrum comparison. Single-ion current integration is used to quantify Geosmin.
NH4-N (mg/L)	SM (4110)	0.02	IC	Sample injected into carbonate-bicarbonate and passed through series of ion exchangers. Anions are separated by their relative affinities for for a strongly basic anion exchanger. Anions passed through s fiber supressor coated with a strong acid solution to conv ert anions to highly conductive acid form, conductivity is measured. Concentration is determined from measurement of peak height or area.
TKN (mg/L)	EPA (351.4)	0.30	Contracted Out	Determined by digestion, followed by ammonia determination by ion selective Electrode by a contract lab.

CURRICULUM VITAE

Kaylan Lee Randolph

Education

Indiana University-Purdue University Indianapolis, Geographic Information Science
Masters of Science, March 2007

Indiana University, Bloomington, Environmental Management
Bachelors of Science, May 2004

Funding and Awards

- Masters Thesis Funded by a grant from the Indiana Department of Natural Resources Lake and River Enhancement Program ($20,062) and funds from the Central Indiana Water Resources Partnership ($198,612)
- Indiana Water Resources Association Outstanding Graduate Student Researcher Award (2006)

Research Collaborators

- Veolia Water Indianapolis, LLC
- Indiana Department of Natural Resources, Lake and River Enhancement Program
- IUPUI Department of Geography
- University of Nebraska, CALMIT (AISA Sensor Fly-over)

Professional Experience

	Center for Earth and Environmental Science (CEES), IUPUI
March 2006 - Present	Visiting Research Associate
Aug. – Feb. 2006	CIWRP Remote Sensing Research Assistant
May - Oct. 2005	CIWRP Water Quality Summer Research Assistant
	Family Practice Center and Department of Geography, IUPUI
May 2005 - Present	Research Assistant

Publications

Journal Articles

Randolph, K.L., J. Wilson, L. Tedesco, L. Li, and A. Wilans. In preparation. Hyperspectral remote sensing of cyanobacteria in case II waters using optically active pigments, chlorophyll *a* and phycocyanin.

Research Reports

Li, L., D.L. Pascual, L.P. Tedesco, K.L. Randolph, R.E. Sengpiel, and B.E. Hall. 2006. Developing a survey tool for the rapid assessment of blue-green algae in Central Indiana's reservoirs. 2005 Lake and River Enhancement Report, Indiana Department of Natural Resources. 44 pp.

Contributor to

Tedesco, L.P., D.L. Pascual, L.K. Shrake, L.R. Casey, B.E. Hall, P.G.F. Vidon, F.V. Hernly, R.C. Barr, J. Ulmer, and D. Pershing. 2005. Eagle Creek Watershed Management Plan: An Integrated Approach to Improved Water Quality. Eagle Creek Watershed Alliance, CEES Publication 2005-07, IUPUI, Indianapolis, 182 pp.

Conference Presentations

Randolph, K.L., L. Li, L.P. Tedesco, and J. Wilson. 2006. Remote Sensing of phytoplankton in case II waters using optically active pigments, chlorophyll *a* and phycocyanin. North American Lake Management Society 2006 International Symposium, November 8 – 10. Indianapolis, Indiana.

Randolph, K.L., L. Li, L.P Tedesco, J. Wilson, and D.L. Pascual. 2006. Remote Sensing of Phytoplankton Using Optically Active Pigments, Chlorophyll *a* and Phycocyanin. Indiana Water Resources Association Spring Symposium, June 21 – 23, 2005. Purdue University, Lafayette, Indiana.

Seminars and Meetings

Randolph, K.L., J. Wilson, L. Li, L.P. Tedesco. 2006. Remote sensing of cyanobacteria in case 2 waters using optically active pigments, chlorophyll *a* and phycocyanin. Central Indiana Water Resources Partnership December 2006 Meeting, Indianapolis, Indiana.

Randolph, K.L., R.E. Sengpiel, D.L. Pascual, L. Li, L.P. Tedesco, J. Wilson. 2006. A rapid assessment tool for mapping blue-green algae. Veolia Water Indianapolis, LLC, Technical Advisory Group October 2006 Meeting, Indianapolis, Indiana.

Tedesco, L.P., L. Li, D.L. Pascual, K.L. Randolph, R.E. Sengpiel, B.E. Hall. 2006. Indianapolis Water Resources Research. Veolia Water Australia July Meeting, Adelaide, Australia.

Tedesco, L., L. Li, D.L. Pascual, K.L. Randolph, R.E. Sengpiel, B.E. Hall. 2006. Eagle Creek Reservoir Conditions Associated with June 2006 *Pseudanabaena* Bloom. Veolia Water Indianapolis, LLC, Technical Advisory Group June 2006 Meeting, Indianapolis, Indiana.

Randolph, K.L., L. Li, L.P. Tedesco, and J. Wilson. 2005. Remote sensing of phytoplankton pigments, chlorophyll *a* and phycocyanin, in small, inland reservoirs. Joint Remote Sensing Seminar. Purdue University, Lafayette, Indiana.